SCALABLE PATH PLANNING AND SIMULATION VIA NUMERICAL RING PREDICTION AND PATH OPTIMIZATION THROUGH MODEL-CENTRIC GPU DATA ANALYSIS

A Dissertation
Presented to
The Academic Faculty

by

Zhengkai Wu

In Partial Fulfillment
of the Requirements for the Degree
Doctor of Philosophy in the
School of Electrical and Computer Engineering

Georgia Institute of Technology
May 2019

SCALABLE PATH PLANNING AND SIMULATION VIA NUMERICAL RING PREDICTION AND PATH OPTIMIZATION THROUGH MODEL-CENTRIC GPU DATA ANALYSIS

Approved by:

Dr. A. P. Sakis Meliopoulos, Advisor
School of Electrical and Computer Engineering
Georgia Institute of Technology

Dr. Douglas B. Williams
College of Engineering
Georgia Institute of Technology

Dr. Gee-Kung Chang
School of Electrical and Computer Engineering
Georgia Institute of Technology

Dr. Fumin Zhang
School of Electrical and Computer Engineering
Georgia Institute of Technology

Dr. Andy Sun
School of Industrial and Systems Engineering
Georgia Institute of Technology

Date Approved: [Nov 20, 2018]

To my professors, family, and friends

ACKNOWLEDGEMENTS

First and foremost, I would like to thank my Ph.D. advisor, Professor A.P. Meliopoulos, for being the best advisor that I am very fortunate to meet with. His insights and encouragement have brought great motivation for my work as bright light in the shadow to overcome obstacles. I have known him ever since I started my Ph.D. journey at GT. He is a very nice guy and knowledgeable professor while coaching lots of students with efficiency.

I would also like to thank Dr. Chang for his kind guidance in and out of class. His insightful suggestion provides me great motivation and guidance for composing Ph.D. dissertation and making better plans towards the success of the journey. I would like to express my deepest gratitude to Professor Douglas Williams serving as my committee and for past Lego robotic project with him from which I learned a lot. Despite his busy schedule, he always made valuable advice for my research and life in a new country. I am thankful for all other professors who help for my proposal and thesis committee members for giving me valuable comments for my work. Dr. Fumin Zhang is also very supportive during my lectures with him. I am grateful to have him serving as my committee member as well. I would also like to extend my sincere gratitude to Dr. Andy Sun for serving as my dissertation committee and for his valuable time contribution in reviewing the draft. Their insightful comments and suggestions have made considerable contribution to the completion of this work.

I wish to express my deepest gratitude to Dr. George Riley (who has passed away) for his patience and encouragement towards my Ph.D. Thanks for all instructors, secretaries and coordinators at GT who helped and cared me in the past, within and

outside Electrical and Computer Engineering Department as well as people in Manufacturing Engineering Department for the interdisciplinary support during past project. Thanks for whoever that has provided technical consultancy and support including those labs and companies that shared software, hardware, CNC machine training and computational data resources, which contribute to experimental platforms. Special thanks for the invitation of AeroDef Manufacturing in SME for providing travel support and WHPC (Women in High Performance Computing) for supercomputing conference opportunities in Salt Lake and many other supportive organizations during conferences.

Most importantly, I am grateful for all my family, friends and professors as well as colleagues including my lab mates while completing this dissertation work. The goal of Ph.D. really takes a long time with dedication to achieve. Without your company, my time during this journey wouldn't be so enjoyable. Many thanks for whoever helped and guided me in the past. Without your encouragement and lead, my journey of Ph.D. would not be such fruitful with lasting memories for a life time.

TABLE OF CONTENTS

LIST OF TABLES

LIST OF FIGURES

LIST OF ALGORITHMS

LIST OF GLOSSARIES

CNC: Computer Numerical Control

STL: STereoLithography

CAD: Computer-Aided Design

GDP: Gross Domestic Product

GPU: Graphical Processing Unit

HDT: Hybrid Dynamic Tree

AMR: Automatic Meter Reading

ARCH: Autoregressive Conditional Heteroskedasticity

FMS: Flexible Manufacturing Systems

CAM: Computer Aided Manufacturing

AIMA: Autoregressive Integrated Moving Average

SOBI: Second Order Blind Identification

ICA: Independent Component Analysis

SARs: Severe Acute Respiratory Syndrome

FEA: Finite Element Analysis

MRI: Magnetic Resonance Imaging

FMM: the Fast Multipole Method

BEM: Boundary Element Acoustics

VM: Virtual Machine

SaaS: Software as a Service

IaaS: Infrastructure as a Service

PaaS: Platform as a Service

SUMMARY

Manufacturing via Computer Numerical Control (CNC) has gained popularity as it enables complex systems to be automatically produced. There is a need to increase the capability of CNC to enable manufacturing of ever more complex systems. In this thesis, a Step Ring path planning scheme by real-time simulation of multi-axis machining generating 2D and 3D visualization and controllable G-code optimization for model-specific Computer Numerical Control (CNC) manufacturing is proposed and applied. The main integration steps of our scheme are: (a) in pre-processing, the main tasks are model structure analysis and 3D reconstruction (Example: Buzz - Georgia Tech Logo Image) with data fitting through Grid simulation as well as machine path validation and Voxel Model in graphical simulation is introduced. (b) processing of ring path planning model, Isoscallop Analysis of Surface Quality is applied for real-time simulation of path parameter tuning and Blackbox tuning of ring path as a function. (c) ring prediction algorithm is tested for estimation of Ring boundary for optimal local path within linear constraint. And (d) in post-processing, G-code optimization is implemented with scalability of path planning by GPU (Graphical Processing Unit) simulation of accessible path sequence through path partition. G-code optimization is attained by both adaptive filter for partition and data compression. For accessible path sequence analysis, parallel data structure of map kernel structure is also analyzed.

The innovations of our scheme are a scalable path planning solution based on local ring prediction and accessibility map sequence data analysis towards parallel optimization. The input Buzz STL model is a 3D model built from 2D image features

after model fitting based on feedback control of entire simulation process and sustainable planning. The achievement of real-time application in graphic visualization with the help of GPU allocation and smart data modeling is going to drive low-cost and high-quality surface machining for both time saving and event planning. High-precision 3D simulation may help analysis over other functions of machining and software GPU simulation such as generalization of various platforms of multi-axis machines and provides distributed guidance for digital manufacturing and Computer-Aided Design (CAD) software development.

For digital manufacturing and CAD design, efficiency and accuracy matter. Digital metric is important as key component of this thesis. Task partition enables multi-tasking and parallelism i.e. independent tasks that can be run in parallel. Therefore, digital metric for task partition and evaluation is presented after basic ring path planning in subtractive 3D printing to provide application insights regarding automatic system integration and advanced processing of data. One important feature is path sequence generation with accessibility map and optimal orientation, which is analyzed with simulation output via GPU computation and varying sampling rate for performance estimation. Accessible sequence of path is key to linearization of nonlinear path with connection to modeling and optimization.

Cloud computing metrics for virtual measurement and simulation with case study are also described as computational tools of storage sharing and distributed device of network communication. Cloud simulation includes two aspects: (a) simulation of case study for demonstration of 3D path planning task (b) performance metric for evaluation of energy saving. To attain energy efficiency or green computation on these digital

devices such as GPU and cloud, methods of case study example are analyzed with service-oriented cloud and feature classification of workload partition of user behavior analysis that help attain these goals of optimization.

Feature protection is an important part of this thesis work as it connects both control and path validation features with bounded constraints. Path protection was initially introduced for the purpose of control and error tolerance. In the path protection scheme, path validation and collision avoidance are included for error tolerance in CAD design. Protection is also described with digital metrics in feature-awareness design with map interface for bounded monitoring of feature classification and better maintenance of system.

Overall, we demonstrate a successful step ring path planning approach of both local and global scale. The simulation is done through GPU path planning and model-specific graphics rendering and simulation, using pattern based geometric STereoLithography (STL) models with target shape in 3D printing that can be reconstructed from image data for multi-axis machining. Digital manufacturing and path protection using digital metrics and other performance monitoring designs are also described. In addition, graphic interface with parameter feature selection for path protection and maintenance is described. For data diagnosis and searching speed of a certain feature, we analyze branch number for path sequence generation and also discuss the role of branch in Hybrid Dynamic Tree (HDT) data structure and grid resolution with 3D Buzz structure analysis demonstration. The path planning process is tested both by simulation and machining with double-feedback control. Step ring path planning

contributes to numerical computing and future dynamic estimation regarding linear and nonlinear model and measurement of bounded control for path simulation.

CHAPTER 1. INTRODUCTION

Cross-disciplinary work has been providing profound research opportunities for past breakthroughs in scientific progress. Combined simulation techniques with advanced GPU based software data analysis provide optimized solutions for CAD design and application. CNC design based on subtractive 3D printing techniques is the innovation of the tested ring path planning. CNC provides advanced machine coding for optimal automation of machining design and fast mass production. Design software and modeling based on innovative software simulation provide predictive analysis before actual path implementation with fault-tolerance and inspection of quality assurance. Compared to other software for CNC machining, we try to combine parallel techniques for path planning so that strategic path planning methods for optimal metric selection can be user interactive and machine efficient. In this thesis, a path planning scheme is done based on ring step scalable path by real-time simulation of multi-axis machining generating 2D and 3D visualization and controllable G-code. The optimization of G-code for model-specific Computer Numerical Control (CNC) on Okuma machine is implemented as post-processing of data. The major simulation solution of path planning includes data-preprocessing, parameter tuning of path simulation, and data-post-processing. The main tasks are model-oriented data analysis and fitting through interactive simulation for path validation. Isoscallop analysis of surface quality based on ring step path simulation is applied for volume representation of geometric 3D model in an interactive way. At last, the post-processing provides scalability of path planning by adaptive partition based on

graph analysis of software output G-code so that sub-graph local optimal region is generated for distributed computing and cloud computing application.

Analytics and visualization systems play a key role in enhancing both operational and non-operational awareness. In particular, they can offer the operator, analyst, or decision-maker refined information that will support critical maintenance, refurbishing or replacement decisions. While data representation by visualization can provide vivid analysis of data mining for decision support, the current asset management software is constrained to either geo-referenced grid visualization or to variable trending and charting. This thesis work provides a framework for data integration and analytics that combines abstract path planning 3D manufacturing data and visualization concepts for cost budgeting and energy saving. Based on a simulation framework, we present a monitoring system that provides integrated visual analytics and decision coaching. The system aims to explore the visualization potential to represent simulation metrics and feature extraction for classification measurements in monitoring and data analysis for simulation system service.

The innovation contributions are as follows:

- We link together the technical areas of condition assessment using a weighted index as input or as learning feedback result. We identify the links across geographic areas by providing a system evaluation class and maintenance service level.

- We design a feature classification color evaluation for software interfacing with map design.

- We design metric selection for classification related to data-mining to realize seamless relationship analysis.

- We simulate a classified feature awareness strategy for asset management to enhance the cost allocation for optimization.

- We design a budget monitoring method using data classification. This is formulated as a linear programming problem given a set of constraints.

In addition, we address the cloud computing and grid modeling application in subtractive 3D printing based on device level analysis such as GPU and parallel system integration in performance modeling and simulation. Our major approach is based on application perspective and cloud simulation to 3D printing modeling scenarios and parallel application platform of GPU so that time and energy could be optimized within time restriction. The application design is based on user-oriented request order and support data structure of hybrid dynamic tree into parallel system platform so that user satisfaction can be attained via user data streaming into system with planning strategies and data monitoring demo. The approach includes: model based analysis with performance modeling and application in tree topology and time perspective based on software prototype loading geometry; prediction based on smart meter data and geometry estimation and remodeling application based on parallel grid kernel and adaptive 3D tree structure in image processing; cloud computing analysis by modeling and application level design for scheduling strategies demonstration, as well as 3D printing application by user workload classification to satisfy product making via input modeling through

whole software system integration under parallel GPU architecture for workload optimization planning for performance and energy saving.

The software component for path planning simulation highly maps the real machining output after particular tool sizing experiment, thus the simulation in 3D volume geometry in each pass can demo the real machining output of actual mapping tool in full develop mode. The 3D volume visualization of cutting operation happens by 3D geometry rendering of each material removal process that actually runs on GPU to reduce the parallel latency between user interaction and software rendering time. The optimal planning can be attained and estimated once we figure out better path planning time by modeling geometry if the same depth of volume rendering is picked on average.

The work of this thesis can also help alleviate typical machine shop operations. In normal days, machine shop is busy with timed business schedule and business analytic case is charged with labor cost similar to auto shop. If the software planning tool can provide enough simulation and planning of both the 3D visualization and workload estimated consumption, we could monitor and optimize time of machining operation by modeling perspective via geometry sizing and input user requested geometry workload, and we would have our integrated design of 3D CAD design and CAM path planning more embedded into software parallel platform with smart meter data analytic as demand referenced forecast connecting both historical workload of system user and flexible individual input model schedule request.

The structure of this thesis includes eight chapters. The first two chapters introduce problem background of subtractive 3D printing and literature research of step

ring-based path planning and related fields. Literature review is described in Chapter 2. Chapter 3 describes algorithms for ring predictive feature-based modeling in path planning and post-optimal G-code optimization by data compression. Ring scalable black-box parameter tuning, as well as 3D reconstruction and design on 3D printing grid modeling by double-feedback process for simulation precision via example Buzz feature extraction. Chapter 4 describes strategy in path planning. Chapter 5 shows data analysis in accessible sequence of map and describes numerical modeling of geometry boundary optimization as well as analyzed path protection. In addition, data integration by pre-processing, tuning, post-processing of 3D path planning simulation is done beside software component frame. Chapter 6 shows numerical modeling for estimation and parameter tuning. Chapter 7 describes digital cloud metrics and accessibility map kernel structure analysis for parallel workload study. Our research shows classification of cloud workload may enhance efficiency. Finally, Chapter 8 summarizes the thesis work and provides thoughts for follow up research.

CHAPTER 2. LITERATURE SURVEY

In this chapter, we introduce the project background of subtractive 3D printing, and provide literature review towards its research gap based on graphical models and computational algorithms by GPU simulation towards optimization.

2.1 Subtractive 3D Printing and Its Research Gap

CNC machine is a computer numerical controlled multi-axis machine for milling and turning operation. CNC machining provides strong material cutting power because of its strong cutting force and fast speed. Conventional 3D printing works with plastic material for additive fabrication based on STL model.

In contrast, subtractive 3D printing using CNC machine is a new way of 3D printing with the same STL model but more machining capability and diverse material flexibility. For comparison, conventional 3D printing works through a 3D printer with additive path planning to build successive layers while the subtractive 3D printing simulates material removal in subtractive ways for CNC machining with GPU software simulation via parallel computing features. GPU (Graphical Computing Unit) speeds up both visualization and computation and it runs multi-kernel application for path visualization and simulation in a parallel way. The scale of path is the key due to range and storage limit of CNC platform.

The major research purpose is model-based 3D visualization by path parameter tuning via GPU simulation and the model fitting and remodeling of system integration for path planning by local scalable solution towards efficiency. Through data analysis, we

would optimize model of 3D CAD design and computer aided manufacturing (CAM) towards path planning with more user interactive decision towards efficiency and optimization in embedded system software, this is one of the motivations. Another research gap is parallel data analysis of accessibility map computation [1] through adaptive depth-based volume rendering by on GPU path simulation when we consider orientation.

2.1.1 Model Analysis and Fitting as Pre-processing Validation

Model analysis and fitting are through simulation parameters and machining. For sustainable manufacturing, model validation procedure is described in system point of view during dynamics for efficiency of labor productivity, including sensitivity and behavior pattern during model validation [2]. In addition, model fitting of model scale and position in space affect system sensitivity of path planning and accuracy of simulation process. On the other hand, parallel computation capability, such as cloud manufacturing and service-oriented platform including public and hybrid platform as well as private community platform, calls for key challenges in manufacturing to merge with new technologies in cloud computing [3]. Parallel computing and high-performance computing tools based on GPU simulation and software product are thus developed towards efficiency and flexibility. The aim of FMS (Flexible Manufacturing Systems) is to achieve efficiency for mass production, and piece wise linear approximations and heuristic algorithms are reviewed to work for nonlinear constraints based objective functions [4]. Regarding model geometry and parameter validation, voxel model is good for structural analysis and topology design of surface modelling and optimization not only in automation industry, but also in computer aided design software [5].

Manufacturing grid system and its optimal selection-based analysis in resource and service has been studied [6-10] to provide parameter setting and mapping solution. Our demo Buzz model is validated by fabrication.

2.1.2 Voxel Model in Graphical Simulation

For graphical models, voxel model techniques are highly applied in graphics-based application. Study in [11] gives an idea of how to generate look up table, block density as well as index buffer for 2D and 3D textures via GPU with simple voxel and marching cube introduction. Shoji [12] introduced indirect FMM-BEM for voxel model analysis and applied field for electrical field of biological samples via GPU acceleration and Pseudo code template for CUDA kernels of the fast multipole method, along with multiple graphics processing unit execution. Crassin [13] introduced a system that achieves real-time rendering performance for several billion voxels and showed how their introduced pre-filtered geometry model and approximate cone tracing can be used to efficiently achieve blurry effects and real-time indirect lighting. He also presented a solution based on an adaptive data representation depending on the current view and occlusion information, coupled to an efficient ray-casting rendering algorithm, extracting information during rendering to guide data production and streaming [14]. The resulting solution can efficiently render large volumetric data sets interactively to real-time rendering performance for several billion voxels. Rees and McColgan [15] provided statistical analysis for multiple comparison and general methods of pre-processing as well as fluid registration for Voxel Based Morphometry.

Simulation based on grid and numerical input are important for accuracy and statistical analysis. Sugiyama et al. [16] presented a new simulation method for solving fluid-structure coupling problem, which has been developed with all the basic equations numerically solved on a fixed Cartesian grid for fluid and solid motions using a finite difference scheme with various verifications and validations of the present full Eulerian method for numerical accuracy. Scahill et al. [17] described a voxel-based analysis of nonlinear-registered serial MRI to demonstrate the most statistically significant regions and global entropy in advancing of Alzheimer's disease (AD). Differences between groups by statistical analysis and change detection of individual overtime by fluid registration are introduced after MRI Acquisition and Pre-processing. Study in [18] introduced issues and methods such as steady state temperature initialization involved in accurately predict SARs via the development of realistic anatomical data sets, in which voxel-based descriptions are created by dividing the space occupied by the object being described (e.g., the human body) into a 3D grid of small, equal sized volume elements known as voxels. In [19], a new simulation method for solving fluid-structure coupling problems suitable for voxel-based geometry has been developed and a volume-of-fluid approach is applied to describing the multi-component geometry. Study in [20] introduced finite element analysis as an invaluable tool for investigating the biomechanical function of complex skeletal structures. Voxel-based FEA on millions of voxels/elements that are needed to model small sections, as well as issues such as color-mapping strains, clipping and adding displacement field is discussed in [21].

2.1.3 Isoscallop Analysis of Surface Quality

Isoscallop analysis is a cared topic in machining operation as the isoscallop scale and shape affect the surface quality of machining parts for material simulation based on tuning parameters. Simulation of surface geometry for path validation based on the 3D volume representation for virtual path visualization helps validate path before physical machining in fabrication. Regarding software algorithms in material surface machining, software algorithms based on the product surface isoscallop analysis is presented with strategies based on product scallop heights and parametric equations of sculpture surface quality measurement [22]. The 3D volume visualization of cutting operation by 3D geometry rendering of each material removal process may take a lot of time by CPU computation.

2.1.4 Post-processing and Scalability of Path by GPU Simulation

Compared to similar work in 3D printing and tool path planning, offsetting algorithms based on top of volumetric data structure for graphical rendering simulation also use HDT (Hybrid Dynamic Tree) tree [23] as graphical simulation basis but differs in its surface geometry scale and adaptive filtering as post-processing of scalable path based on pre-processing of model fitting due to model reconstruction from image for path sensitivity and accessibility sequence analysis. In addition, ring path prediction is similar to machining spiral strategy [24] but differs by GPU simulation for path planning of selected ring set cover of model in software visualization.

2.2 Statistical Data Analysis and Filtering based Data Mining

Statistical data analysis is widely applied in data mining and machine learning regardless of area. A new statistical method for wind forecasting is presented in [25]

based on independent component analysis (ICA) and autoregressive (AR) model exploiting the time structure like second order blind identification (SOBI). [26] presents a short-term wind speed prediction using linearized time series model estimated by regression analysis on logarithms of wind speed data. Autoregressive Integrated Moving Average (AIMA) model is developed to forecast short term power load of New South Wales in Australian, and then rectify residual errors using method of weighted mean[27] residual errors are then rectified by weighted mean. [28] investigates regime switching in the volatility of load time series to capture the nonlinear characteristics of volatility. It combines two types of regime-switching GARCH models with Generalized Auto-Regressive Conditional Heteroscedastic (GARCH) models. The ARCH (Autoregressive Conditional Heteroskedasticity) model is an advanced statistical model that is efficient in investigating the volatility characteristics of time series [28, 29]. [30] improves the state forecasting accuracy by presenting a block-diagonal state transition matrix based on regression analysis and uses extended Kalman filter to correct classical dynamic state estimation (DSE). Time series is widely used in load forecast. [31] describes an algorithm of non-stationary time series forecasting using ensemble of autoregressive models with time-varying structure. Recursive splitting is implemented, and individual models are defined and demonstrated combining fuzzy logic controller in forecasting with different time frequencies. [32] presents a time series forecasting model based on real measurements of load power through two components: a trend component and a cyclic (periodic) component, which are identified separately using a regression algorithm and spectral techniques. [33] establishes the neural network and Chaotic Time Theories with an optimal time lag for performing short-term forecast of power load. Support vector

machine works for nonlinear modelling and is also applied with enhancement for electricity forecast [34, 35].

Filter are important for data forecast and machine learning. [36] uses Kalman filter for short-term load prediction of residential customers to examine the potential impact of automatic meter reading (AMR). [37] illustrates short term demand forecasting on smart meter data by polynomial fitting (using time polynomials to fit load curve) with interpolation using apparent power sample points.[38] presents a variable data learning window and diverse learning data weighting combinations to improve short-term load forecasting in buildings for demand side management and energy efficiency. [39] also studies asymmetric ARCH models for short-term load forecasting. [40] uses a two-step methodology comprising a classification and an adjustment steps for short-term load forecast in non-residential buildings. Pattern, feature and data numerical characterization are also useful data trace representation. Forecasting is a general term while prediction is more specific. [41] presents a self-learning algorithm of prediction by incremental pattern characterization in electricity consumption based on smart meter readings. [42] uses spatial autoregressive model to analyse the spatial characteristic between power demand and GDP, and develops an adaptive forecasting for mid-long term load with the combination model. Feature selection is helpful for building energy prediction with two well-known probabilistic regression techniques--linear models and Gaussian process regression [43]. Data mining approaches are thus applied to forecast energy consumption by extracting patterns, for example use Neural Network and Support Vector Machine to come up with a precise prediction ranging from hourly electric energy usage to weather data in a predefined period of time like three days ahead [44].

2.3 Solution of GPU Scalable Path Planning via Graphical Model and Accessibility

We focus on path planning problem of subtractive 3D printing based on STL model, which include linear 3 axis path by numerical ring cover for graphical region and accessibility map for path orientation. The accessible graph connects accessibility regions by path sequence and is updated based on accessible point position. The software provides visualization, statistical and numerical analysis, and model-centric function via Graphical Processing Unit (GPU) as it runs parallel computing applications. We apply ring numerical prediction algorithm and compute accessibility map with data analysis mapping ring scale to map sequence with data structure including sampling result of map resolution. In addition, adaptive filter is described as post-processing solution of path scalability towards storage efficiency and flexibility. At last, parallel optimization of GPU cross-layer analysis of GPU pump kernel for improvement of map accessibility is analysed.

2.4 Digital Metric and Cloud-based Power Management

2.4.1 Introduction of Power Management

Power management is becoming more and more important for modern computer systems, especially for large-scale systems composed of thousands of servers. The advances in micro architecture and fabrication technologies have led to increased performance capabilities in modern computing platforms, which are being accompanied by a dramatic rise in the power densities exhibited by hardware [58]. Overconsumption of power causes many problems, like electricity consumption, bill cost, and even system

failures. As a result, there have been various power saving techniques in response to the increased importance of power saving (e.g. [51, 63, 68], etc.). Cloud computing is another important area of modern computer system [55, 65]. As a promising super structure for corporate, enterprise and academic computing, cloud computing has the attention of many big companies (e.g. Google, Amazon) [46]. A cloud can be defined as a pool of computer resources that can host a variety of different workloads, including batch-style back-end jobs and interactive user applications [45].

The importance of power saving and promising effects of cloud computing bring about the idea of a "green cloud" [56]. For data centers which implement cloud computing, it's operators still have to purchase and provision servers and other IT equipment as well as maintain the facilities components, therefore it is important for a green cloud to predict demand at least to some extent so that people may not over-provision (building, hardware, software, and other things) for fear of running out of resources due to an unexpected surge in demand. Power budgeting is therefore rendered for online power management in several aspects [58].

2.4.2 Background of Power Budget Management in Data Center

The job of power budget management is to ensure that the aggregate power consumption of the platform does not exceed the specified power budget, or that it adheres to some average over time. Accordingly, power budgeting should be flexible and cover the power consumption satisfying certain Service Level Agreement (SLA, e.g. response time). There has been substantial work performed on power budgeting, exploiting hardware management capabilities like processor frequency scaling [51, 63].

Power budgeting is important, where reasons include the following (Karsten Schwan 2010):

– to meet a data center-level power constraint, by imposing constraints on certain sets of resources and on the applications that use them; one purpose is to constrain total power usage; another purpose is to ensure fairness across multiple applications (power proportional behaviour is a favorite recent topic for e.g., hadoop codes);

– to constrain the resources used by an application, with power being one of the first level metrics desired by data centre operators, again, to meet centre-level power budget constraints, and then, to also have a better basis for charging models;

– to achieve improvements in total power consumption, a key goal for web companies like yahoo and Google, since their total power bills are starting to approach levels similar to the levels of equipment purchase bills.

Effective active power budgeting could differentiate both homogeneous and heterogeneous data centre resources and build application-aware VM budgeting [58]. That's why we think of workload classification by power budgeting for different services in cloud computing. Besides, existing hardware techniques (e.g. queuing techniques, control method using DVFS and MPC [68] and hybrid means [49]) of power management for current data centres do not address enough fault-tolerance and dynamic performance characterization by workload types. Their control references are based on constant power budget distributed to fixed locations and do not adapt to the dynamic user workloads of the web service of a cloud in varying locations.

The case for power management in cloud computing is quite different from current data centers in the following aspects: varying user behaviour and request, dynamic web workload change, fault-tolerance issue in large scale and mixed cloud services.

2.4.3 Fault Tolerance in the Cloud

To estimate fault, we can use the miller's Mills Fault seeding theory [60]:

$$\frac{\text{detected seeded Faults}}{\text{total seeded faults}} = \frac{\text{detected non-seeded faults}}{\text{total non-seeded faults}} \qquad (2.\mathbf{1})$$

As the mechanism of tree logic could be made into software system for clouds, fault tolerance and its detection for software testing are easier for the classification tree. Posterior estimation of untested faults in the system could be predicted from Equation 2.1.

2.4.4 Synthetic Data for Simulation

In this thesis, we implement power simulation using defined metrics and provide evaluation of power saving by synthetic data [47, 50, 61] in three cases: power capping with uniform Pc, power capping with classified Pc1, Pc2 and Pc3, and power consumption without capping.

2.4.5 Solution of Power Capping

Power capping could save power during outages and meet the power requirement at certain times [61]. Although CPU computes 30% energy of the total power usage by computer, it is significant when user workloads are large in broad scale of cloud. From ElasticTree [54], we know that network energy is reduced too by the power saving from

optimum network tree. Large-scale simulations and network implementations in real cloud services and environmental software system development, remains to be done in the future.

2.4.6 Related work of Power Management in Data Center

Power management has become critical for large scale server systems and HPC machines. Previous works for data center power saving, use methods like turning servers on and off based on demand [48], dynamic voltage and frequency scaling (DVFS) [68], and spare servers [62] to manage power. Recently, coordinated design based on multi-level power management for the data centers is also presented [61].

Models for performance [53] or power [68] are built to make use of frequency scaling in different power phases. Most power management methods for data centers are based on power distribution units (PDUs) and RACKs distributed by fixed locations on physical level (groups or enclosures [61]).

On the other hand, power budgeting techniques include platform level controllers that perform fine grain throttling to meet power limits [57], power budgeting processes using non-uniform allocations across nodes in data centers [51, 59],and a compensation approach using power budgeting during different periods of varying workload to manage power from a VM-centric point of view [58]. Power capping saves power without affecting performance for I/O intensive workloads[50].

Power aware techniques for cloud computing have already been presented [45, 64]. Other methods try to manage a cloud's workload [66, 67] or use VMware in order to

lower power consumption. ElasticTree on data center network has already been proved as an effective method for saving power [54]. The network tree is actually presented to improve video quality in cloud computing for the masses, and this paper is similar to [52] for a P2P network, but differs in that it uses tree distribution for the power budgeting in cloud services.

CHAPTER 3. EXPERIMENT ON PREDICTIVE RING PATTERN VIA 3D DESIGN FOR SCALABLE PATH PLANNING TOWARDS EFFICIENCY

In this chapter, we provide definition of ring path planning via graphical models and describe computational algorithms with GPU graphical simulation towards optimization.

3.1 3D Design from Image Feature by 3D Reconstruction

3.1.1 Image Feature Extraction

We apply the same model in STL format used in 3D printing, but use CNC machining for production of these models. To design the model, we want to have user preferred input feature such as image we want to put together to a sculpture or logo. To demonstrate the idea of 3D design model from image feature, we use similar 3D reconstruction from image contour point feature to rebuild the 3D geometry shape. The process of making image feature into 3D geometry STL model as path planning input takes CAD design process to complete. The CAD design could be done by CAM/CAD software, to build with simple curve or lines or points we input from point cloud data. We use Georgia Tech logo Buzz to demonstrate our idea and extract the contour key points from image feature for the 3D Buzz model.

3.1.2 3D Scaling and Registration for 3D Reconstruction Model

Scaling and registration is another phase in 3D modeling for STL input of CAD design. The original coordinate of the model may not be the same with path planning software coordinate, so we map the right origin position with the path planning software and make sure the coordinate of the 3D model is the same with machine space coordinate in order to have the right mapping precision between the software output of G-code and the path planning CNC machine axis. Figure 3.1 shows the scaling process after the 3D reconstruction of the CAD design. We shape the model to the optimal size for machine path planning operation, so that the path has right sensitivity and scale for the CNC machine to operate from the 3D input.

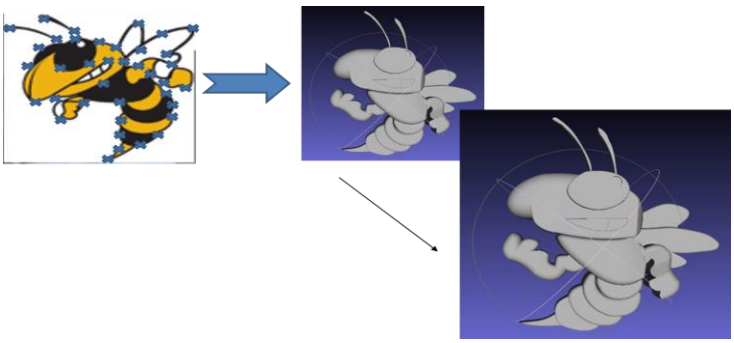

Figure 3.1 3D Scaling and Feature Exatraction of Buzz

3.1.3 Application of 3D Reconstruction Model Significance

The image feature gives application feasibility from user input design of Sculpture such as photos so that image profile may get 3D printed for body profile. In addition, artistic design may also be built by the path planning form 3D reconstructed model. Moreover, the 3D reconstruction also gives important feature extraction from the expected medical part of the patient such as teeth and other bone structure feature for analysis in order to have right sensing and inspection of the original shape of the body for

concave making up or rebuild. Therefore, it does have important application significance in medical and in artistic design.

In addition, to make up important structure that may not be easily produced from original making such as car collision part or aircraft part, we may use the 3D model and build up material test for fixing these parts so that the few missing parts may be rebuilt to fit the original design or for material test and force experiment in different conditions. Therefore, the applied technique does have a lot of application fields for connection of 3D printing and also advanced manufacturing application on CNC. Virtual path planning and simulation could adapt path planning without lab environment or for space product.

Last but not least, due to analysis of cloud and parallel simulation study via GPU testbed and task-oriented service cloud, our simulation approach also facilitates the cloud manufacturing application such as Manu-cloud design, so that location free and thin-client may be applied into industry and VM virtual machine as user interactive tools, such as phone app or robotic jet plane.

3.2 Introduction of Ring Path Planning in Subtractive 3D Printing

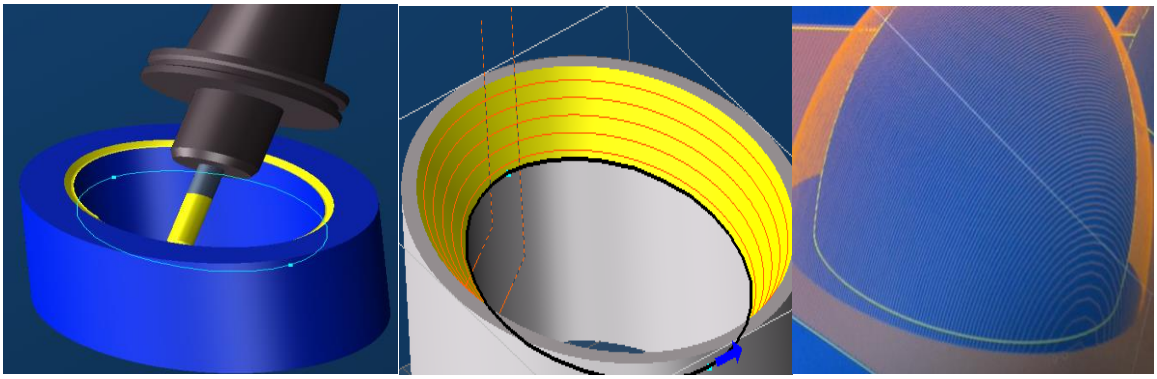

Figure 3.2 Ring Distribution and Spiral Tool Path Simulation

This section will answer the question based on ring structure. Figure 3.2 shows the ring distribution based on the spiral tool movement and its orientation. The ring is controllable 3D linear spiral circles of maximum radius |r| by defined number of rings and ring step distance that are distributed across the 3D geometric structure. By ring we have fast searching for nearest neighbors of volume computation. The ring simulates the spiral machining strategy of the tool tip direction as it passes along the geometric surface. The boundary of the ring path circles classifies the points of contact along the geometric body that contribute to actual volume selection for pattern processing of interest area. How to achieve path planning efficiency based on graphical model and numerical computing based on selected model design pattern? This chapter will answer the question based on ring structure. Bounded ring gives 3 axis linear path domain.

The set of ring circles also represent an interested area of path planning geometric input as only selected region within the ring cover will be used for volume generation of interactive path planning. Thus, the scale of the ring determines the area of center region that is segmented for target model region. The area outside ring circle region is segmented off the volume picked for path rendering operation.

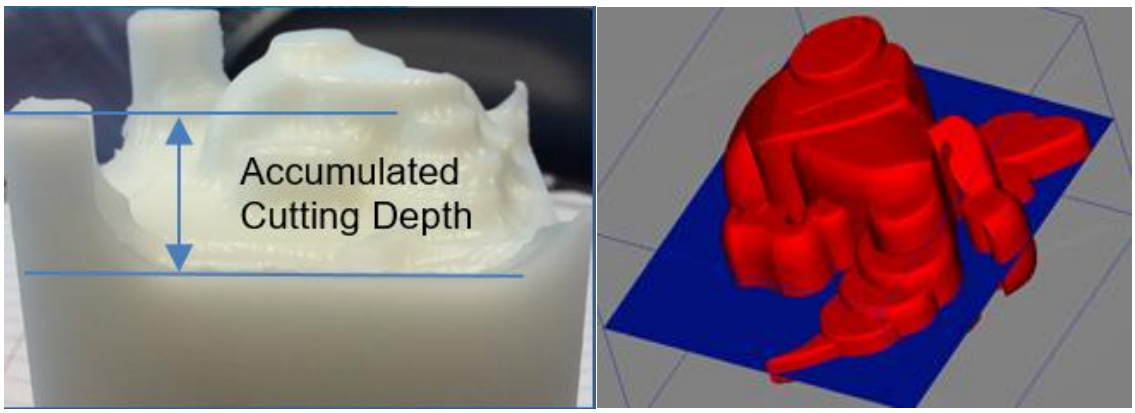

Figure 3.3 Accumulated Cutting Depth and No-cutting Plane

The ring gives numerical value to the measurement of region size along its distribution location. The number of ring circles represents the size of tilted region that can be covered within ring edge circle. Both radiance of geometric surface normal variation and the size of the boundary ring edge determines the ring number. The ring circle size represents its horizontal and vertical data of ring distribution in 3D space. The

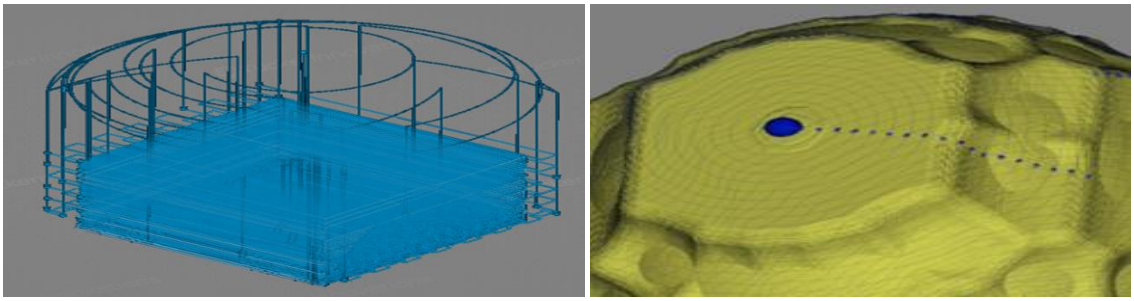

Figure 3.4 Path Retraction and Iterative Ring Path Distribution by Depth Layer

more tilted for surface cover of ring region for orientation variation of tool tip, the more ring circles for the target zone. In addition, the larger the target area, the larger number of ring circle based on fixed gap or step over distance.

As we place the ring circles across the surface area, we give height information of each ring path layer in distributed layer position of ring circles. The path planning is made based on the layer-based removal of volumetric path iteration that the tool tip goes deeper by depth of tool cutter. The tool tip will go all the way down to mill the surface off the stock geometry above the plane of non-cut zone while do path planning. Figure 3.3 shows the distributed ring path circles along 3D space and path layer distribution that is evenly across geometric body for planning operation. The dot is the ring origin of path planning start which is the initial location of ring path planning circle. The vertical lines represent path retraction in Figure3.3. Figure 3.4 shows the accumulated cutting depth of a stock and the geographical position of non-cutting zone of loading the ring model path

settings via target plane segmentation of Buzz model. The accumulated cutting depth of all layers are determined by the non-cutting plane location placed across the body of the geometric model.

3.2.1 Scale of Ring on Geometric 3D Pattern

The scale of ring is the foundation of scalable ring path planning as it determines the scalable region within interested area. As we scale the ring size of boundary cover set, the size of volume selection is also scaled for rendering operation of stock geometry.

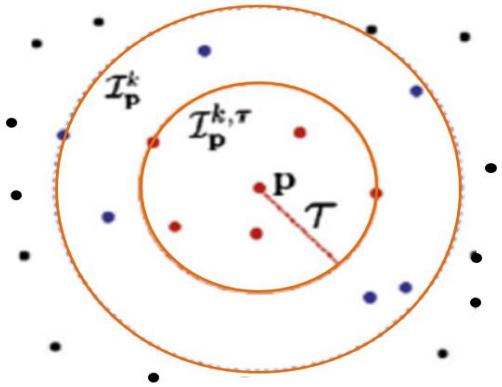

Figure 3.5 Distance of Ring Circle for K Nearest Neighbours

The scale of ring determines the distance of the k nearest neighbours around point p within boundary. The ring determines the geometric pattern within distance range. Figure 3.5 shows the distance relation of ring circle and scale as well as k neighbour vectors Ip with centre point p within a certain distance T. The implementation provides ring-based search. The points are classified into different color zones by distance.

3.2.2 Local vs. Global for Scalability of Path and Accessible Sequence

Local ring path is partial cover of the geometric model while global ring path is full cover of the geometric model within target zone above non-cutting plane. In our case, the local ring path can be viewed as volume with restriction and global ring path can be viewed as volume without restriction. Global ring path can be applied for automatic path generation without linear system concern of path retraction generation, and is used while the rotational movement is enabled for 5 axis tool path planning. In our simulation solution, we pick local ring path for linear system generation so that a path trajectory is linear for all 3-axis path movement to travel across its target region. Both local ring path and global ring path follow the search of nearest neighbour and selected end volume generation in 3D space, and will determine the size of input volume while computing the load and simulate graphical rendering of geometry. 3-axis path considers [x, y, z] coordinate vector for 3 dimensions in 3D space, it is given with linear movement as no rotational angle is given for tool freedom of motion. Assume a geometric surface is partitioned into multiple orientation zones that are accessible for tool movement, then the local ring gives volume restriction across these oriented zones for accessible space classification towards our end goal of generating a valid path orientation. The input cover set of local ring will lead to transformation of output cover set that is accessible within boundary based on our path searching algorithm.

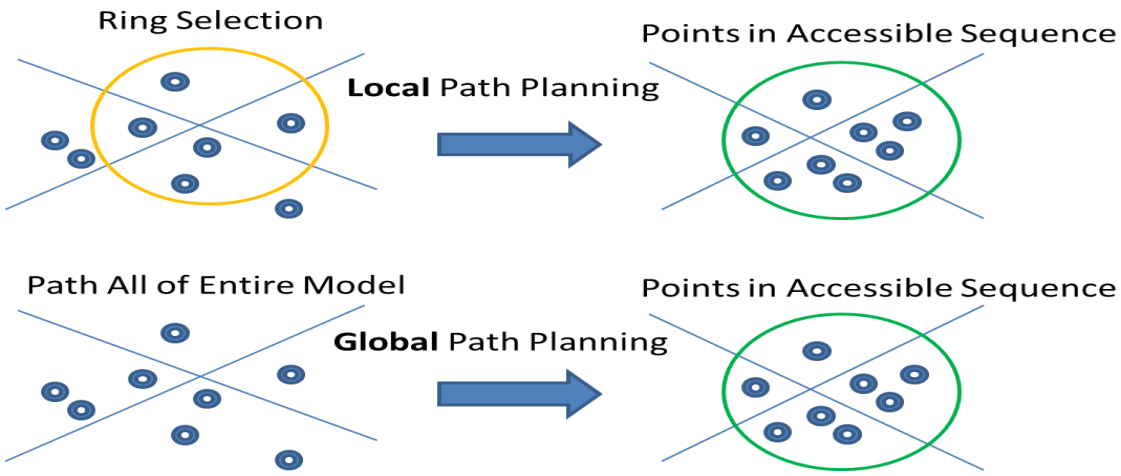

Figure 3.6 Local vs Global Ring for Accessible Sequence Mapping [69]

Figure 3.6 gives comparison view of ring scale of local vs. global while generating accessible sequence for classified points in 3D accessible space. The result will lead to path planning output as the accessible path will be updated based on ring selective searching and the input of the volume generation based on target ring path region. It is highly understandable that the global path has less user interaction as the path data collection are all picked as input of volume generation while local path considers more user decision while choosing a region within interest. Thus local path gives more flexibility while choosing path location while global path saves manual effort while automatically computing all path regions of entire geometric surface area. The domain of ring cover area can be viewed as sub-zone of a large data set mapped to small clusters. Each cluster can be viewed as domain specific solution of local ring so that the centered geometric area is highlighted for particular interest of path planning purpose. This gives benefit to ignore material waste of machining uncared region or an unsuitable region for machining due to whatever reasons, such as model geometry limitation of machining or machine axis limitation of operation range and freedom of motion. This applies

particularly for region of holes or patterns including complex geometry surface with non-symmetric design.

The control of the ring edge is based on feedback control law for boundary constraint restricted retraction while tuning ring path parameters based on major three feedback information: fabrication error, simulation pattern error, and retraction of path generation as we avoid retraction path in 3−axis with selected ring edge boundary in each local path iteration across the surface layer by layer.

3.2.3 Geometric Pattern Simulation

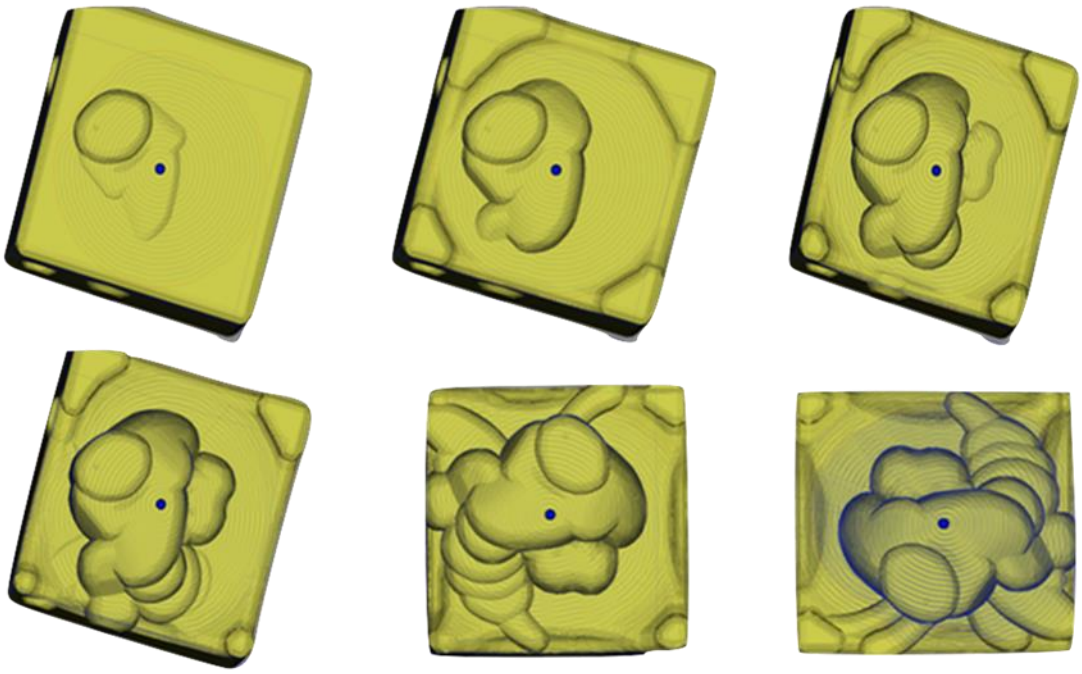

Figure 3.7 Iterative Ring Path for Accumulated Pattern Simulation [69]

The path pattern is highly defined by the geometric shape of STL input model. It is generated starting from the center of the ring. The path pattern of each ring path

iteration follows each layer removal by subtractive removal of layer by depth of stock surface. The iterative process of surface geometry pattern is determined by the size of ring selected for each local ring path while generating linear path in 3 axis movement. The accumulated target pattern should satisfy the end target that is aimed for machining operation for fabrication of subtractive 3D printing output. The variation of path pattern is highly determined by the variation size of ring cover as we simulate the cutting process step by step based on layer removal by depth. Figure 3.7 shows the demonstration of selected Buzz model for iterative process of path layer removal for pattern simulation. The ring step numbers are 21, 24, 27, 33, 34, 121 rings for each iteration due to its planned movement and 3D surface coverage.

3.2.4 Path Retraction and Jumps

Path retraction is what we want to limit in linear path planning. It happens when the orientation change is too large for the tool movement to stay in connected path loop. Path retraction will trigger tool tip movement off the surface of geometric stock and lead to more tool travel distance in space. Jumps of tool retraction gives orientation move from position to position while starting a different set of connected path points within the same region. A tool jump adjusts path orientation and gives more freedom of movement in 3D space as it provides angular variation that is usually nonlinear beyond linear 3 axis coordinate zone. In our simulation solution of step ring prediction, we aim to have no path retraction within selected ring cover region. The jumping condition can be roughly described by $\| p_I - p_k \| > A_i$, while p_I and p_k are normals of two contact points as the end of previous path sequence and the start of the next path sequence. A_i is the threshold

condition that determines a jumping condition within orientation variation limit of tool movement.

3.3 Ring Numerical Prediction of Graphical Models

3.3.1 Pattern based Ring Prediction Algorithm for Layer based Path Planning

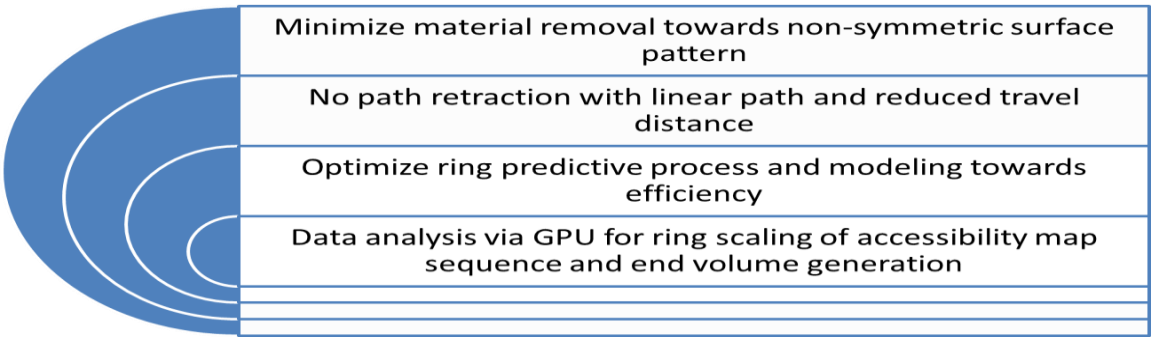

Figure 3.8 Objective of Ring Predictive Path Planning

The objective of Step Ring Predictive Path Planning can be shown in Figure 3.8. The key ring variables are selected including layer depth, step over distance of ring circle, and the number of ring circles. Figure 3.9 shows the impact of parameter for geometric pattern.

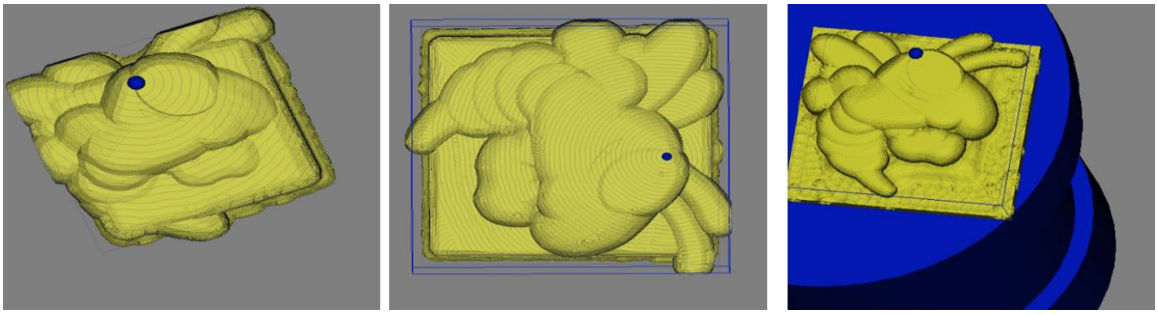

Figure 3.9 Ring Path Parameter of Step Distance, Max Cutting Depth--1 mm, 1mm; 1mm, 2mm; 0.5mm, 1mm

The scale of ring is the foundation of scalable ring path planning as it determines the scalable region within area of interest. The scale defines the boundary of region as path planning target. Given a design stock, the optimization of linear ring path planning region matching the peak pattern is defined as the maximum peak of matched pattern with height of selected area Sp:

$$S_p = \mathrm{MAX}(\eta_P) \tag{3.1}$$

Equation 3.1 shows Sp definition. Selected area S_p is subject to constraints $g_i(x) \leq R, h_i(x) \leq R, Z_i(x) \leq d$ in 3D space.

It is a function of three variables for parameter turning of path towards path efficiency and optimization of user decision. The Input of ring path is the region of target pattern for volume removal of accumulated pattern simulation. An optimal path satisfies the storage limit of physical CNC machine in fabrication and user selection of model sizing and orientation as well as the volume density due to geometric resolution and path variables. The process of parameter turning can be described in Figure 3.10 as a Blackbox system. The major inputs of layer depth, step distance and ring number for bounded region are key parameters of path planning simulation. The ring path defines the search boundary of target for pattern selection purpose as well as geometry resolution towards path planning solution. Accessible sequence formulates after ring path planning simulation while generating volume rendering for comparison. G-code path is the output of the path planning result after transferring the path data by geometry relation in physical space. G-code runs on CNC machine as user programming code for intelligent control purpose for machining operation to create path planning target.

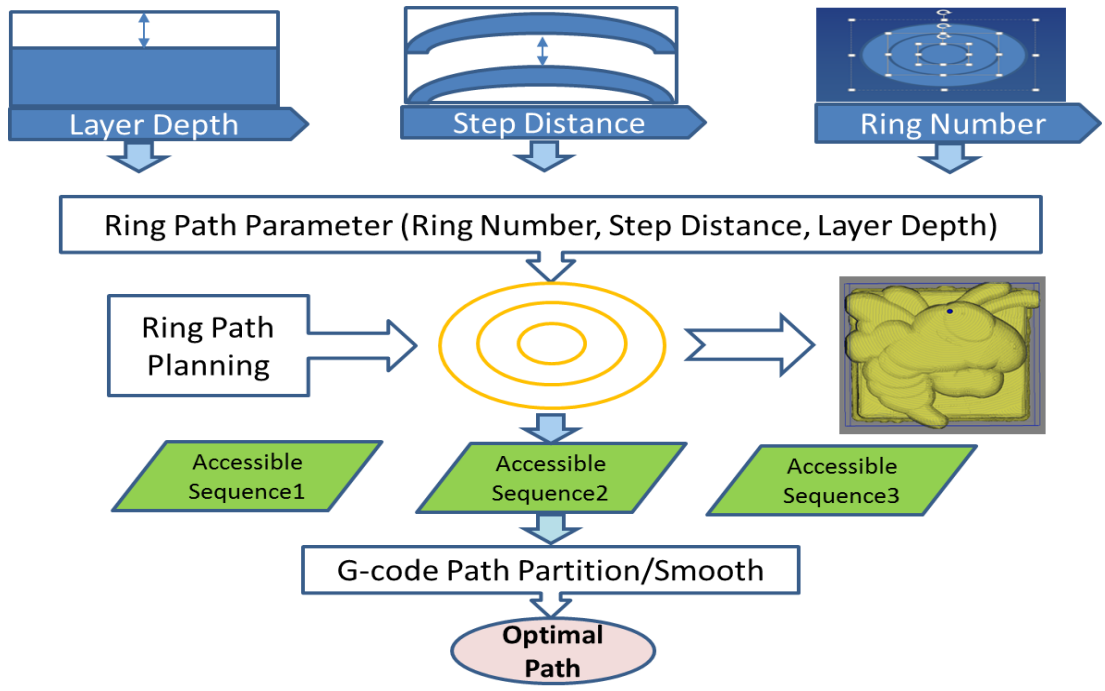

Figure 3.10 Blackbox Ring Path Simulation Parameters and Data Flow

The ring local path for benefit of complex geometry planning is in Figure 3.11. The model of Kingkong is used as input of ring path planning target. The region of ear is local compared to the body as global. For local path area such as the ear, the ring covers

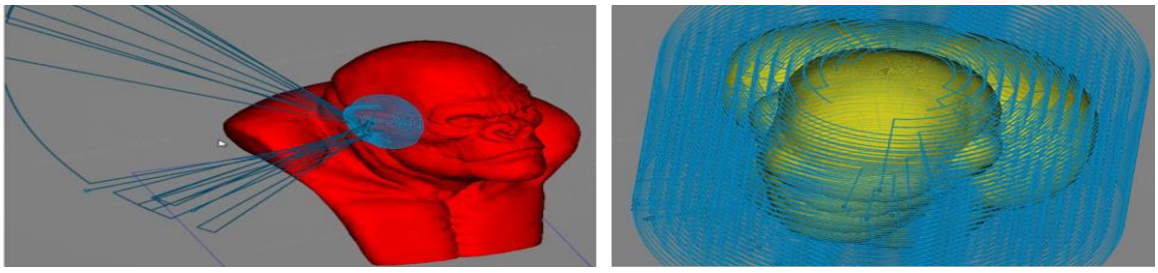

Figure 3.11 Local Ring Path for Partial Travel compared to Global Ring

smaller area of region for path planning operation, while for global path area of the body, the ring covers entire body as path planning region. The global path is rough compared to the local path regarding refined details for high geometry resolution.

Pattern-based Ring Prediction Algorithm for scalable path planning is described as Algorithm 1. The input parameters of ring are step distance, ring steps, subtractive layer depth for cutting path. We consider feedback condition as no path retraction of each layer of ring cover to control the ring edge. The entire problem is viewed as path optimization of local linear path of 3 axis.

Algorithm 1 Ring Prediction Algorithm

Algorithm 1 Ring Prediction by path parameters

1: **procedure** RingNum (step distance g, layer depth d)

2: make rough initial guess of ring number r

3: **for** each ring iteration do

4: Increase ring number of circle by c

5: Edge← GrowRingBounds (c, r)

6**:** **if** Edge triggers path retraction (simulation feedback & fabrication feedback)

7: Decrease c'=c-1 until no retraction and keep c'>=0

8: **else**

9: set state of r'=r+c' as new ring number

3.3.2 *Image Reconstruction based Model Fitting and Path Validation for Sustainability*

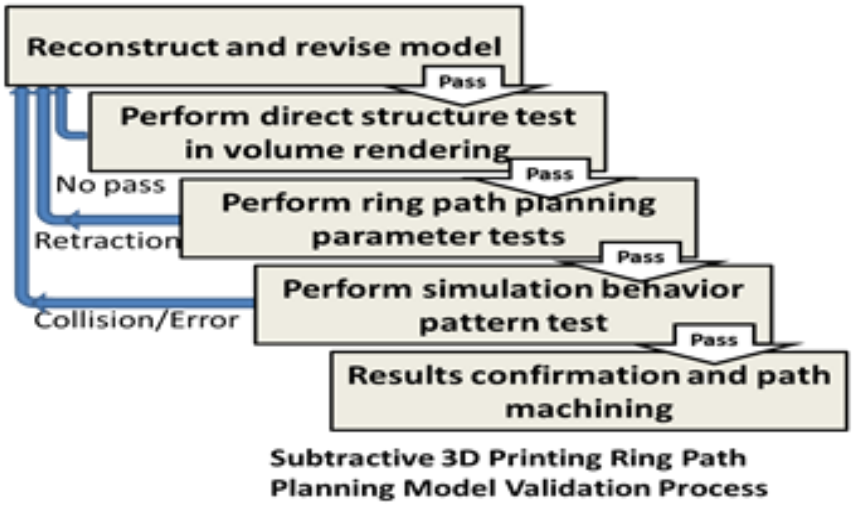

Figure 3.12 Model Validation Process for Subtractive 3D Printing [69]

For system accuracy, we need model validation for path. The model validation process is done based on reverse engineering for mapping of system accuracy of reconstructed model between simulation and fabrication. Figure 3.12 shows the sustainable process of information-based feedback control. There are feedbacks from both simulation and fabrication results to double-proof the system accuracy of simulation software based on geometric selection. There are three feedbacks for information of

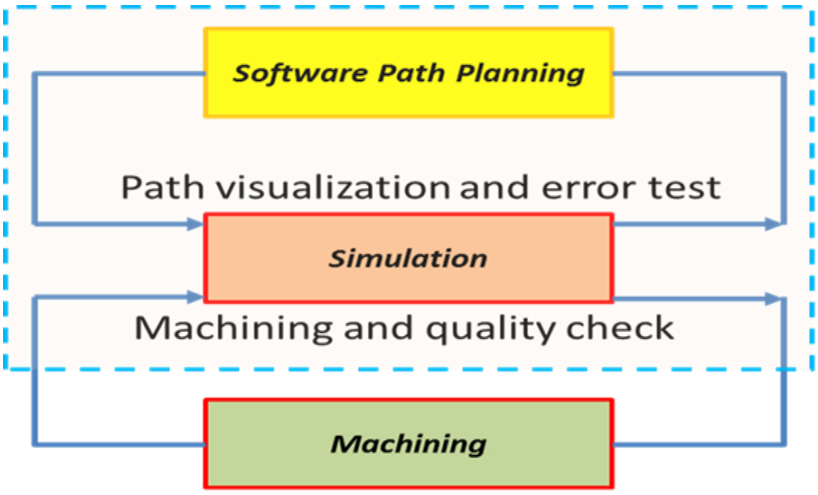

Figure 3.13 Double Feedback Loop [69]

resulting difference compared with reference target for accuracy of parameter tuning based on each planning process. Figure 3.13 describes the feedback control process as we tune the parameter of model and path variables for double-feedback information for quality check based on simulation result of input model.

3.3.3 Grid Analysis for Model Fitting and Topology Structure Analysis

Figure 3.14 shows the STL model and its no-cutting plane of path for 3D

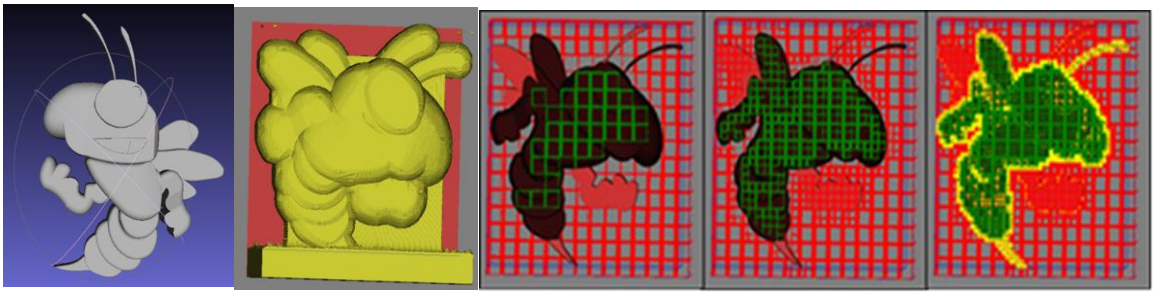

Figure 3.14 Reconstructed Model and Grid Classification Image [69]

simulation. Adaptive Grid gives topology classification for model structure analysis. We also adjust parameters of orientation, scale, position in 3D space for model fitting purpose, so that we can do model rescaling based on reverse engineering for model reconstruction and path planning accuracy of the system. The decision variables of model fitting based on image reconstruction are model orientation, decomposition ratio and 3D position, while feedback variables of path planning are pattern resolution, path sensitivity, geometric deformation, simulation path retraction as well as path collision. In numerical perspective, the distance of grid depends on the grid resolution while geometric pattern is measured and recognized by shape intersection with grid lines. In addition, color grid in adaptive HDT depth highlights image classification view of model geometric topology in 3D visualization.

3.3.4 Graphical Simulation Result of Model Visualization vs. Machine Platform

The simulation results include generated path visualization of each path iteration, volume rendering output of simulated geometry stock surface, and final fabrication product. The results show ***3D material and path simulation by graphics rendering.*** The 3D scallop simulation results show simulations by proper selection match actual machining output. The simulation of each path iteration is based on the cutting depth preselected to demonstrate the accumulated path iterations, simulated 3D visualization of model geometry and actual machining product. Figure 3.15 shows the mapping of three for Buzz model and is what we pick software simulation to aim for so that any design model and path planning accuracy can be visualized ahead of time in virtual environment simulation before physical platform operation. Thus we can save time and cost of material waste for precision machining based on accurate planning path to avoid error

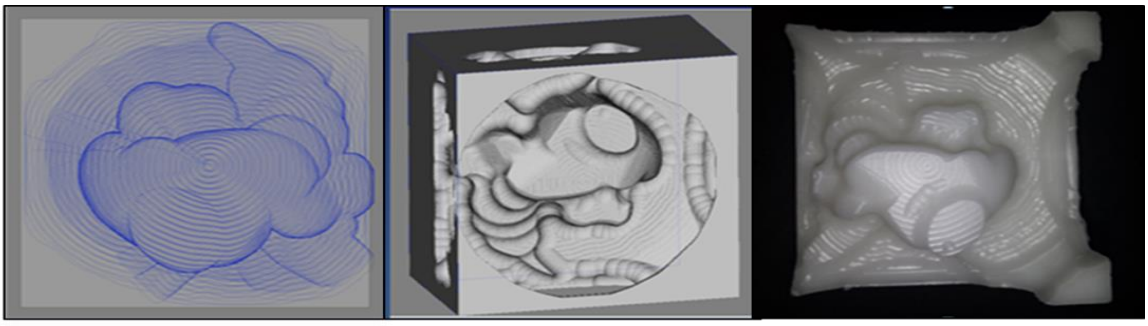

Figure 3.15 Ring Prediction Path Simulation [69]

waste and fabrication deformation to guarantee the quality of product. The results validate virtual path simulation as software design application need precision check from function design for validation.

The rendering could also be applied for entire machining frame of the CNC platform for motion simulation of tool path. Figure 3.16 also shows the subtractive 3D printing visualization results of graphical motion rendering for machine path simulation compared with real Okuma machine.

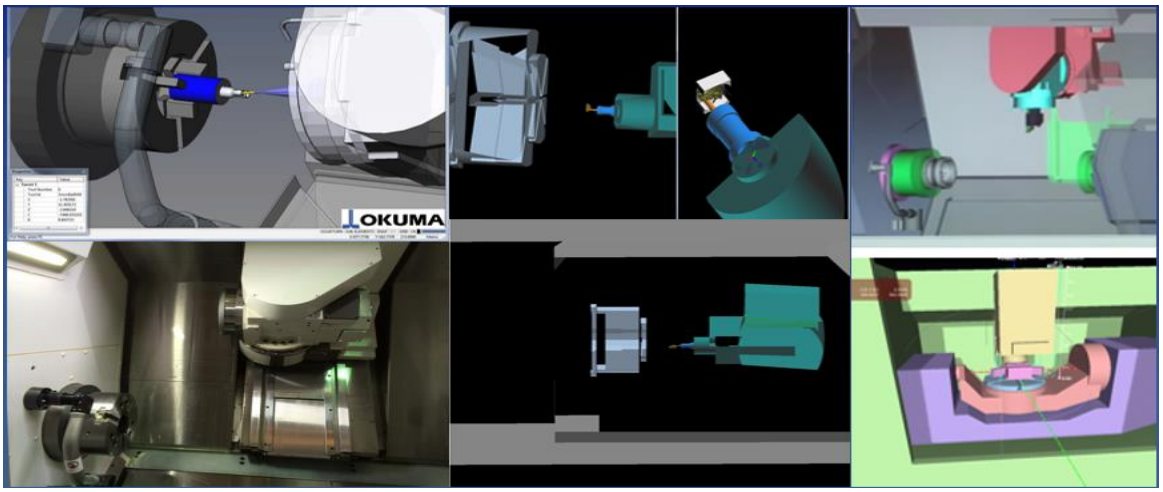

Figure 3.16 Path Simulation and Volume Rendering matching Fabrication

3.4 Post-processing towards Adaptive Filter for G-code Optimization

3.4.1 Graph Partition via Adaptive Filter for Path Division

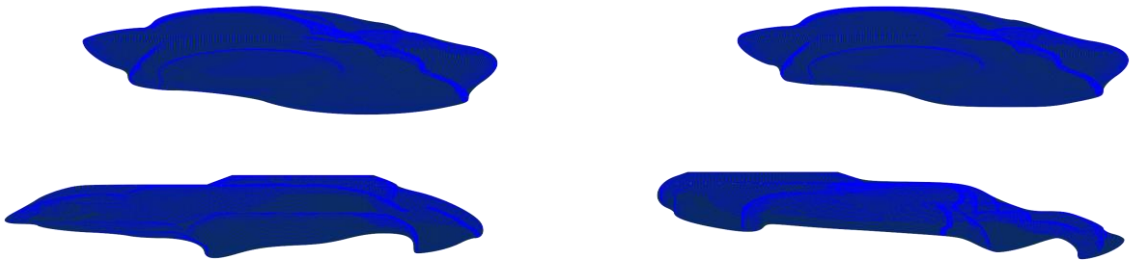

Figure 3.17 First Division G-code Simulation of Buzz [69]

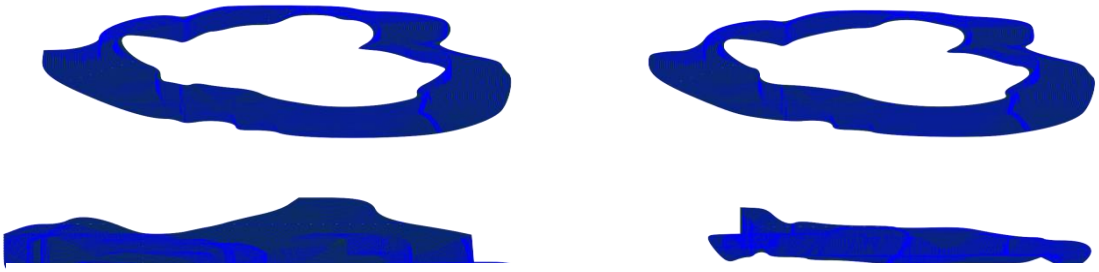

Figure 3.18 Second Division G-code Simulation of Buzz [69]

A scalable path helps reduce file storage within limit. The G-code optimization challenges are segmental graph partition and motion data compression towards scalability. Path partition by adaptive filter can attain load distribution with any flexible ratio. Figure 3.17 and Figure 3.18 show the output G-code graph after partition as first and second division of path of Buzz model machining. Storage limit and graph topology may be two direct benefits of this partition effort.

Partitioned G-code simply has fewer processing lines, therefore partition manage to reduce the limit required for storage processing purpose on CNC machine, especially old CNC machine style with limited storage space. Partition of G-code also helps to reduce orientation limit beyond machine operation zone, such that we could reorient a path simply by reposition of the stock geometry and mapping to the new G-code line for a better graph orientation to keep path topology information complete.

3.4.2 Motion Data Compression

Due to sampling reason, high resolution data points may not reflect enough orientation variation for G-code produced from the path sampling from geometry volume. As some feature points along the path simply do not reflect any orientation move simply,

it is merely for geometry resolution purpose. We want to remove the raw data G-code, not only because of its time consumption for handling large volume geometry workload output, but also because of saving of storage space especially for large processing sequences of data when the scale becomes significant. Only path points reflect with orientation change of tool position need to be kept for path G-code route. By data compression, we remove most redundant points due to resolution of geometry generation, and keep only the critical information of G-code for orientation change. This way, we could attain G-code with better smoothing route as well as raw data compression as no information of route path is lost during the process. The end goal is to remove redundant data information non-relevant to the motion. Data compression saves up to 30% storage limit in our results.

3.4.3 G-Code Optimization Algorithm

G-code is the numerical control programming language that runs and control CNC (Computerized Numerical Control) machining operation. G-code path optimization challenges include segmental graph partition and motion data compression towards scalability. A scalable path helps reduce file storage within limit. Path partition by adaptive filter can attain load distribution with any flexible ratio. Data compression saves up to 30% storage limit in our results. The combined solution for optimization could solve adaptive ratio partition of G-code such that it works in a controllable scale.

Though G-code works on CNC machine, the path planning component through simulation gives rough G-code before the optimization process. We first apply data partition then apply motion data compression just for G-code refinement. We combine

path points on the same orientation that appear on repeated position as redundancy at

Algorithm 2 Adaptive Filter of G-code Optimization

1: **procedure** Partition (N (G-code line), S (storage))

2: ***Task1*** (Adaptive Filter): N=total G-code Line

3: Initialize ND=1

4: Ni=N/ND (Division Ratio),

3**:** **while** Ni > S as Storage Boundary

4: ND' =ND*2 for one division

5: Update Ni'=N/ND'

6: **if** Ni'<S,

7: return Ni' as individual lines

8: **else** ND'=ND*2 **continue**

9: ***Task2*** G-code Compression (G1, G2). G1, G2 are consecutive G-code lines

10: **for** i←1 to max_G1-1 do

11: **If** G1 line == G2 line for point direction

12: Insert G3 line ← combine G1 line step with G2 line step

13: Delete G1, G2 line

14: **else** keep G1, G2 as consecutive lines

different time scale. After G-code optimization, we aim to attain path scalability across machine orientation space and geometry feature space. The refined G-code may have no redundancy of data or less redundancy of data.

Overall, the implemented solution for G-code optimization include the adaptive filter for path division and data compression for removing path redundancy, which are shown in Algorithm 2. The post-processing algorithms of G-code optimization include tasks of path partition filter and data compression.

CHAPTER 4. EXPERIMENT ON OPTIMAL REGION DETERMINATION FOR STRATEGIC PATH PLANNING

This chapter discusses the simulation and control strategy in optimal path planning. The analysis approach focuses in morphological region analysis and list examples of geometry path planning strategies from the basic geometry component by region. Sensitivity analysis gives the foundation of control stability of path. Protection strategy of path by tolerance and control component is described at the end from system perspective to highlight the big picture.

4.1 3D Morphological Filtering by Optimal Region

4.1.1 2D Multi-Region Perspective for 3D Model

Figure 4.1 3D Multi-Pattern Combined Black-Painted Egyptian Model

Figure 4.1 is a tested 3D printing product of existing 3D model [1], and it is rebuilt through subtractive 3D printing machining process. It shows that one 3D model sometimes could be combined by multiple small 3D models of different patterns, such as teapot, dragon, Egyptian Ladies together are all components of 2D regions embedded on the same 3D surface. Therefore, multiple 2D regions are actually considered while formulating a hybrid model.

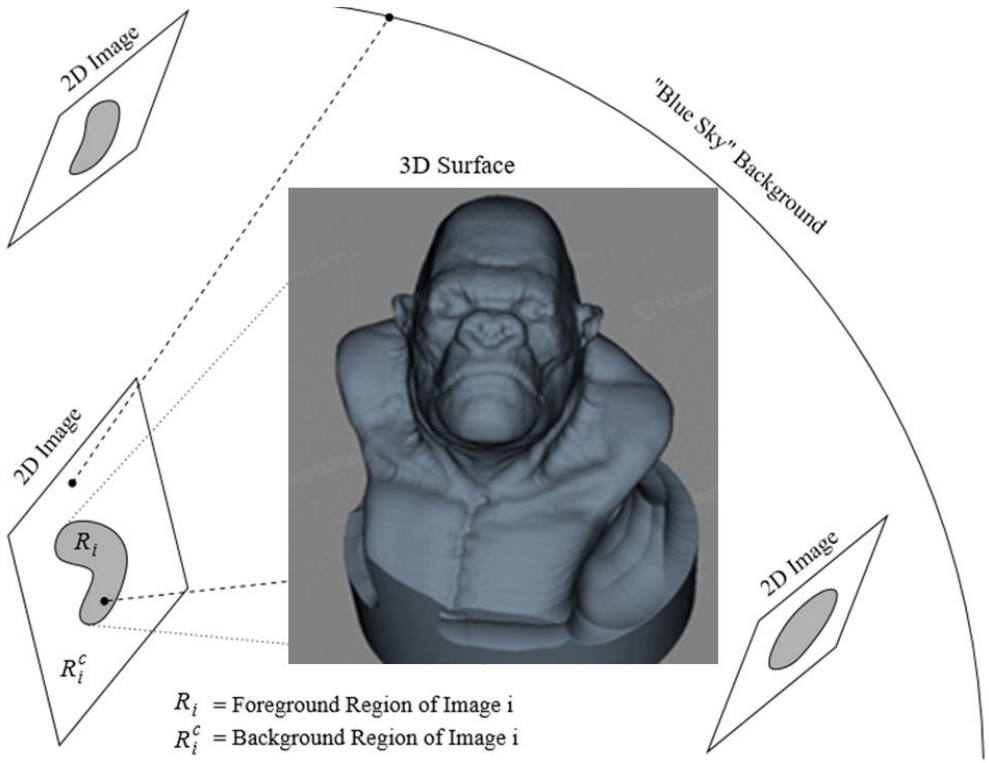

Figure 4.2 3D King Kong Model into 2D Region

For one complete 3D model of complex shape and geometry, it could be viewed from multiple perspectives for understanding details from different orientations by taking regional photos as 2D images. Ideally, a 3D object can be viewed from multiple orientations to give 2D perspective plane for intersection image of 2D region reflecting

its orientation surface. Using these 2D images, 3D model could be reconstructed by image features and orientation angles of image intersection planes. The 2D perspective of 3D oriented region then gives a 2D mapping chart based on the original 3D object which can be recovered from shape information of a certain orientation plane. Figure 4.2 is the illustration of 3D model KingKong into multiple 2D perspective regions by different oriented planes.

4.1.2 Morphological Filtering for Image Segmentation Region

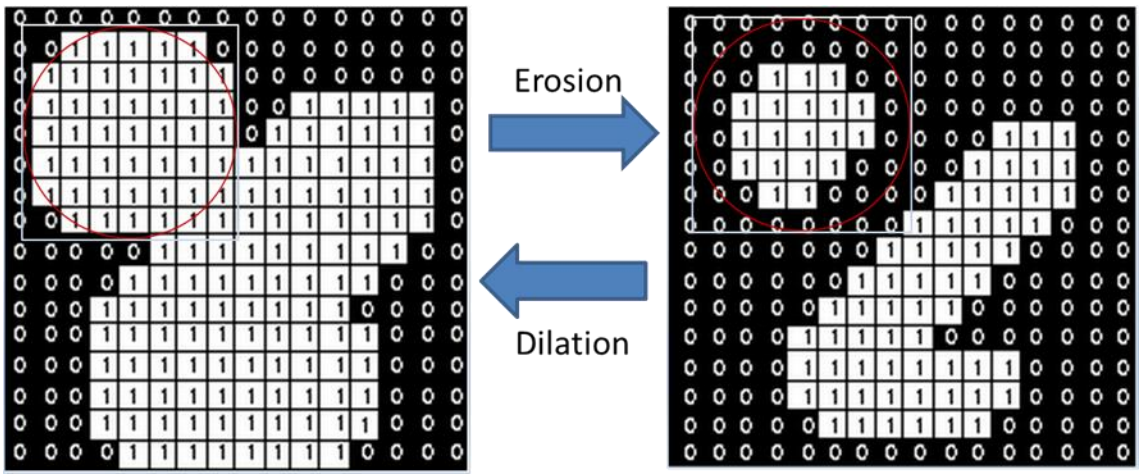

Figure 4.3 2D Region Segmentation by Erosion and Merging by Dilation

Morphological filtering gives erosion and dilation as duplex operation of the original shape. Erosion may help segmentation of the region for the obvious local structure feature part away from global connected region with general outline structure. Dilation may reverse exact behavior of the erosion process due to its duplex attribute for operation of erosion. Thus, once an object shape is segmented by erosion of 2D model it can be reconsidered together to its original shape. Figure 4.3 shows how a 2D region get

segmented when erosion happens and dilation reverse and merges the segmented area to the original complete body.

4.1.3 Morphological 3D Decomposition of Local Geometry Region

Morphological decompositions are geometry representation of object into components. The rule of morphological decomposition follows:

An element S decomposes into several smaller ones:

$$S = H1 \oplus H2 \oplus H3 \oplus ... \oplus HN \tag{4.1}$$

Equation 4.1 shows the decomposition of S by morphological operation. The reverse process as combination of components by union or path merging. For accumulated path we look at the reverse process merging local optimal region. The steps towards optimal path based on morphological decomposition may include: Figure 4.4 shows example of 3D KingKong model into 3D decomposed component as cylinder and facial globe component so that both components have their own orientation planes for path planning.

We decompose geometry into simple component for optimal region.

- Path planning for each component geometry pattern
- Merge local optimal region as accumulated path
- Kernel size of filter is critical in partition – determine optimal sizing K
- Look at Trade-off between speed and quality for path region benefit

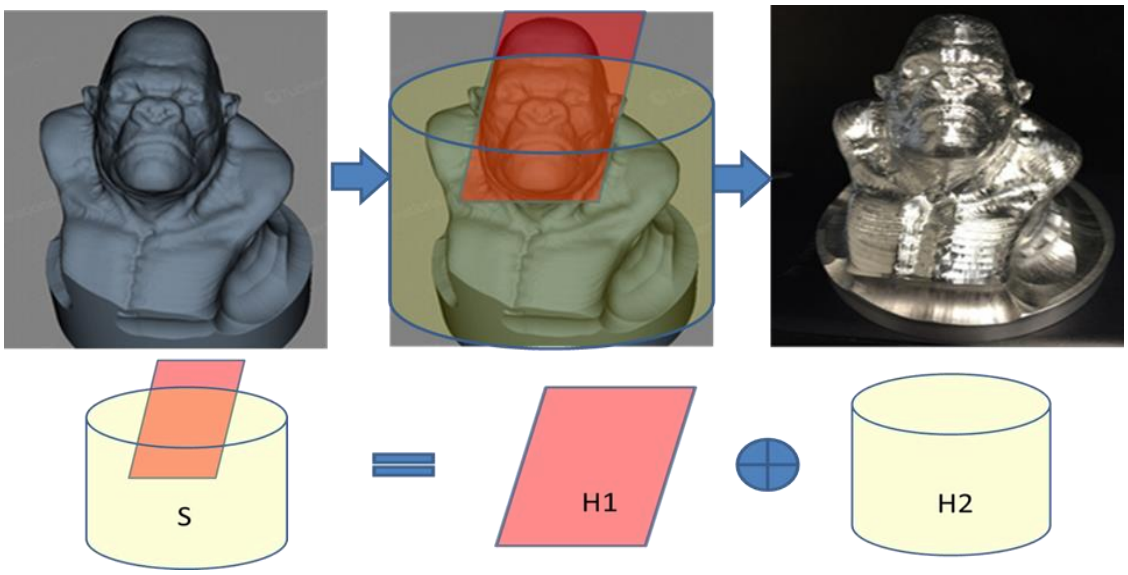

Figure 4.4 King Kong Decomposition into Simple Geometric Component

4.1.4 The rule of Morphological Decomposition for Optimal Region

The Rule of merging operation is based on union of optimal region of decomposed geometry objects, take A,B for example:

$$P(A \cup B)=P(A)+P(B) \text{ if } P(A) \cap P(B)=0 \quad (4.2)$$

Equation 4.2 shows the merging relation of union operation between two regions of A and B. A and B are separate elements of region without intersection. Figure 4.5 shows A as the Head Model and B as the Cubic Model of Stock. The Union operation of these two becomes the final intersected object. The object merging output can be displayed also using cylindrical stock given bounded area of the geometry target path planning region.

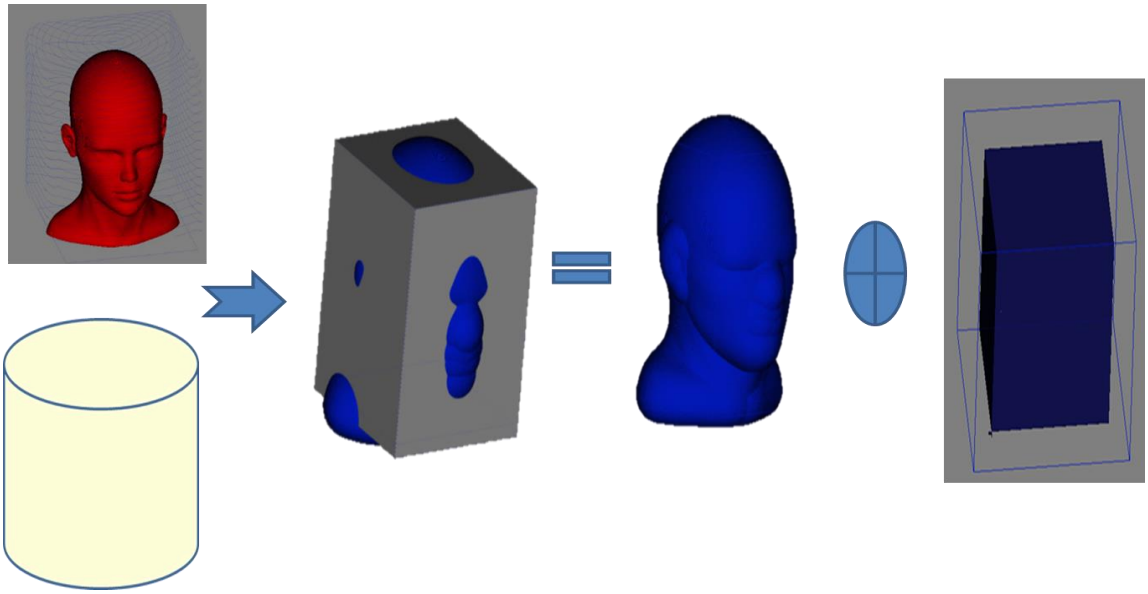

Figure 4.5 Model Morphological Decomposition and Merging

4.2 Path Planning Examples on Optimal Region

4.2.1 Comparison of Geometry Model Path Planning Region

Local ring path refines geometry feature into finishing path based on roughing path operation for fast processing of contour information to get general shape of objects. We have three examples for comparison:

- King Kong Model – two morphological regions
- Draft Model – symmetric region
- Fan Model – roughing & finishing region

Figure 4.6 shows the path planning steps of two different regions of 3D KingKong Model. The entire model is decomposed into face region and body region for

path planning purpose, as face requires more refined path planning strategy while body is fairly symmetric compared to single face target.

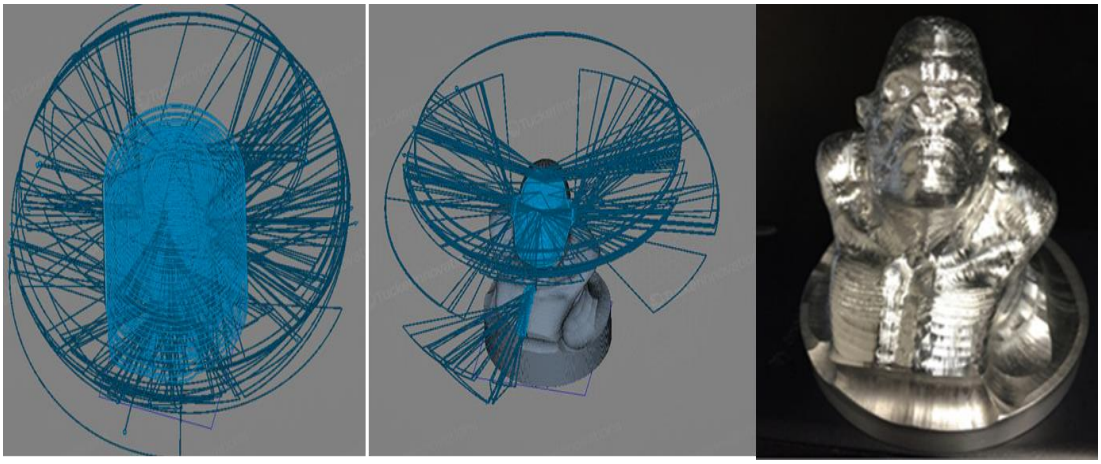

Figure 4.6 King Kong Path Planning Region of Two Areas

Figure 4.7 and Figure 4.8 show the other two model path planning region. Figure 4.7 is the Draft model as it has one symmetrical center which is picked as origin of the ring path. Figure 4.8 has Fan region as symmetric geometry region and body cylinder as another symmetric region, therefore the path planning has two regions for consideration for region-based path decomposition.

These Figures are used to demonstrate path decomposition feasibility for composing a large complex geometry design. Sometimes, in order to have multiple regions of geometry details machined with accuracy, we need to take different approaches of smart path planning strategy for each region compared to machining the entire geometry object. For symmetric object, we could take identical pattern out for path planning and then repeat the pattern with different orientations. For example, we could consider Fan tip with one orientation for path planning and repeat the same strategy for

the rest of the Fan tips, or we could choose all Fan tips together as one complex 3D model for target of path planning. One Fan tip is considered local compared to all Fan tips together from multiple orientations as one global target model.

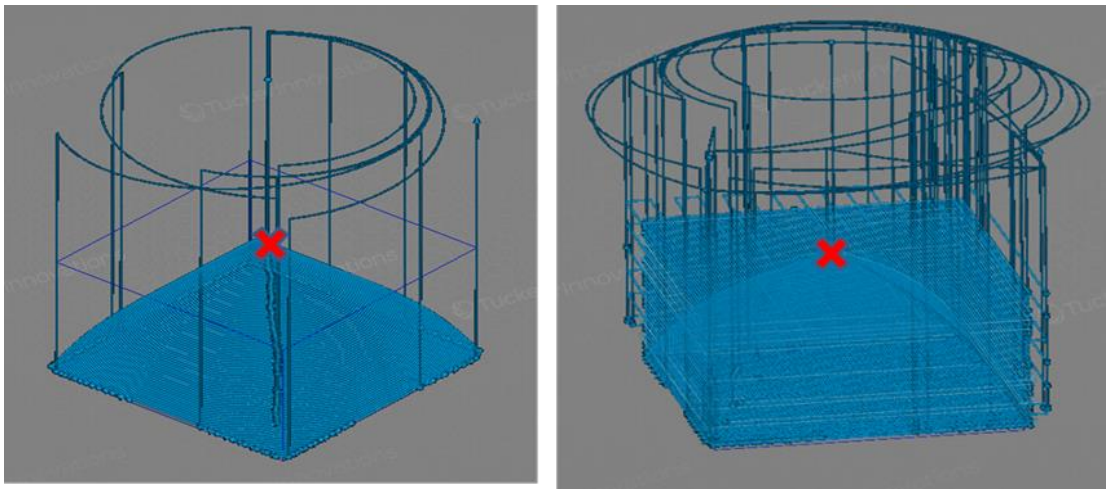

Figure 4.7 Draft Model Ring Path Region of Multi-Layer Sub-Plane

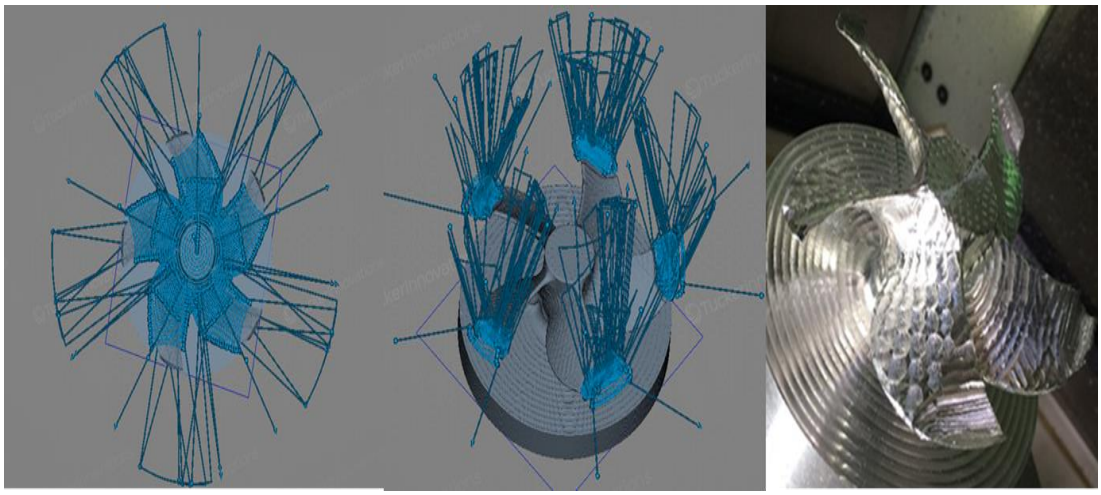

Figure 4.8 Fan Model Region of Ring Path of Symmetric Region

Complexity of path decomposition is determined by the object it uses to partition the region, as we normally pick reference of simple geometry component for non-

symmetric 3D geometry surface, shape dependent path, morphological filter decomposition.

4.2.2 Tool Path Motion Pattern of 1, 2, 3 D Cases between Ring and Other Path Types

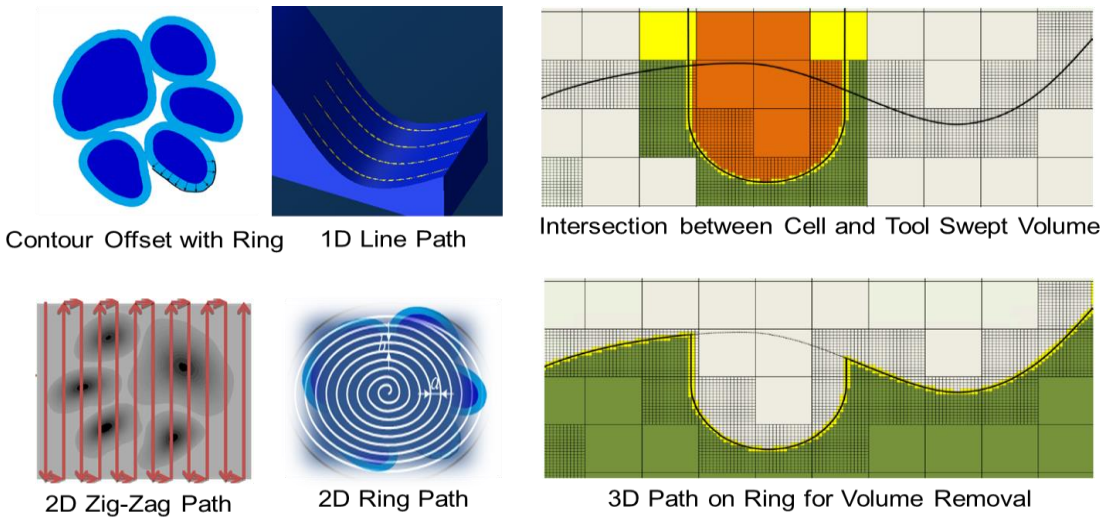

Figure 4.9 Path Planning Pattern Examples

Figure 4.9 shows the 1D, 2D, and 3D comparison of selected path planning patterns based on its feature characteristics. 1D path pattern comes from GibbsCAM software demo version while illustrating the simplest path of line wave form in parallel as path trajectory curve. 2D pattern shown in Figure 4.8 is general zigzag path that integrates with tiger paw pattern. The 3D path pattern illustrates how the applied ring path planning works with adaptive resolution for path trajectory, particularly in volume offsetting of target surface intersection with tool cutter for material removal simulation. For the path planning of tool tip movement, the example of path planning pattern includes 1D path of line movement from same direction, 2D zig-zag movement path and 3D ring spiral path which is the tested ring path planning solution. The intersection

between tool tip and surface offsetting area within ring-bounded zone becomes the material removal area as layers of path get removed during surface intersection with machine tool tip.

4.2.3 3D Sequence, Contact of Point, and Volume Geometry of 3D Candle Holder

Figure 4.10 shows the serial of planning steps for illustration while generating results of 3D path. It has four basic steps for model representation of feature characteristics including ring path in 3D accessible space, 2D sequence generation for accessible orientation, contact points generation of 2D sequences and volume generation for 3D geometry representation. These steps make the geometry model better represented and become feasible as path simulation data in a subtractive way in volume removal process for material cut off simulation.

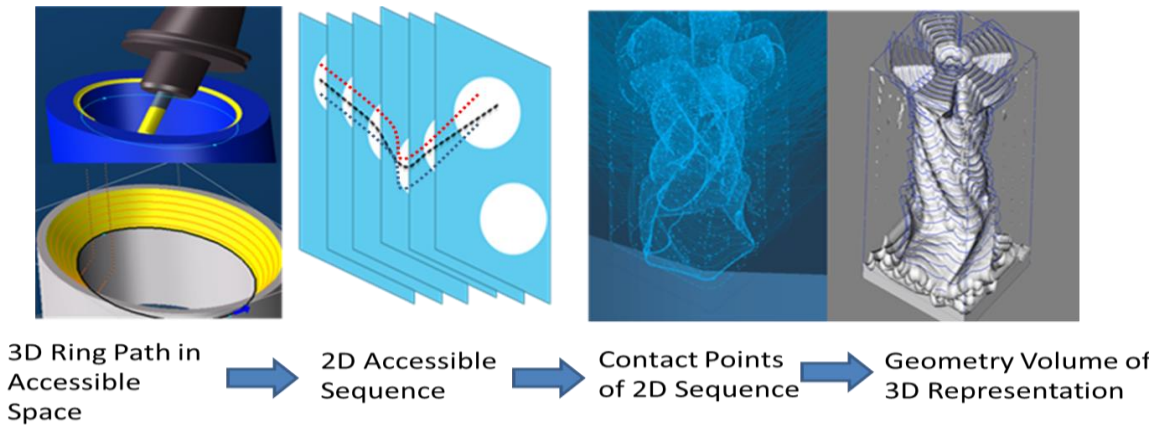

Figure 4.10 Candle Holder Path Sequence into 3D Volume Removal

4.3 Merging Accuracy of Morphological Region by HDT Grid

4.3.1 Morphological Element Sizing

"s1 and s2 are a pair of structuring elements identical in shape, with s2 twice the size of s1, then

$$f \ominus s2 \approx (f \ominus s1) \ominus s1 \tag{4.3}$$

If we have Sd =d *S1, then

$$F \ominus Sd = (f \ominus S1) \ldots \ominus S1, \text{ d times operation of s1} \tag{4.4}$$

Then the accuracy of final morphological accuracy depends on the resolution of data which is determined by data structure of end grid resolution of Hybrid Dynamic Tree structure.

4.3.2 Morphological Step Determination

- Level of Morphological Depth is based on previous level of details
- Therefore the accuracy of morphological body becomes the depth of HDT branch level, assuming level of merging is D
- HDT Tree branch level is based on the data structure and branching factor.
- Resolution level determine the details of morphological steps

4.3.3 Morphological Filtering and Accuracy by HDT Grid Data Structure

Storage for morphological level by ring boundary-based searching include: data storage by sequence of volume, topology geometry region decomposition and geometry resolution precision. How an end voxel is decomposed into satisfied resolution is determined by the Hybrid Dynamic Tree (HDT) data structure. The end of HDT is

branched into multi-level grid with adaptive depth input of tree branches. The level of tree branch depth D is impacted by the grid resolution given its level of branching distance from the root of the tree. Figure 4.11 shows the illustration graph for end voxel resolution accuracy by one branch decomposition of HDT.

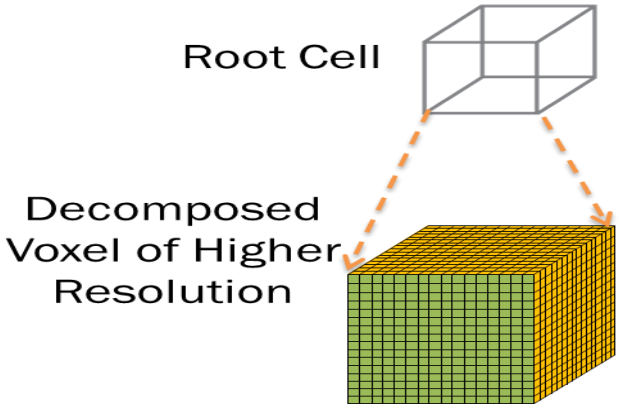

Figure 4.11 End Volume Resolution by Voxel Accuracy at One Branch Decomposition

The morphological filter resolution of 2D region for 3D model is determined also by the 3D grid resolution for its end leaf pixel of intersection with geometry surface contour and thus also affected by the branch level depth D. Adaptive grid based on HDT is given by adaptive D of tree branching distance level, therefore gives more refinement of data resolution towards higher precision. Figure 4.12 is a self-drawn HDT of simple shape with resolution and tree depth, and it gives an interpretation of why deeper branch level depth D will make the data resolution more accurate.

The reason why we involve branch number analysis in our simulation of path sequence output is due to the role of branch in HDT structure. As for branch relation with

grid resolution, the branch of tree helps distribution of data across 3D space and determines the searching speed of path regarding a certain feature.

The branch distribution of HDT affects the topology of tree and the structure of

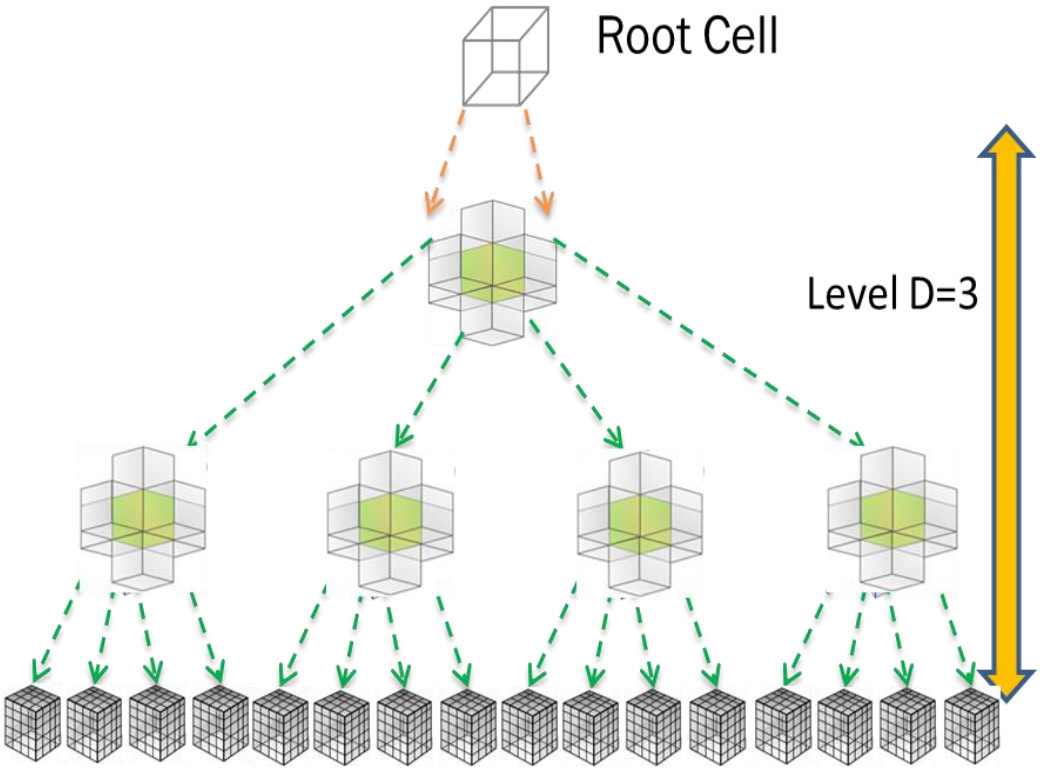

Figure 4.12 Branch Distribution in HDT Data Structure for Grid Resolution of Morphological Filter

grid. The grid resolution therefore can be calculated based on its branching depth distance level D. The partition of the grid is based on the tree branching depth level, the D determines the depth of the tree branch also the resolution dependent on it.

The grid is partitioned highly by the cell of grid resolution sizes into adaptive resolution of the path that is represented by volume geometry. The end resolution of smallest unit is assigned by user through interactive path parameters. Reasonable

parameter setting determines the volume computation time and accuracy as well as path redundancy that whether we have enough information to meet model resolution requirement. The resolution of grid determines the visual perception of 3D quality as well as real time performance of simulation of path motion. The grid thus become 3D foundation of geometric mapping of target. The graphical part is not the focus of the thesis work, so we skip the complexity diagnosis and keep the basic introduction of grid and tree branching due to analysis perspective for understanding of the data structure to support grid level structure as the 3D unit of volumetric analysis.

4.3.4 Grid Modelling for Geometry Region Segmentation

Figure 4.13 shows how an adaptive grid model with HDT depth help partition a color region by image segmentation for different geometry shape. Based on the grid structure of 3D model, we keep changing the depth of HDT tree input and can get color segmentation of 2D image data based on its perspective plane. The classified color of the image segmentation area gives hint of internal area of geometry location. As the grid is adaptive into more depth as previous analysis of higher tree branching level, the grid measurement for resolution is also more refined.

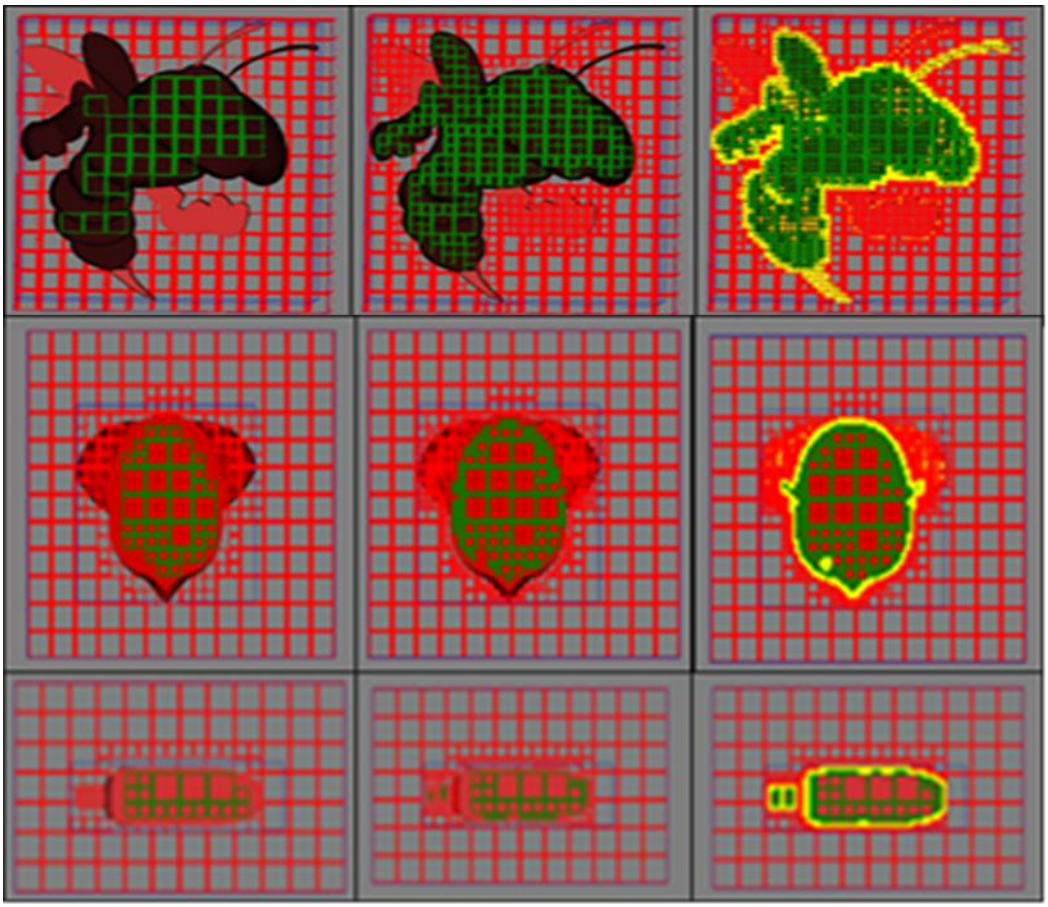

Figure 4.13 Grid Modeling for Buzz and Head Geometry Region Segmentation [69]

Buzz and Head model is used as illustration of geometry comparison. The original models of Buzz and Head are shown by Figure 4.14. The automatic recognition of a geometry model based on grid intersection usually applies to computer vision and machine learning operation for automatic sensing and object condition diagnosis. Different geometries may have unique patterns of path and also geometric 2D image intersection contour based on its original feature. The automatic detection for object recognition based on geometry feature comes from the grid intersection pattern and its contour information.


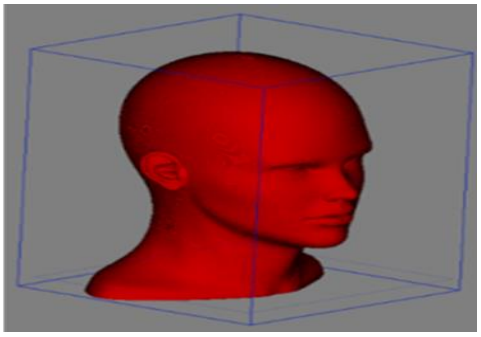

Figure 4.14 Buzz and Head 3D Geometry Model

Basically, a 3D grid gives the following benefits:

- 3D Grid Intersection Based on Adaptive Tree Depth for Model Topology Classification – such as Buzz, Head Demo
- Grid Modeling for Model Recognition (measurement of geometry size and shape)

4.4 Optimal Region Determination

To sum up, besides morphological filter and grid segmentation, optimal region is determined based on the description of the flowing sections.

4.4.1 Offset Distance Tolerance Zone

Due to different offset distance around tolerance zone, we have to determine optimal various regions. First, we define region by non-uniform offset and tolerance zone, Secondly, each region has a different offset distance of cutting depth. In addition, subset plane defines partition domain of region.

Figure 4.15 shows the region-based tolerance zones by varying offset distances. Different tolerance zone by surface distribution gives flexibility of surface path of various resolution. Tolerance zone defines its own path planning requirement of local region so that various requirements can be met. Tolerance zone works for bounded control of path planning with constraints.

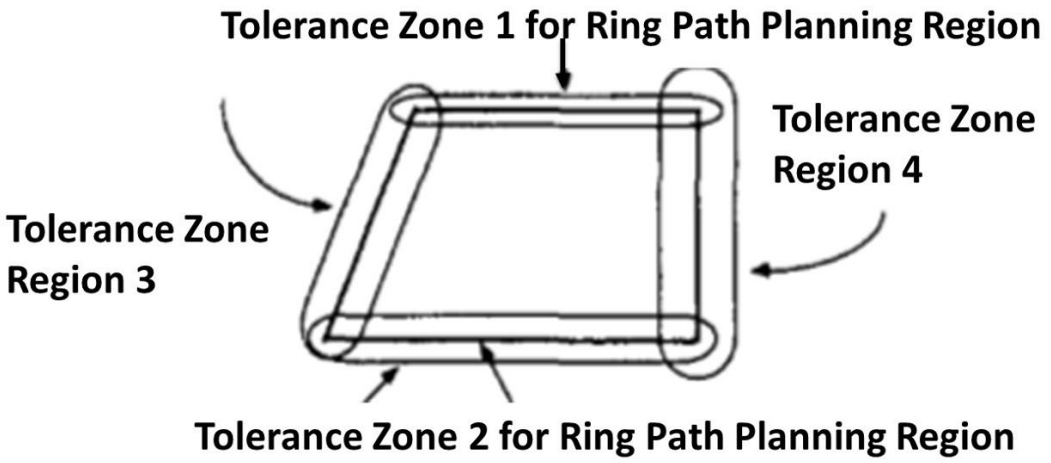

Figure 4.15 Multiple Tolerance Zone for Ring Path Planning Region

4.4.2 Ring Center-based Pattern

To put together different pattern on a same object, we reoriented the surface while machining, and path planning the surface along different orientation with different ring centre, each ring could have its own pattern of geometry path.

Figure 4.16 shows the idea illustration in volume simulation with two patterns. The point is to divide orientation into optimal zones. When we have local solution of different path regions, we have oriented pattern of difference location for path planning. The pattern represents local area of interest that is within target region. Multiple patterns

on various orientation surfaces can be put on local optimal regions with boundary for Ring Path Planning so that we have entire global solution decomposed into these local path solutions.

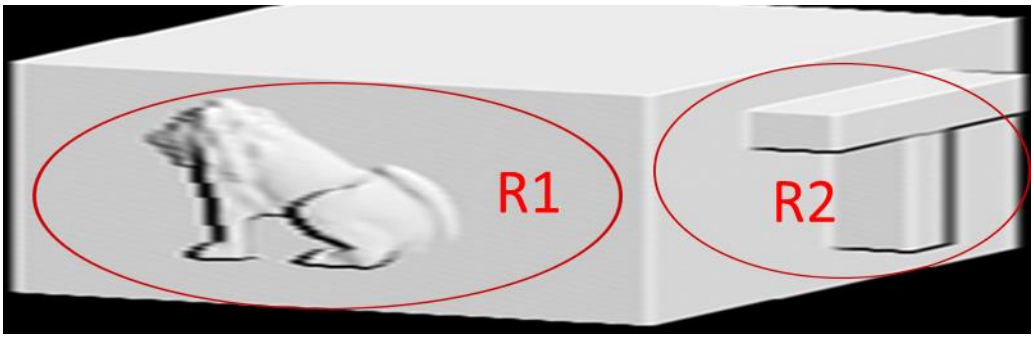

Figure 4.16 Different Center-based Ring Pattern

4.4.3 Decomposition Domain of 3D Partition

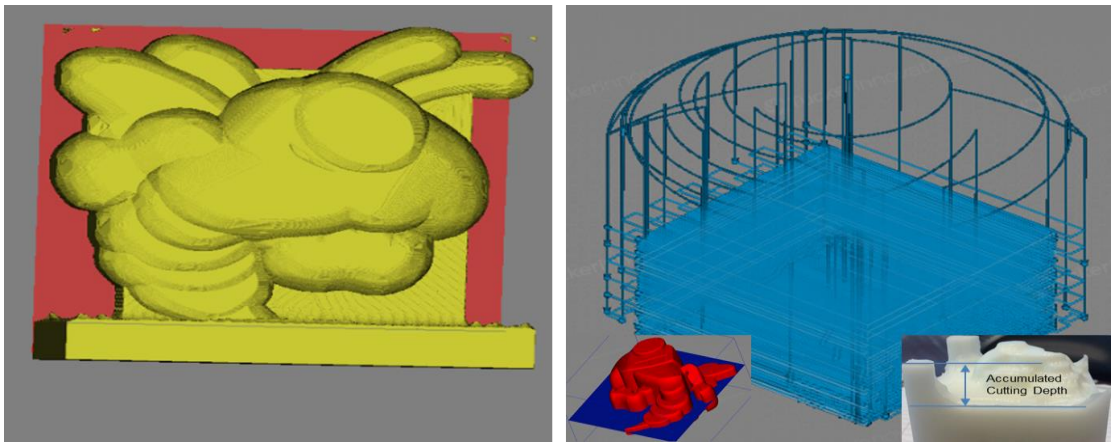

Figure 4.17 Non-cutting plane and sub-plane region

Figure 4.17 shows the target plane of region that we want to cut and the non-cut region which is partitioned by the plane below the plane level. A 3D object space is partitioned into several path planning sub-regions with the sub-plane path along different

height planes. The domain of cutting region can be decomposed into multiple layers of cutting plane for subdivision of path. 3D partition thus provides linearization for nonlinear path as the nonlinear zone reduces into many linear path sequences by subdividing the zone into small slices that is within linear range for path planning. Domain decomposition thus facilitate local feature enhancement and linearization of path sequence planning. Accumulated cutting depth is the depth summation of all linear path decomposition via cutting layers for the final machining product.

4.4.4 Non-symmetric 3D Topology Region by Color Classification via Adaptive Grid

Similar to the description in previous section, a 3D grid gives highlighted adaptive solution and classification by regional segmentation. Grid partition by color interpretation helps intersecting the region into color mapping geometry distinctive part, and region with one color is usually considered one complete subject area with small segmented regions to the other areas of a different color.

4.4.5 Roughing and Finishing determined 3D Region

We could do path planning for the same region but with different resolution requirement. Roughing path covers fast processing of contour information and general outline of the geometry surface. Finishing gives refined detail along the surface region with higher resolution and more refined pattern.

Figure 4.18 demonstrates the difference between roughing and finishing path of horse model and blade simulation regarding volume rendering in the experiment for subtractive 3D printing of path planning practice. The result is tested by simulation

generated G-code path with adjustment to the new CNC machine frame and coordinate orientation. Roughing path of horse is faster with layers marked by black with different heights, while finishing path is slower with more refined resolution for surface smoothness to represent the geometry details. We switch smaller size tool cutter for finishing path and apply larger size tool for roughing path so that the tool won't break and the path can be hybrid optimal with combination of the two. Multiple roughing paths works together until one last finishing path works to smooth the surface geometry.

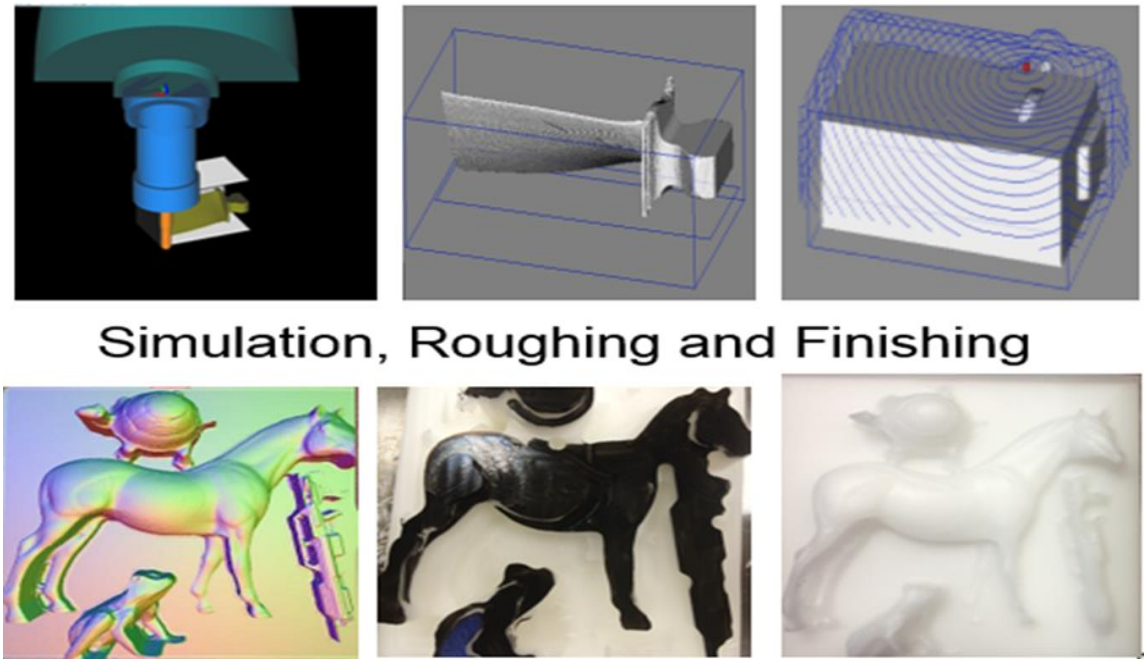

Figure 4.18 Roughing and Finishing by Color Comparison of Horse [1] and Blade

4.4.6 Ring Step based Region of Searching, Scaling Optimal and Height Map

- Region of Searching

One ring step can be used for update for a new position, described as Equation 4.5:

$$\nabla\tilde{y}_i = y_i + \nabla y_i \tag{4.5}$$

For a general search within bounded solution, divided-searching algorithm is normally applied for fast boundary mapping between two sides of the lower minimum and higher maximum value. Equation 4.6 describes the process of divided step update based on k coefficient, k determines the damping distance of the margin size.

$$\nabla y_i = k\frac{(y_{i-1}+y_{i+1})}{2} \tag{4.6}$$

All path contact points are located along a ring circle of path route, Figure 4.19 shows the illustration of points of contact along a tool movement path. It is obvious that the path points density is highly impacted by the frequency of the points extraction frequency or sampling rate.

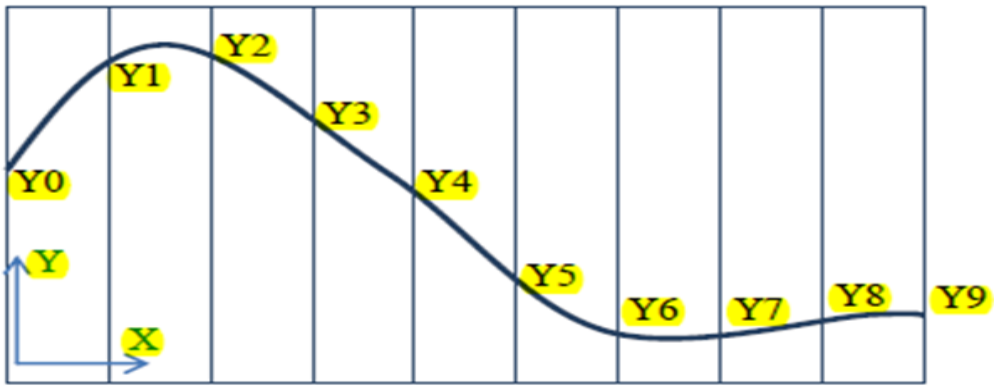

Figure 4.19 Points of Contact along Ring Path

- Scaling Optimal

The scale of ring input is largely either local optimal or global optimal. Local optimal consider bounded input as path data collection, while global optimal considers

entire geometry surface along the 3D surface region. Scaling optimal is highly how the optimal scale can be put to the right region size and location so that the mapping of ring distance searching can be most efficient and fast. Path scalability is highly dependent on ring scaling optimal region as the location of the mapping distance becomes adaptive to the distance or orientation and machine range.

- Height Map [1] and Local Optimal Region

The original height map is used for 3-axis path planning and it compares the path point along of geometry surface for its height intersection with the tool position. We take into consider height map here as we want to discover region-based benefit for local optimal by height information. Compared with 2D ring distribution graph, 3D ring has more height information mapping its peak location, this might recreate peak region for center-based ring circle due to the geometry surface gradient variation. Figure 4.20 shows how a height map get calculated based on the tool intersection with the surface with Hi as surface point of height above horizontal plane and Ti as tool point of height intersection with the geometry surface plane.

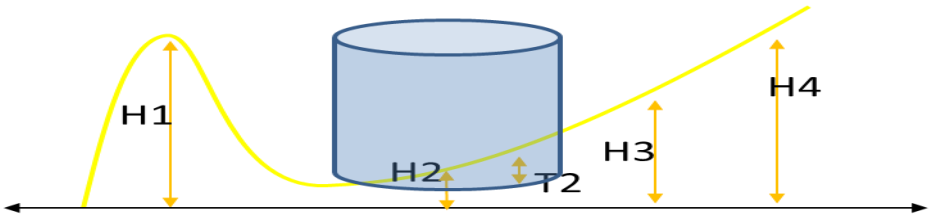

Figure 4.20 Tool Intersection with Surface Plane

Height map of tool tip and surface height minimum gives estimate of offsetting result after ring covers give its circle size along the route. It gives 3D information based

on 2D plane. During subtractive path operation, new height position can be updated by previous one and the distance of tool cutter to the surface, shown as Equation 4.7:

$$Hi = \min (Hi, Hi-Ti) \tag{4.7}$$

Ti is the tool tip cutting depth from the geometry surface, and Hi is the original surface height from the origin plane.

Surface regions with multiple height peaks are shown in Figure 4.21. These peaks could be classified as different regions with ring distribution so that each ring originates from the peak position to retain the convex geometry shape of path distribution.

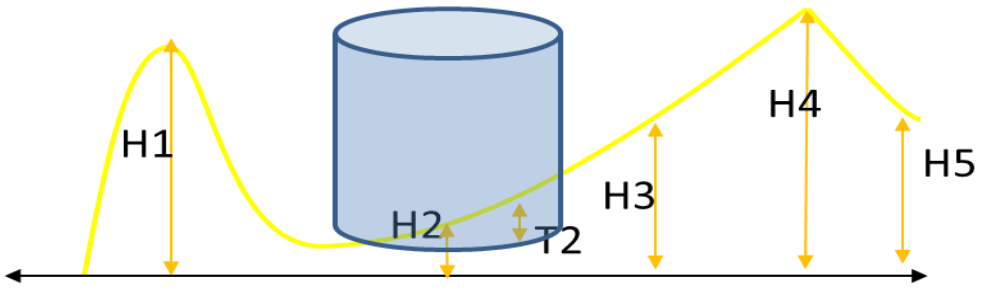

Figure 4.21 Tool Intersection with Multi-Peak Surface Region

4.4.7 Comparison of 2D and 3D Ring Path Planning

With height map considered, we compare 2D and 3D ring path planning and the following may be summarized for comparison purpose.

- Geometry dependent: uniform surface, symmetric body, Non-symmetric surface, pattern of pocket in path
- 2D Ring Path of Pocket:

- 2D geometry is located on single plane of surface
- 2D ring path benefit for path intersected merging
- 2D merging is good for less path length

- 3D Ring Path of Geometry
  - 3D ring path works for complex geometry with multiple depth planes
  - 3D ring path covers nonlinear pattern due to regional height
  - 3D ring path has linear path sequences with boundary
  - 3D merging may not be linear efficient due to regional peak of height, so each ring has to locate on a height region given the ring centre.
- Height based peak of orientated region or height zone exist for 3D space
- Height map is usually used for height information of 3 axis path
- Local optimum gives optimal steps searching within ring size boundary
- Scalability of path considers both local optimal path and global optimal path

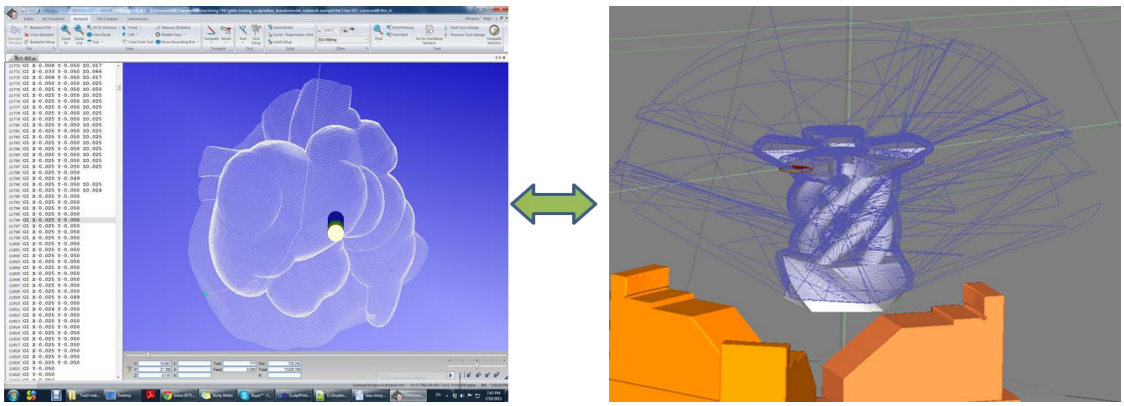

Figure 4.22 Local Optimal Ring of Buzz 3-axis Path vs. Candleholder 5-axis Path

Comparison of Scalable paths for linear 3 axis and nonlinear 5 axis is shown in Figure 4.22. The results come from two different types of G-code via graph simulator. 3D Buzz path as 3-axis path has no retraction only linear path points and the candle holder

path as 5-axis path has lots of retraction path lines. The jumping of the path represents the reorientation of the distance region that need to be connected while switching orientation. 5-axis path has more rotation movement with retracting lines compared to 3-axis path.

The retraction line helps reorient the planning direction and provide new solution space for path sequence connection but takes more jumping distance and safety concern in space. The optimal local path of 3 axis does not have any retraction for the Buzz model path planning and is viewed as linear path sequence within its target region.

4.4.8 Other Path Planning Type besides Ring Step Spiral Path

It is important to compare other path planning solution based on path type as ring path is not the only path planning option:

- Line path movement for one direction of path motion
- Contour offsetting is used for roughing with faster pace and relatively lower resolution compared to finishing of path
- Zigzag path is used for finishing operation
- Ring path works both for 2D and 3D geometry multi-axis path

Differences between these path types matter in time and patterns of motion. Zigzag path takes more traveling distance compared to spiral path movement of ring path motion. The ring takes care of 3D shape in geometry topology by volume operation and calculation, and is more time consuming for its geometry representation but more accurate in high resolution model with parameter tuning operation. Contour offsetting is basic for removal of intersection region between the tool cutter and surface region.

4.4.9 Scalability of Path Region for Accessible Sequence

We want to keep ring boundary in machine space respecting the tolerance region. Scaling of path region is dependent on whether a path sequence is accessible for travel efficiency. In machine space, the ring simulation should be mapped to the same geometry surface for tolerance area. However, we consider more for the following aspects for a scalable region:

- Step normally means the compensation step size of machine parameter as we search optimal solution in machine parameter space or virtual path planning simulation.

- Step is important for accuracy of control sensitivity as we could calculate distance for path control by adaptive analysis in statistical aspect.

- Bounded geometry problem is useful for feature analysis and data fitting solution as we define a feature point outside the material and inside the material region

Therefore, we try to define center-based ring path with geometry-bounded solution as ring step path planning and use ring step to control accuracy and precision of path simulation.

Assume the initial ring center is p^0. The sensitivity is the derivative of compliance function C(p_e), which is the ring in our case with respect to the tool contact point p_e on the surface. To understand the sensitivity of objective function caused by each path sequence generated by ring steps, we have the objective function with explicit form. The explicit form is due to freeform 3D geometric design surface and we have

negative values for sensitivity. For e=1,... N, we have Equation 4.8 considering the sequence element and point of each path:

$$C(p) \approx C(p^0) - \sum_{e=1}^{N} \left(\frac{(p_e^0 - L_e)^2}{p_e - L_e} \frac{\partial C}{\partial p_e}(p^0) \right) \tag{4.8}$$

Pick fixed depth d for the cutting height plane of region, the problem becomes the highest surface summit by given stock topology, which relies on the nearest neighbor definition of search criteria while minimum size of structure is needed to satisfy target pattern. The minimization problem is described as Equation 4.9:

$$\text{Min } f(x) \tag{4.9}$$

The minimization sub-problem for each path sequence of K iteration becomes another optimization problem in Equation 4.10 as we want to minimize sensitivity to be stable.

$$\min \left[C(p^0) - \sum_{e=1}^{N} \left(\frac{(p_e^0 - L_e)^2}{p_e - L_e} \frac{\partial C}{\partial p_e}(p^0) \right) \right] \tag{4.10}$$

subject to constraint: $\sum_{e=1}^{N} v_e \, p_e \leq V$, $0 \leq p_{min} \leq p_e \leq 1, \ e = 1, \dots N$

It is convex function. The Lagrangian functional of the optimization function with dual method for subtractive path planning is as Equation 4.11:

$$L = C(p^0) - \sum_{e=1}^{N} \left(\frac{(p_e^0 - L_e)^2}{p_e - L_e} \frac{\partial C}{\partial p_e}(p^0) \right) + \Lambda(\sum_{e=1}^{N} v_e \, p_e - V) \tag{4.11}$$

For each iteration of path sequence, the function is maximized with respect to adaptive value Λ as we want to remove as much volume as possible, but also satisfy the volume constraint of bounded ring path within target region.

Assume there are N partition of path sequence and each sequence iteration removes d maximum cutting depth, then the target depth of volume removal is the accumulated sub-cutting depth of volume removal for each path iteration. We have Equation 4.12:

$$N * d = Depth_{removal} \tag{4.12}$$

The simulation results include generated path visualization of each path iteration, volume rendering output of simulated geometry stock surface, and final fabrication product. In simulation, the actual step counted is based on the update based on path sequence generation, it is calculated by length of normalized move distance with current position of tool contact point and point on sphere

$$\text{steps\_Count} = \text{length}/\text{curve\_Step} \tag{4.13}$$

$$\text{step} = \text{length}/\text{steps\_Count} \tag{4.14}$$

Our work differs by assigning the center of ring with tolerance zone, therefore give more initial information and guess for searching speed in solution space. A wrong initial position may result in larger searching time or bad solution. The selection of ring center does matter in our path planning simulation for path travel efficiency and machining speed, as wrong origin of ring center may break the path along the route.

Figure 4.23 shows the 3D candle model of path simulation of G-code with graph visualization and machine chuck holder as well as tool cutter. 3D candle is a 5-axis model by its geometry nature as the path motion around it requires complex movement with both linear axis and rotational axis towards nonlinear motion. Due to the complexity of 5 axis geometry shape, path retraction is necessary for path jumping to re-orient a region-based path direction for accessibility. We will look more into what's causing path jumps as path tripping condition in the rest of chapters for accessibility discussion. 3-axis path is simplified way of 5-axis path, though the complexity of geometry sometimes requires 5-axis path operation. The machine requirement for 5-axis path is also very high as the supportive machine structure should work for 5-axis motion. Thus 5-axis CNC machine is very costly compared to 3-axis machine. For simplicity of design, and path economics of cost saving in general conditions, we could try to simplify 5-axis path into 3-axis path by breaking the global region into many local subregions for feasible solutions.

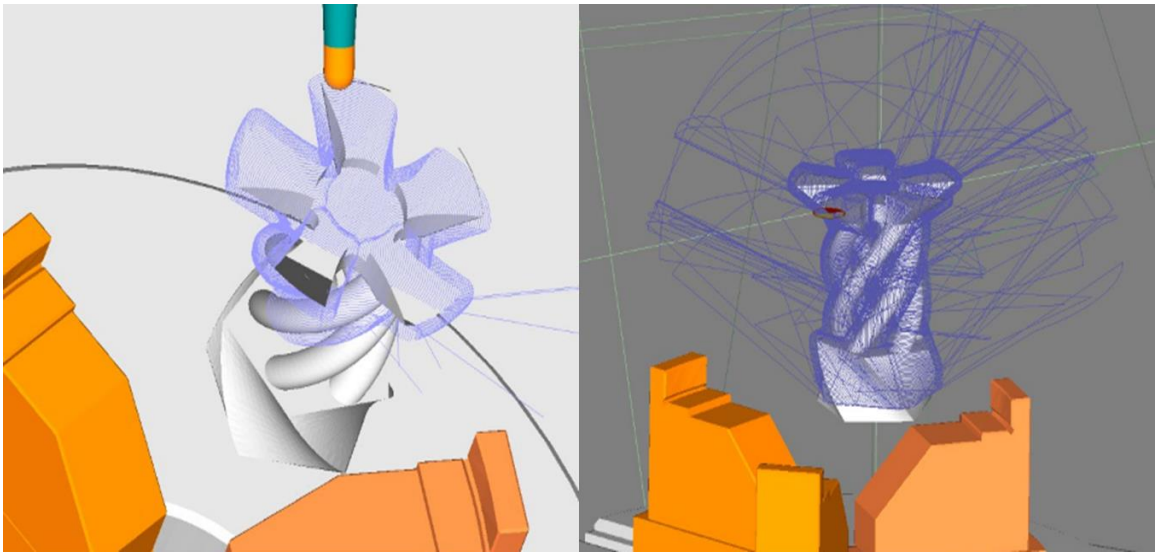

Figure 4.23 3D Path Retraction of 5-axis Candle Holder

4.4.10 Graph Partition by Accessibility Regions

Assume one region is covered by all accessible graph sequence, we partition the graph of entire 3D object region into multiple sub-region for distributed graph processing. We put non-accessible region apart from the accessible region so that the jumping of path between connected regions is more efficient and could be minimized. The topology of the graph could be studied for efficient data distribution so that one large graph area is more centralized compared with other small graph regions. This is because graph centrality has more data transfer optimal benefit compared to other graph topology. The distribution of points along the graph usually follows even distributed mapping based on sampling of feature extraction points, or sometimes could reflect critical shape variation with critical location registered for point position. The scaling study by region should tell different benefits for global and local optimal path. We will discuss more of it in later chapters.

One graph sequence is considered accessible within its own route apart from another graph sequence region. We partition the non-accessible region between accessible sequences so that we could have minimal jumping distance between sub-graph locations. The study of graph jumping is highly dependent on the distance and topology of graph distribution which is determined by the feature extraction of ring path and path parameter input generating the volume data sequence based on geometry model. The goal is to have regional benefit for local optimal of path travel distance within one graph region so that ring path is better located and planned within one sub-graph region. Figure 4.24 shows graph sequence illustration based on sampling of points of contact for graph resolution and accessible orientation for graph formulation in path planning direction.

To sum up, the graph partition by accessible region includes the following benefits:

1. 3D Accessible space into 2D accessible sequence
2. Curve construction for initial curve & iterative optimization
3. Graph theory of connected component of shortest path in a graph partition for path efficiency
4. Min jump for surface orientation radiance distribution region via accessible path sequence between regions

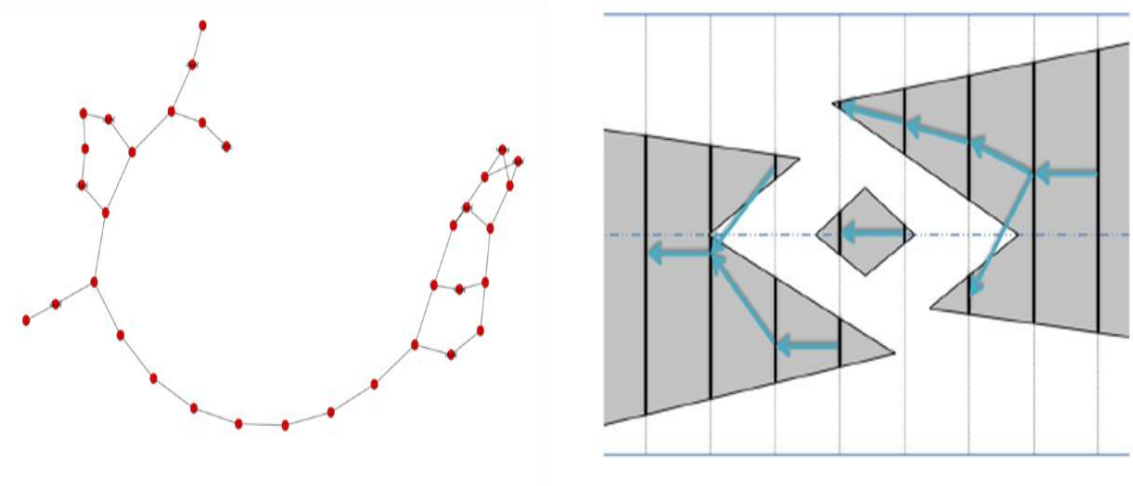

Figure 4.24 Graph Sequence Illustration [1]

4.5 Path Protection and Control

4.5.1 Path Retraction and Jump Conditions

A tool jump adjusts path orientation and gives more freedom of movement in 3D space. The jumping condition can be roughly described by $\|p_I - p_k\| > A_i$, while p_I and p_k are normals of two contact points as the end of previous path sequence and the start of the next path sequence. A_i is the threshold condition within orientation limit of tool movement.

4.5.2 Path Control Optimization and Modeling

Figure 4.25 shows the self-drawn flow for control components of path optimization. The control of the ring edge sets the region, and it is based on feedback control law for boundary constraint restricted retraction while tuning ring path parameters based on major three feedback information: fabrication error, simulation pattern error, and retraction of path generation as we avoid retraction path in 3-axis with selected ring

edge boundary in each local path iteration across the surface layer by layer. We aim at linear path of minimal jumps.

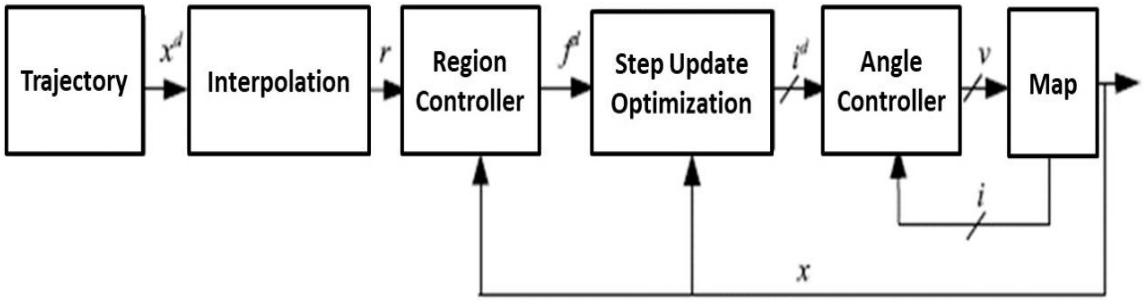

Figure 4.25 Control Component for Path Optimization

4.5.3 Path Protection via Rapid Machine Probe via G-code and Tolerance

Path protection means providing protective measurement or simulation methods so that errors involved in path planning could be reduced and collision of path in machining can be avoided. Path protection provides vision-based prediction for fault tolerance and path validation before errors. To achieve path protection, we use methods such as monitoring tools for graph inspection for path planning regarding trajectory.

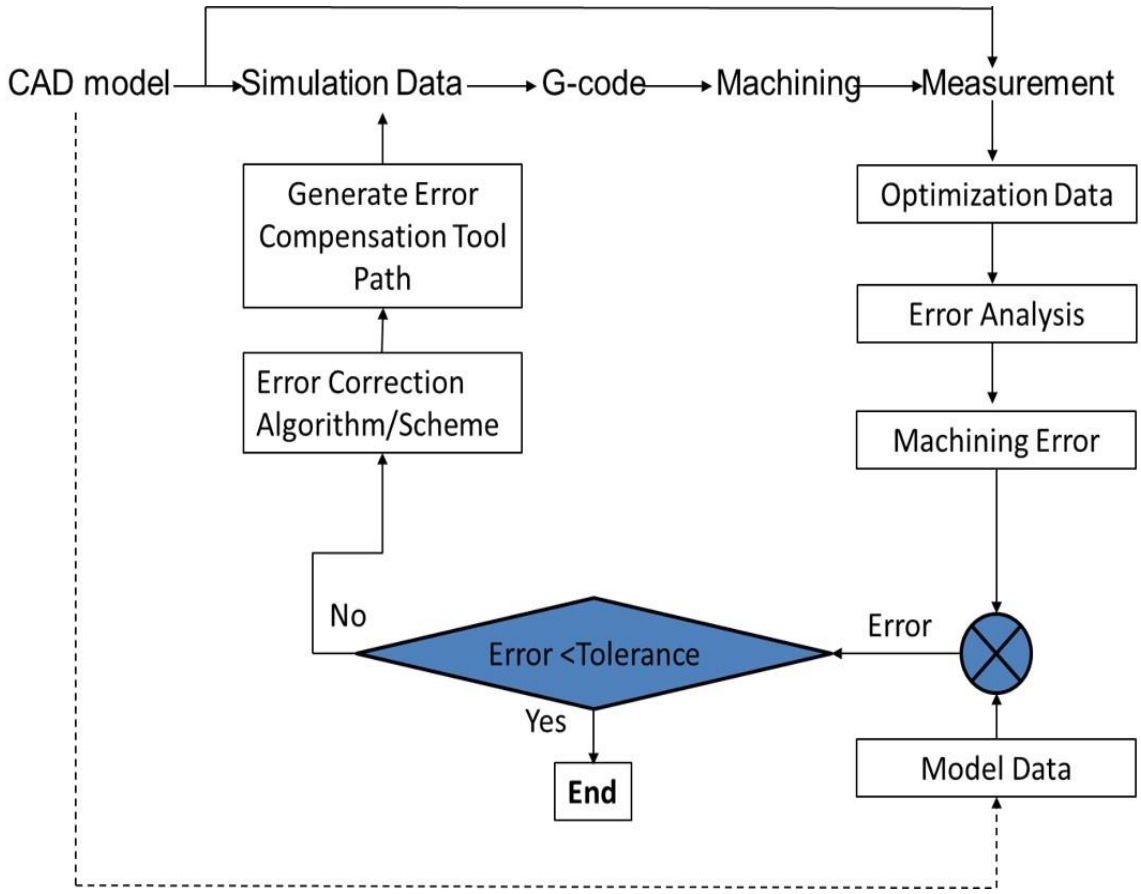

Figure 4.26 Numerical Path Protection by Error Tolerance via G-code

Figure 4.26 shows path protection for ring-step path planning for 3D domain of selected region. It uses control loop for error compensation and path update via numerical estimation of path forward steps. Errors should fall within tolerance for rapid machine probe. Moreover, jump distance of path step should also fall within the tolerance otherwise path will be corrected for error compensation until it satisfies the constraints.

Path protection also involves monitoring of selected feature so that path focus of key parameters can be better maintained. Path protection needs to pass tolerance of errors within control constraints or compensation limit. It could also be attained via error

compensation algorithms for generated tool path. Right diagnosis of problem also helps path protection. Equation 4.15 shows condition analysis of B as given condition of path:

$$P\left(\frac{A}{B}\right) = P(A \cap B)/P(B) \tag{4.15}$$

The variation of path pattern is highly determined by the variation size of ring cover as we simulate the cutting process step by step based on subtractive layer removal by depth.

In general, for 5-axis milling machine, the machine coordinate vector has unique transformation as Equation 4.16 with tool posture position and offset value.

$$\begin{bmatrix} X_M \\ Y_M \\ Z_M \\ A_M \\ B_M \end{bmatrix} = \begin{bmatrix} a_{11} & a_{12} & a_{13} & a_{14} & a_{15} & a_{16} \\ a_{21} & a_{22} & a_{23} & a_{24} & a_{25} & a_{26} \\ a_{31} & a_{32} & a_{33} & a_{34} & a_{35} & a_{36} \\ a_{41} & a_{42} & a_{43} & a_{44} & a_{45} & a_{46} \\ a_{51} & a_{52} & a_{53} & a_{54} & a_{55} & a_{56} \end{bmatrix} \begin{bmatrix} X \\ Y \\ Z \\ I \\ J \\ K \end{bmatrix} + \begin{bmatrix} X_{tr} \\ Y_{tr} \\ Z_{tr} \\ A_{tr} \\ B_{tr} \end{bmatrix} \tag{4.16}$$

The mapping of coordinate helps further analysis between motion of machine and diagnosis of data measurement. State estimation usually works with matrix mapping to represent vectors of target in space. The benefit of putting together multiple information in matrix provides further analysis potential of information fusion. To understand multi-axis machine motion and its measurement position, we put the basic form of axis for machine coordinate. [X, Y, Z, I, J, K] is the simulation data coordinate of cutter location, and $[X_M, Y_M, Z_M, A_M, B_M]$ is the machine coordinate vector of 5-axis milling machine. $[X_{tr}, Y_{tr}, Z_{tr}, A_{tr}, B_{tr}]$ is the compensated machine coordinate center with absolute zero-point as set-up position. X, Y, Z is linear coordinate axis while A, B is the rotation axis

round the linear coordinate axis. The matrix formulation also helps to understand path dynamics of system operation and how compensation and data registration work.

Equation 4.17 shows accessible path sequence with k partition by ring, with B as given condition of path:

$$P_R[A] = \sum_{k=1}^{N} P_R\left[\frac{A_k}{B}\right] \tag{4.17}$$

CHAPTER 5. DATA ANALYSIS OF RING PATH BY OPTIMAL REGION ACCESSIBILITY

We will describe data integration in this section and how analysis of simulation data enhances our solution. As data analysis becomes an important aspect in many research areas especially understanding how experiment works under simulation environment mapping real physical space. Data analysis methods such as big data analysis and machine learning also give highlight of why data is important as it is the input of all study for the model training process. Ring path planning is our approach of selecting user interactive pattern of right scale and size, and optimal region gives precise geometry position by geometry shape and accessible orientations for better path planning operation.

5.1 Data Integration Contribution

5.1.1 Key Data Integration Steps

Overall, the key data integration includes three steps -- preprocessing, training processing, and post-processing. We use preprocessing of 3D scaling from 3D image reconstruction for feature extraction into STL design, training processing of ring parameter tuning optimization, post-processing of graphical path partition and data compression for G-code optimization. Figure 5.1 shows the applied data integration steps from data integration perspective.

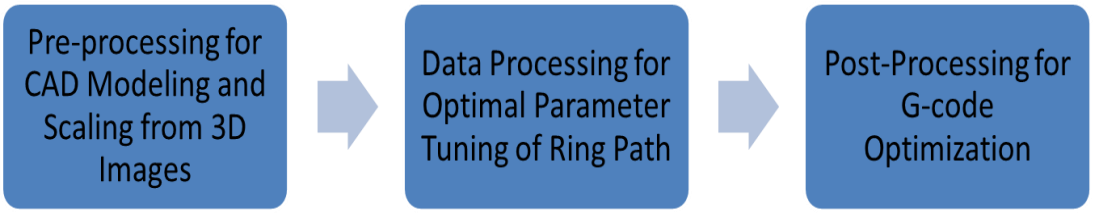

Figure 5.1 Data Integration Steps

5.1.2 Benefits of Data Integration

Data pre-processing gives flexibility of 3D design from image features by user selection, as Buzz demo model via reconstruction from 2D image feature into 3D geometric design provides man-made 3D print model from scratch. Moreover, data training process facilitates parameter tuning for system automation and user interaction. In addition, post processing enhances distributed computing capability and scalable path planning options. Local path from small 3D printing product of hand-made design to large aircraft part can be made via scalable path planning solution based on the applied ring path method as large volume of data or graph can be partitioned into small data sequences for fast processing of local data.

5.1.3 Path Planning Component and Simulation Framework

Software system may be large due to its complexity in function and design. The simulation framework helps understand the basic component that are vital as key steps of path planning that we apply in subtractive 3D printing. Not all planning components are necessary to be listed in our simulation framework, and we try to classify key components by the same or similar feature functions, especially what we contribute to.

This section describes system integration flow and functions of each path planning phase.

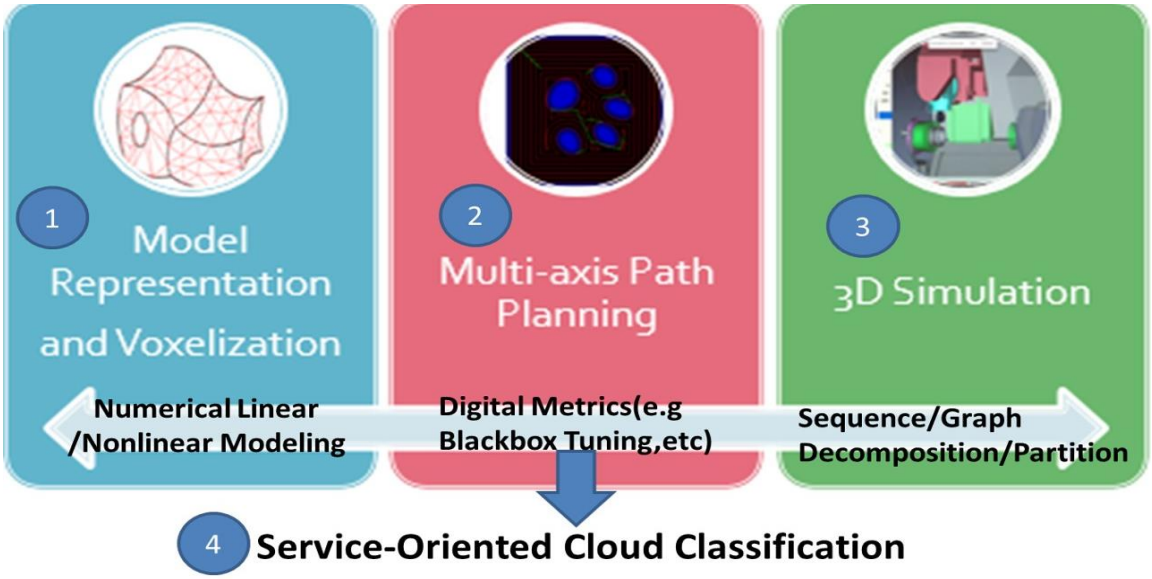

Figure 5.2 Software Function for Simulation

Figure 5.2 shows module structure of data analysis and simulation methods. Major analysis of path planning simulation is based on functional modules as multi-axis machining simulation, 3D model representation as well as multi-axis motion simulation.

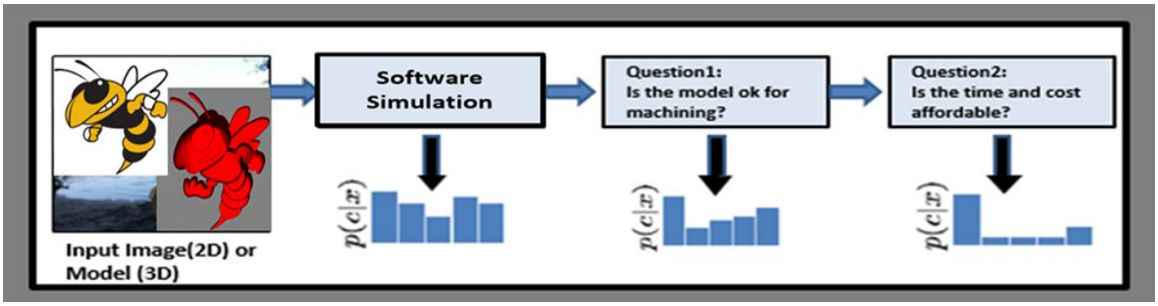

Figure 5.3 Model-based Path Planning of Subtractive 3D Printing [69]

The entire path planning of subtractive 3D printing process includes multi-axis machining for G-code generation, machining simulation of graphical rendering and model-based path representation.

The goal of software simulation is efficient path planning. Figure 5.3 describes the purpose involved in model-based path planning towards a final accessible path by model analysis and validation.The computational challenges of model-based path planning in subtractive 3D printing include many computational aspects as follows: freeform parameter tuning towards path efficiency and user decision pattern, scalability

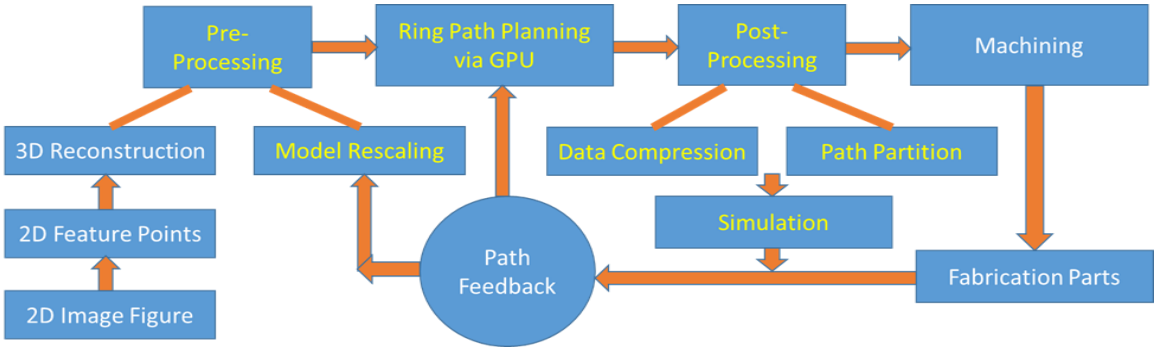

Figure 5.4 Data Processing Steps and Functions

of model integration and high-density path, high geometric cost of rendering and material waste, storage limit of G-code on CNC machine, etc.

Figure 5.4 shows data processing steps. The yellow marked steps are marked as contribution of this thesis. The data flow chart works from 2D data to 3D fabrication, which includes three major phases: data pre-processing for model reconstruction and model fitting based on reverse engineering by feedback, dynamic data pattern processing of accessible region via ring scalable path prediction, and data post-processing for G-code optimization. The data output is made for fabrication material part.

5.2 Data Analysis of Accessibility Map Sequence mapping Data Structure

5.2.1 Ring Mapping to Accessibility Sequence with HDT Branch

Hybrid Dynamic Tree (HDT) is implemented as our data structure for model representation. The Branch of the tree can be categorized as static branch with static and dynamic branch with active voxel for more variations while changing the resolution. We study the relation of branch of tree so that an efficient map structure can be formulated while generating GPU volume as material removal simulation in path planning. The branch of tree determines the searching efficiency of a tree as the topology of tree depth and branch. The dynamic part of tree structure is caused based on the scalable model sizing and resolution enlarging by active voxel distribution. For rough modeling of tree branch

$$Branch_{full} = Branch_{static} + Branch_{dynamic} \tag{5.1}$$

Equation 5.1 displays the branch information regarding dynamics of model adaptive resolution and scalability for topology analysis [69]. The topology of tree branch may determine data efficiency of loading the model and the speed up performance while turning the path parameter for visualization purpose.

The basis of HDT tree structure regarding branch can be shown in Figure 5.5 [69]. We compare the path layer regarding local ring and global ring mapping HDT branch number in Table 5-1 and Table 5-2 respectively for benefit of local optimal solution of path [70]. More tree branches usually mean more processing data for volume operation in GPU computation of accessibility sequence of contact points and longer latency for end volume generation. Data analysis is the numerical foundation of graphics. Here voxel is the smallest element to consider 3D graphical information. Active voxels are mapped to

dynamic branches which carry information in an active way. Static voxels are mostly in static branches that remain unchanged during simulation. Branching factor determines how many branches each tree allocates workload with branch number.

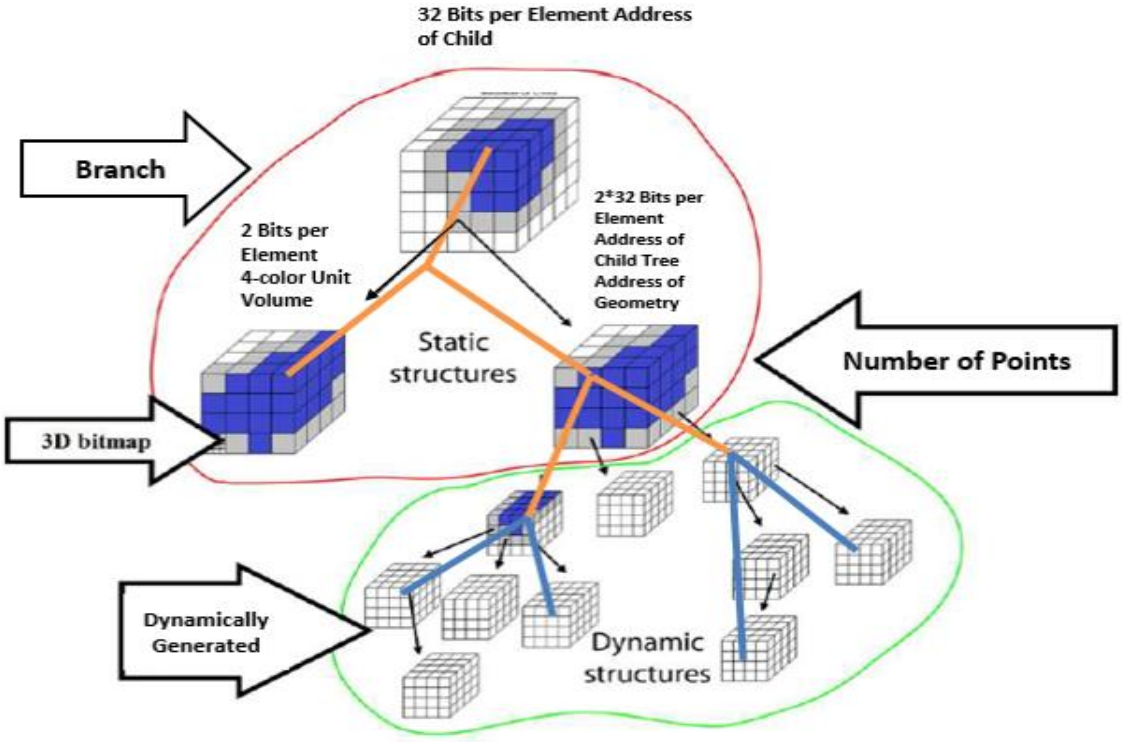

Figure 5.5 Data Structure and Branch Topology of HDT [69]

The current system platform used is windows 7 enterprise running with Visual Studio (VS)2010 with GTX 780ti GPU and GTP 980ti GPU from Nvidia and Intel Core Processor (TM) CPU i7-4771 3.5GHZ 3.5 GHZ, with installed memory 32GB on 64-bit operating system. High multi-core processors may have less rendering time for path generation and map processing. Benefits of understanding branch relation with accessibility map and volume are fast searching algorithm on data query by branch information and branching optimization\prediction for fast data access and distribution.

Table 5-1 Local Step Ring Based Path Planning by Depth [70]

Step distance(mm)	Depth(mm)	Ring no.	Branch number	Branch consolidate time(s)	Generating end volume(s)
1	6	21	1	0.049	2.477
1	6	33	1	0.075	4.694
0.25	3	131	1	0.052	8.81

Table 5-2 Global All Paths of Full Model Path Planning [70]

Step distance(mm)	Depth(mm)		Branch number	Branch consolidate time(s)	Generating end volume(s)
1	6	Path all	11	0.1	7.602
1	6	Path all	25	0.067	3.972
0.25	3	Path all	22	0.048	8.569

5.2.2 *Ring Scale Mapping to Accessibility Sequence by Points and Time*

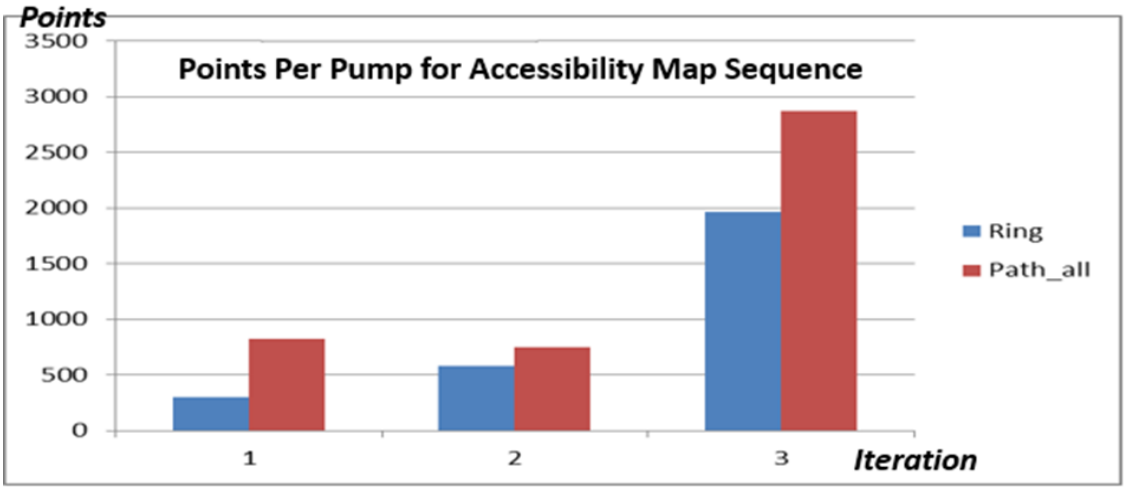

Figure 5.6 Points per Pump in Map Sequence [69]

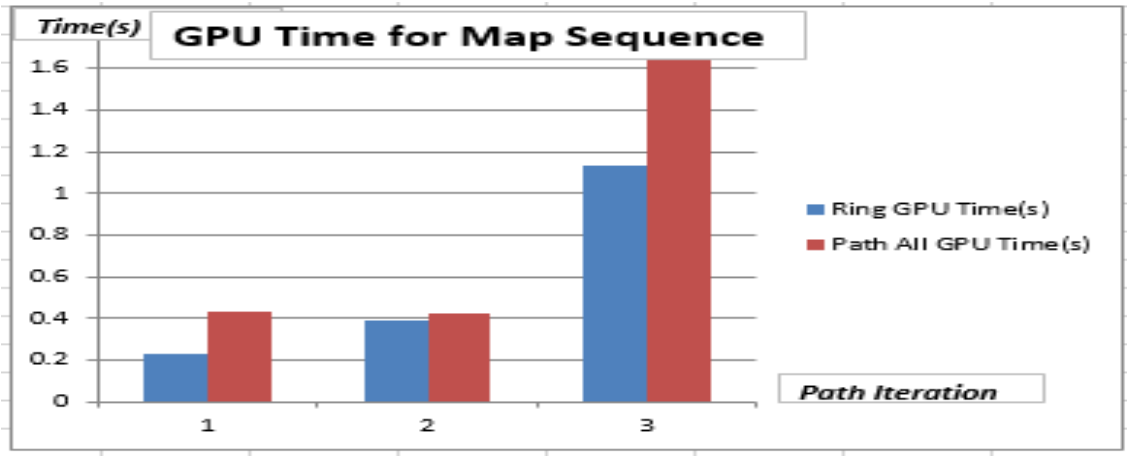

Figure 5.7 Time Relation of Map Sequence to Local Ring vs Global Ring Path [69]

Figure 5.6 shows the points per pump relation with map sequence. Pump is the sequence simulation concept of virtual mapping for load moving unit as flow. As there exists a mapping relation between a ring and a point, we can similarly analyse the relation of a set of rings of its ring completion and a set of points of accessible

sequence. Figure 5.7 shows the time relation of mapping between map sequence to local and global ring of path. As contact points of geometry surface is rendered by GPU volume representation and also supported by data structure of HDT as the basis of scalable resolution model.

5.2.3 Ring Mapping to End Volume Generation for Computation Time

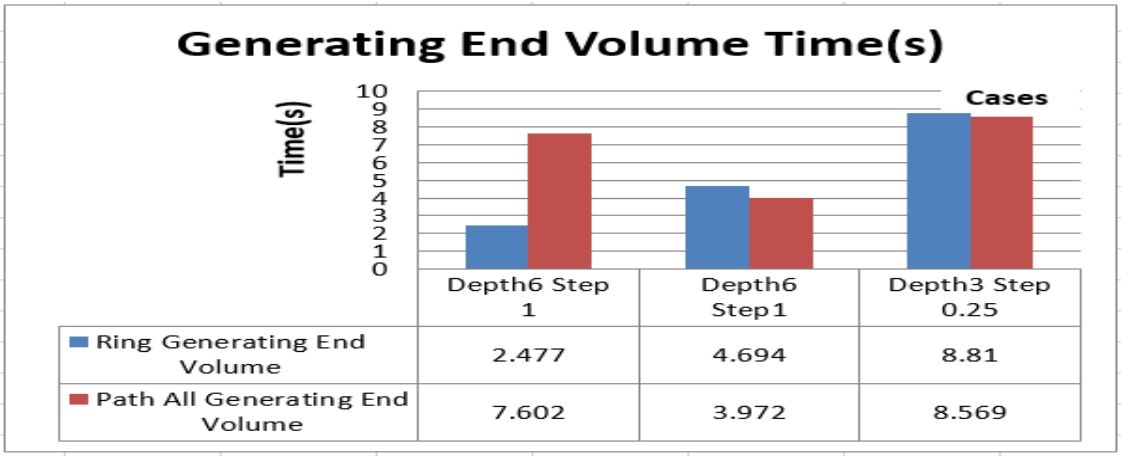

Figure 5.8 End Volume Generation of Local vs Global Path [69]

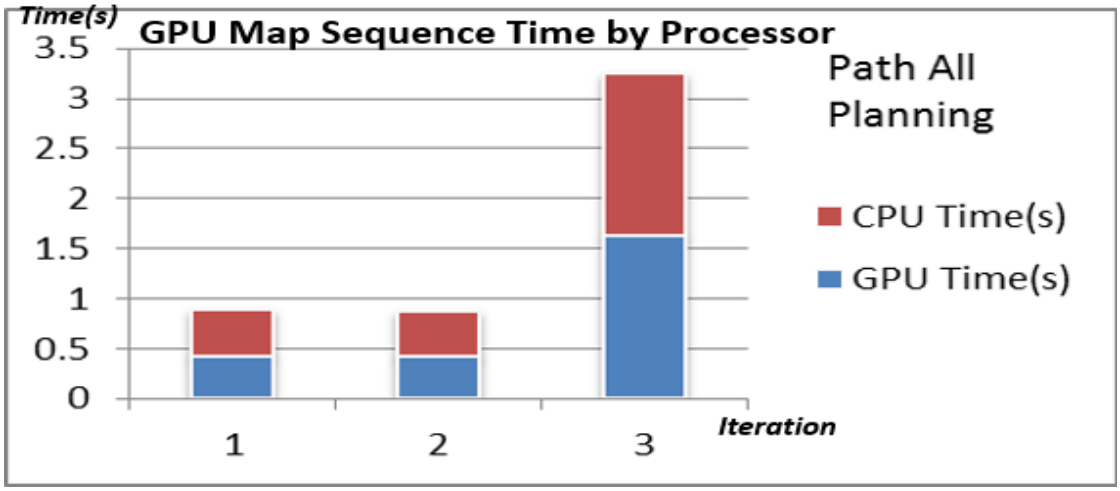

Figure 5.9 GPU Map Sequence Time by Processor [69]

The mapping of end volume generation based on ring number also shows local optimal solution by time response compared to global ring path. Figure 5.8 analyses end volume generation by major ring parameters of ring number, path layer depth, and step distance.

5.2.4 Processor Comparison of CPU vs. GPU for Map Sequence Generation

The result in Figure 5.9 highlights map sequence computation time for small workload between CPU and GPU. For visualization of graphics modeling, GPU benefit over CPU is obvious. GPU could highly speed up graphical simulation especially for high resolution display which helps Isoscallop Analysis. Isoscallop Analysis by simulation validates the planning parameters for layer-based path iterations.

5.2.5 Domain Specific Solution on Sub-Region Partition

Data analysis results show the scalability of local optimal ring on GPU. The local optimal ring gives solution of path planning in large scale for scalability of path planning. This leads to flexible platforms and path efficiency without retraction. Local optimal ring also gives domain specific solution based on 3D geometric pattern of linear 3 axis path. We want to look at the 3D space from 2D plane intersected region for multi-level set regions. The benefit of multi-level set is to give regional study of local variables while planning the path from accessible orientation.

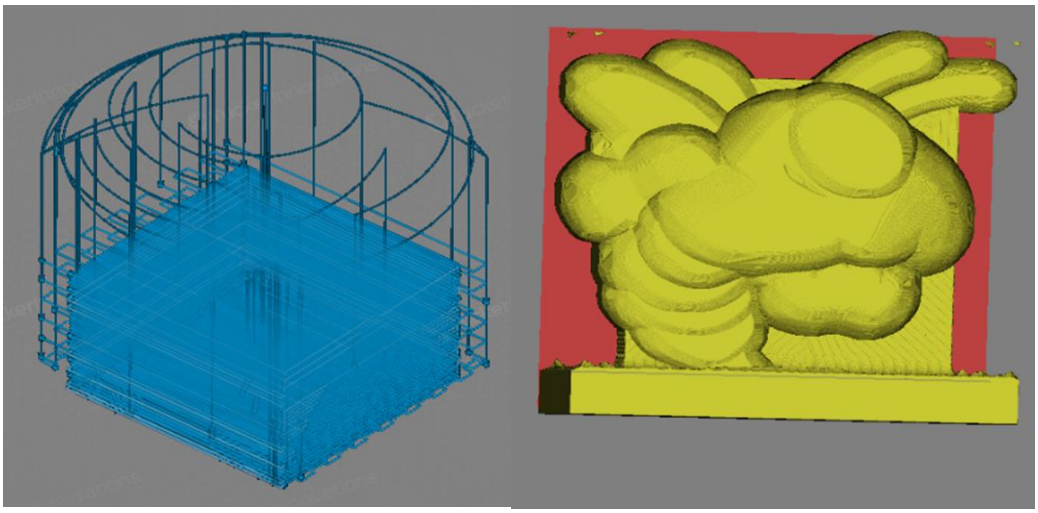

Figure 5.10 Multi-Level Set Partition of Sub-Region for 3D Model

Figure 5.10 gives a general view of how the partition plane gives partition of sub-region for even distribution of data across 3D geometric space. Successive offset volumes provide a sequence of XYZ points for a target tool path and economic analysis based on "domain specific solution" in accessible linear region described as union of sub-components. Equation 5.2 formulates this relation.

$$Er=U\varepsilon l \tag{5.2}$$

5.3 Accessibility Sequence Modeling

5.3.1 Depth based Sequence of Path

One ring sequence is located by a ring depth defined surface cutting plane, which becomes the sub-region partition of the 3D space. As the tool depth goes deeper for the planning path, we get the sequence of path points on the assigned depth partition plane via the ring parameter of cutting depth for numerical ring modelling function or rather surface offsetting distance in graphical term. The idea mapping between numerical math

and graphical simulation should be perfect as the iterative process mimic material removal operation while doing tool offsetting algorithm within the ring-bounded region. The accumulated cutting depth is a summary of all these cutting depth partition for each sub-plane of ring cutting path.

5.3.2 Sequence of linear space (X, Y, Z) – Sequence modelling

Take candle holder 3D model for example, the orientation affects the model relative position for path planning coordinate shown in Figure 5.11. The geometry has its own orientated coordinate aside from the machine space as the world coordinate. Considering the relative move, we put the sequence of path as pervious location and take new updated information merging the previous for data fusion. This could give a kinematic motion of how the path get extracted along the route of tool travel.

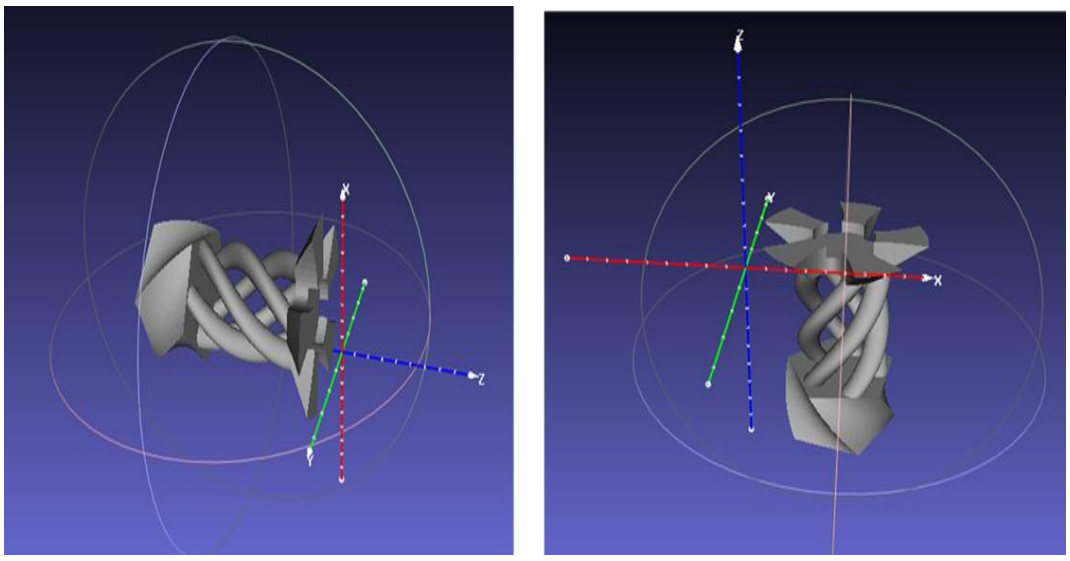

Figure 5.11 Candle Holder of Multi-axis Orientation

Sequence modeling is useful for data-based probability estimation. Two points of data formulates a sequence of path direction, that we could apply it similarly for estimation of depth sequence analysis for graph region.

5.3.3 Depth Sequence for Map Intersection by Graph Theory of Partition

If we partition a path loop into multiple sequences, if each sequence rests on the same plane of height level-set then we consider the sequence in a sub-region of one depth partition. One depth sequence may formulate a graph or sub-graph region, which is part of intersection area for map accessibility study. The following aspects are thus related to our theoretical graph topology with user interactive metric:

- Graph Theory of Connected Component in Path for maximal removal efficiency and min Orientation Jump based Radiance Distribution Region of Ring
- Dynamic path programming with user metrics of material removal surface or pattern-based travel speed
- Graph Cut Theory of Path Travel Efficiency –Breath First Search (BFS), Depth First Search (DFS)
- Cloud GPU network distribution for data allocation and sharing topology

5.4 Optimal Orientation Searching via Multi-axis Accessible Sequence

5.4.1 3+2 Freedom of Path for Geometry for Accessibility Orientation along Sequence

For 3-axis sequence of path, sequence modeling is enough for mapping 3D coordinate to the linear path vector of X, Y, Z position. The path is nonlinear when evitable rotation is needed. That's when we consider rotation for orientation. A machine rotation happens when part of geometry motion is considered static, as they have relative motion with each other, therefore we consider geometry target as static in geometry space with machine motion and consider machine as static with geometry target motion in machine space.

Figure 5.12 shows the machine motion following A, C orientation angular

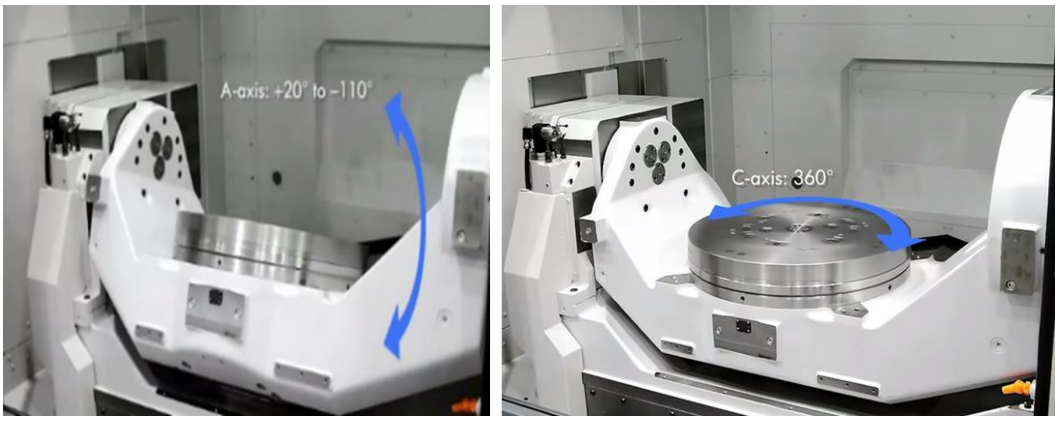

Figure 5.12 Machine Coordinate of A, C Rotational Angles

rotation. A, C provide two directional rotation of machine motion, gives the flexibility of 5 axis freedom along the tool path sequence. Take Okuma machine for example, with A, C angular move, most 5 axis parts could be produced from the CNC machine. The path planning component give output G-code for operation of CNC machine for path machining.

5.4.2 *Nonlinear Path Orientation Space for Rotation (Theta, Phi) into 3D Accessible Space*

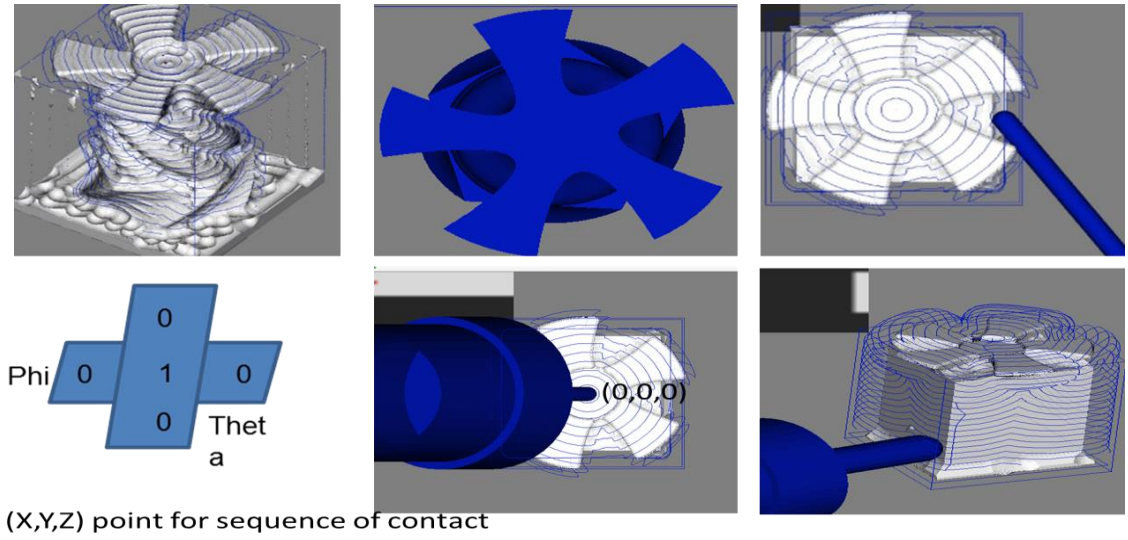

Figure 5.13 Candle Holder Ring Path Planning Angles for Accessible Orientation

Once we have a tool path sequence, the orientation mapping happens along the orientation of the tool which is based on actual tool contact position. We analyse the contact of point for data accumulation of extracting from geometry volume as the tool movement orientation space is basically given by the intersection of two orientation angles namely phi and theta to determine a feasible direction. The accessible direction is marked by access map as non-zero value of the intersected orientation. In orientation space, the non-zero value gives the label of confirmation for passing the angular intersection position of two orientations. With this information the accessible direction on a particular path point is given by the access map. A bunch of access map gives sequences of path tunnel regarding feasible orientation space. 3D space is thus partitioned into 2D accessible sequences between a series of access map planes intersecting the

individual path sequence. The accessible path happens within the accessible tunnels and gives the right information connecting the access map orientation plane on each path sequence point. Figure 5.13 is the illustration of the path simulation for candle model based on its ring path origin as the start of ring circle and the access map marking area for accessible direction of angular motion. The sequence is composed of accessible point of contact along the path planning route. The accessibility map is then formulated by the access map construction by loading path sequence points in 3D solution space. All accessible points of path are pumped as sequences of path for workload computation of accessible path. Accessible orientation is calculated based on access map information following the sequence path point of contact for tool touch position. Two orientation angles are considered due to CNC machine axis setting of two rotational orientations besides linear axis. Theta and Phi are labelled as general orientations and the intersection of both feasible orientations is the accessible direction for rotation.

5.4.3 3D Transformation between Points (X, Y, Z) in Vector Space

$$\mathbf{P}' = \begin{bmatrix} 1 & 0 & 0 \\ 0 & 1 & 0 \\ 0 & 0 & 1 \end{bmatrix} \mathbf{P}\cos\theta + \begin{bmatrix} 0 & -A_z & A_y \\ A_z & 0 & -A_x \\ -A_y & A_x & 0 \end{bmatrix} \mathbf{P}\sin\theta + \begin{bmatrix} A_x^2 & A_xA_y & A_xA_z \\ A_xA_y & A_y^2 & A_yA_z \\ A_xA_z & A_yA_z & A_z^2 \end{bmatrix} \mathbf{P}(1-\cos\theta).$$

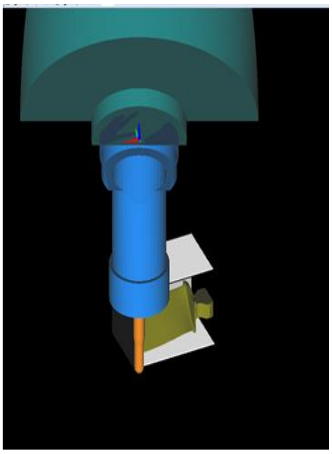

Figure 5.14 3D Graphics Simulation of Motion

Considering geometry part as stable, we have the tool movement motion. If we consider machine motion as well, we need to have the general mapping relation with the 3D geometry of CNC machine to the tool path.

Figure 5.14 shows a 3D graphical simulation of matrix mapping based on the orientation assuming **angular** movement in 2D follows certain translation relation with 3D motion. P is the position vector representing 3D object. P' is the updated position by orientation motion. Then we have the 3D machine motion simulation in 3D graphical form. The simulation scene of machine tool and target mapping are also displayed in Figure 5.14 as simple illustration of 3D graphical components in path planning of machining. This is useful for path validation of fast collision check by 3D monitoring function.

The linear mapping in 3D motion for machine motion simulation in 3D graphical space provides relative motion of path inspection to avoid collision. Right mapping of path reflects the relative movement orientation and position so that a machine tooling is moving towards the target of geometry stock. This provides a general way of checking the path traveling orientation for error analysis and fault tolerance. Accurate precision of path planning motion should be based on machine position registration and a few other precision factors mapping machining operation.

5.4.4 Orientation Partition Region of Spider Net Searching

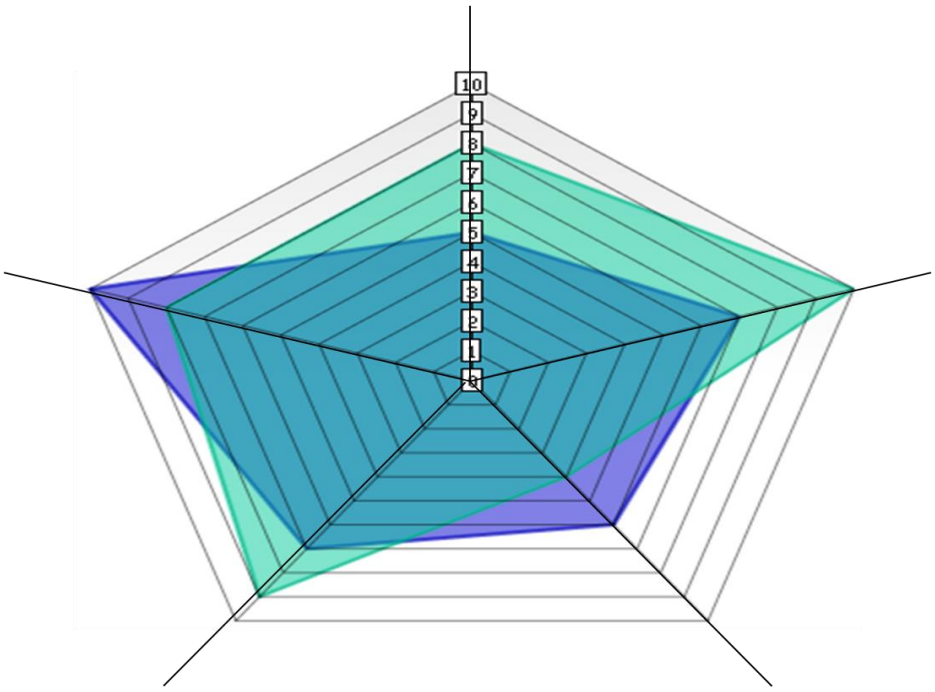

Figure 5.15 Spider Chart and Orientation Zone [83]

Generally speaking, the ring gives fast searching region by distance, while whether we could search by angular position is also within interest. The spider net is just one way of searching based on the orientation move.

The spider net is another way of checking accessible direction. The difference from accessibility map is it gives fast access of radial distribution of orientation zone mapping the target angular region. The angular region maps the most relevant distance and position closest to the right geometry feature so that a particular location can be approached. A radial shaped spider net is shown in Figure 5.15. Each radial line is marked by different orientation angles or metric attributes. Different color region could be marked by user selected metric for distance or speed score so that comparison between orientations may be generated. This way we could mark orientation-related attributes and classify the region by score into different color zones.

As Figure 5.15 reveals, user selection metric could be set with evaluation score regarding the distance of spider chart from origin based on its orientation zone. Each orientation could be tied to a certain attribute of region. The path along the chart formulates its region of graph. For spider net graph, a region is partitioned with several symmetric orientation given a sub-angular region with ranged degree of freedom. Spider graph may give us reference of fast approaching not from ring distance but from angular motion of orientation searching, providing a different region partitioning of fast searching by orientation with distance metric and assigned budget level of boundary. For subtractive 3D path planning, spider chart may help stability study in path planning by orientation region and fast searching by oriented direction with partition.

Compared with accessibility map, spider net path gives fast searching from orientation zone for partition region besides the distance location, and the ring path is based on accessible orientation mapping of every single point along the 2D sequence in 3D accessible space. Spider net is a broad way of oriented searching and may be faster than accessible map in certain cases. For simulation purpose, accessible map is better depending on the dynamic data structure for interactive offsetting operation within ring distance searching region for visualization benefit. Though spider net may be location fast for oriented position searching, it does not simulate orientation computation with the 3D visual material removal process as accessibility map.

The benefit of spider net is that we could divide orientation region into zones based on orientation feature classification. For example, we could label orientation region by partition of the angular space into stable, safe, or dynamic zones for path planning simulation. The label of the region is based on experience and training data of the

simulation output. This way we could label the angular space not just by accessibility but with more attribute assigned by specific metric of measurement. Accessibility map could be enhanced this way for condition analysis and machine diagnosis of geometry part making regarding different features. We may connect the features by classification of similar features to the same partition region of spider graph. This is useful for path planning besides accessibility orientation with user add-on features on path selection, for example a critical pattern or certain mark points for monitoring or sensing purpose.

CHAPTER 6. NUMERICAL FUNCTION FOR NONLINEAR AND LINEAR MODELING VIA RING DISTANCE REGION

This section gives math description of modeling for path parameter tuning and optimization. It helps define the nonlinear feature of capturing the ring path and accessible sequence. Application perspective of data for condition analysis and predictive modeling for path sequence control. It ties the geometric modeling to grid modeling regarding resolution and bounded solution so that the parameter system can be facilitated with the monitoring feature.

6.1 Ring Path Planning by Distance Region of Tolerance Zone

6.1.1 Nearest Searching of Ring by Distance Region

The iterative offsetting happens between tool tip and part surface material within the scale of ring cutting distance area. The searching is embedded into data structure based algorithmic program. Figure 6.1 shows the illustration of 3D voxel with Ring.

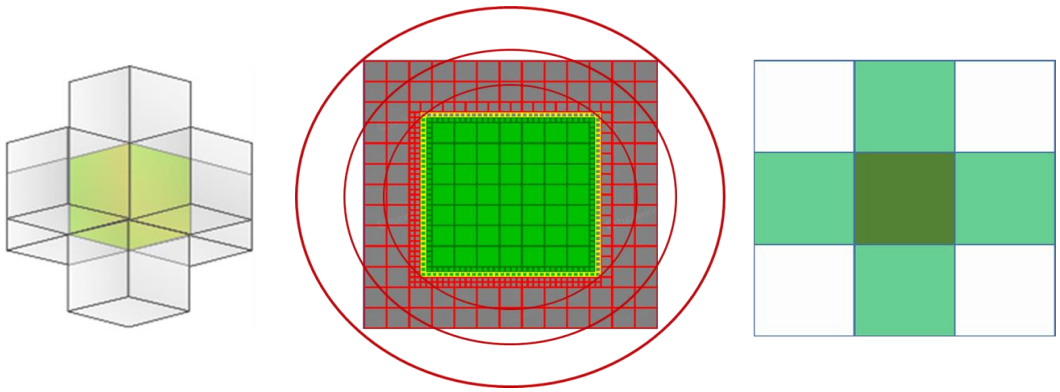

Figure 6.1 Nearest Search with Ring Distance Region

6.1.2 Tolerance Zone of Ring Path in Machine Space by Distance

The ring gives distance-based searching around a center location as origin for initialization of searching towards the bounded solution. The bounded solution is considered a tolerance zone within which the geometry surface is bounded for linear path optimization of machining. The solution domain describing tolerance zone of machine object is modeled as an optimization problem[71]. The distance-based ring centred region gives area partition by distance, as the ring area is defined into multiple distance based nearest ring circle on each path player. Figure 6.2 shows the tolerance zone of 3D Buzz design on the milling part within ring boundary circle.

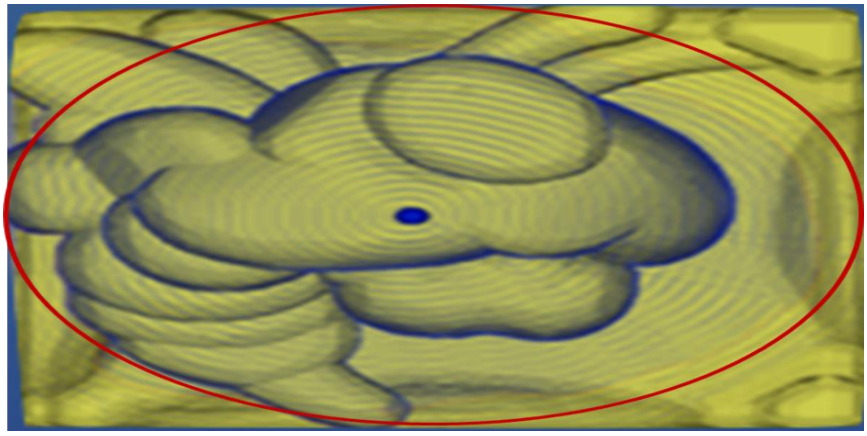

Figure 6.2 Buzz Ring Circle for Tolerance Zone

- Each ring is objective function r^2 for the nearest search in rigid body parameter space for path solution domain, such as formulated in Equation 6.1:

$$\text{Min Obj} = \sum r^2(\text{xi, Ring(S, d)}) \tag{6.1}$$

where xi is points of contact of selected feature, Ring set the zone

- The non-uniform geometry tolerance zone along the entire part for each surface is a function of the surface S and the offset distance value d as cutting depth of ring input.

- Similarly, we put each ring as tolerance zone of linear path in Equation 6.2:

$$\text{Ring}(S, d)=\{x\in R^3 || \text{dist}(x,S)|<=d\} \quad (6.2)$$

The verification of the tolerance T_F for each feature of sub-set surface is formalized by center-initialized ring circle.

6.2 Mathematical Function of Ring Path Modeling

6.2.1 Nonlinear Function of Ring Path Modeling

Numerical "Ring" into linear path is a complex process, in simulation is iterative searching between intersection area along the surface offsetting distance by assigning ring cutting depth. Wk is the condition of the ring optimization function, the solution gives path coordinate (x, y, z) point in 3D space. The linear movement only takes the 3 axis points as there is no rotational need for orientation searching, just offsetting is happening within ring boundary defined by the ring circle size.

$$A_k(W_k)=f_k,\ w_k=(y_k,u_k,p_k) \quad (6.3)$$

As formulated in Equation 6.3, the step ring is the nonlinear function of bounded ring condition. A is the optimization function for W ring input based on ring parameter variables y, u, p which is indicated as step distance, ring path depth and ring circle size. The optimization satisfies the bounded condition for the searching of solution within the

goal of Fk which is usually defined as 0 in function form. When defined in a 3D grid, the solution searching process based on three ring parameters of Wk become ring condition input based on the distance of ring circle size cover area from the ring origin center. Take Buzz model for example, the bounded ring given the maximal reachable area within its tolerance zone of geometric part. The ring gives the distance of searching area from its center such that the optimal solution of path exists based on user defined metric condition.

6.2.2 Linear Function of Ring Path Optimization

All ring has different cutting depth, F is the nonlinear ring cutting effect by accumulation linear ring for path planning of bounded surface area for linearization, f is a number of linear function solution. As formulated in Equation 6.4, a nonlinear function can be summarized by linear function of ring path sequences putting together. Therefore the right decomposition of a nonlinear path could formulate many linear paths.

$$F\,(r) = \sum_{i=1}^{N} f\,(r_i) \tag{6.4}$$

N is the total number of ring cover sequences that are input with different cutting depth d_i for accumulated cutting depth

Sum of each ring depth $\sum_{i=1}^{n} d_i$ is total cutting depth target.

As formulated in Equation 6.5, ring cut height of the i-th iteration of linear path layer can be described as

$$H_i = A_i X_i + B_i \tag{6.5}$$

X_i is defined by the ring-bounded area with key parameters, A_i is the coefficient for linear path solution of searching linear function mapping based on ring vector input of three coordinates for a point of contact position P(X, Y, Z) and H_i is the height of ring circle cutting layer located on a certain orientation plane and Hi is the height-defined i-th iteration of path layer for material removal. B_i is the cutting margin by material left beyond the ring circle of selection area.

As formulated in Equation 6.6, accessible path solution P with k partitions by ring then becomes accumulation of path sequence P_i as discrete path solution in functional form:

$$P[A]= \sum_{i=1}^{k} P_i \left(\left[\frac{A_i}{B} \right] \right) \tag{6.6}$$

Each ring index i is based on its accumulation of located plane layers. A_i is the linear mapping function based on the ring point coordinate vector, and B is given condition by the target of design.

6.3 Application of Path Sequence Modeling

6.3.1 Bayesian Modeling for Stochastic Optimization of Path Dynamics

The purpose of Bayesian modelling is based on condition analysis given the previous information. As we have two points for connection along the sequence, both point accessibility conditions are required. Changing of one-point condition such as cracker of path or change of user metric selection may affect accessibility of point one and also affecting the resulting accessibility of the sequence connecting point one and point two. Bayesian modelling thus provide stochastic analysis of path dynamics based

on changing conditions. Path dynamics could be caused by change of user section metric or collision of another path orientation. Feature extraction requirement may also be another reason why one-point accessibility condition is changed.

6.3.2 Bayesian Modeling via Sequence Condition

All sequence models can be put together as condition-based probability sequence model. Equation 6.7 shows the merging of two path accumulation, where D is point of new tool position, and A, B as previous sequence points:

$$P(D/AUB) = P(D/A) + P(D/B) \text{ if A, B are independent} \quad (6.7)$$

- For extension of this idea, in fact the following aspects are also true, assuming the first path sequence is A, the second path sequence is B. As formulated in Equation 6.8, the total depth of cut is summation of all sequences.

$$D=Depth\_A + Depth\_B \quad (6.8)$$

- Nonlinear curve can be summation of linearized partitioned curves with lower precision, although linearized accuracy depends on partition ratio of the nonlinear function for the closest estimate.

- Take condition of class C1, C2, C3 into consideration, then we could have fusion of data in all conditions by C1, C2, C3 as evidence of data measurement.

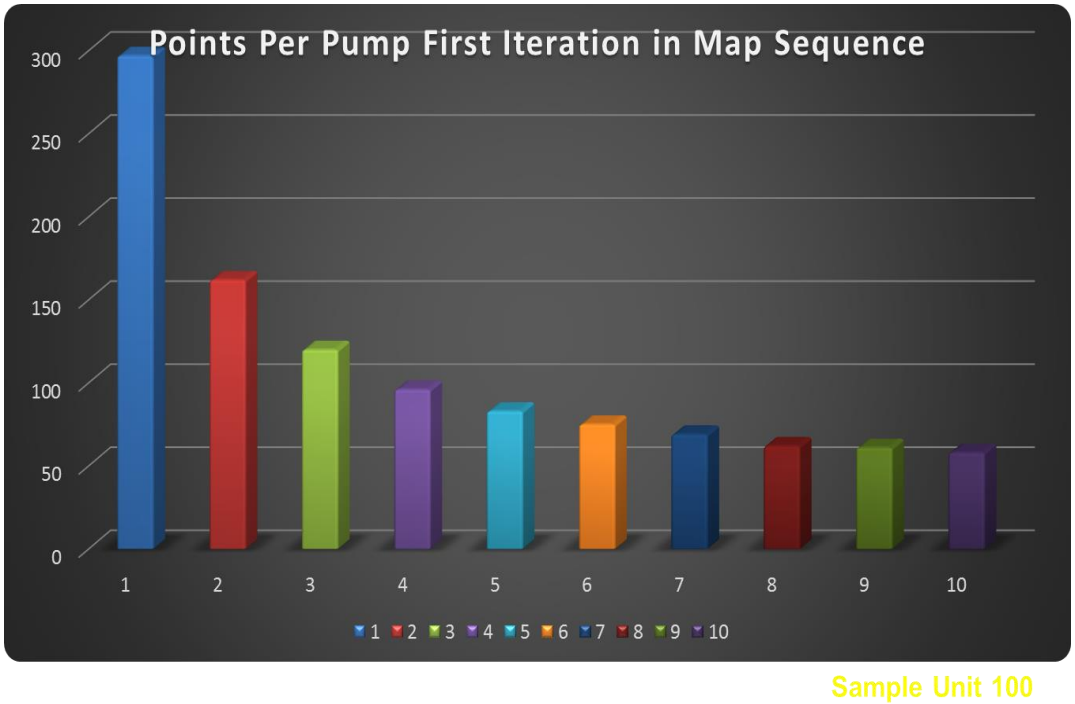

Figure 6.3 Map Sequence of Points per Pump for First Path Iteration

We can simulate the points for each sequence of path based on the cutting depth of ring path input. The points based on sampling frequency of Buzz model path is shown in Figure 6.3. The more points of data collection for the same time frame, the less points of margin for sampling gap distance.

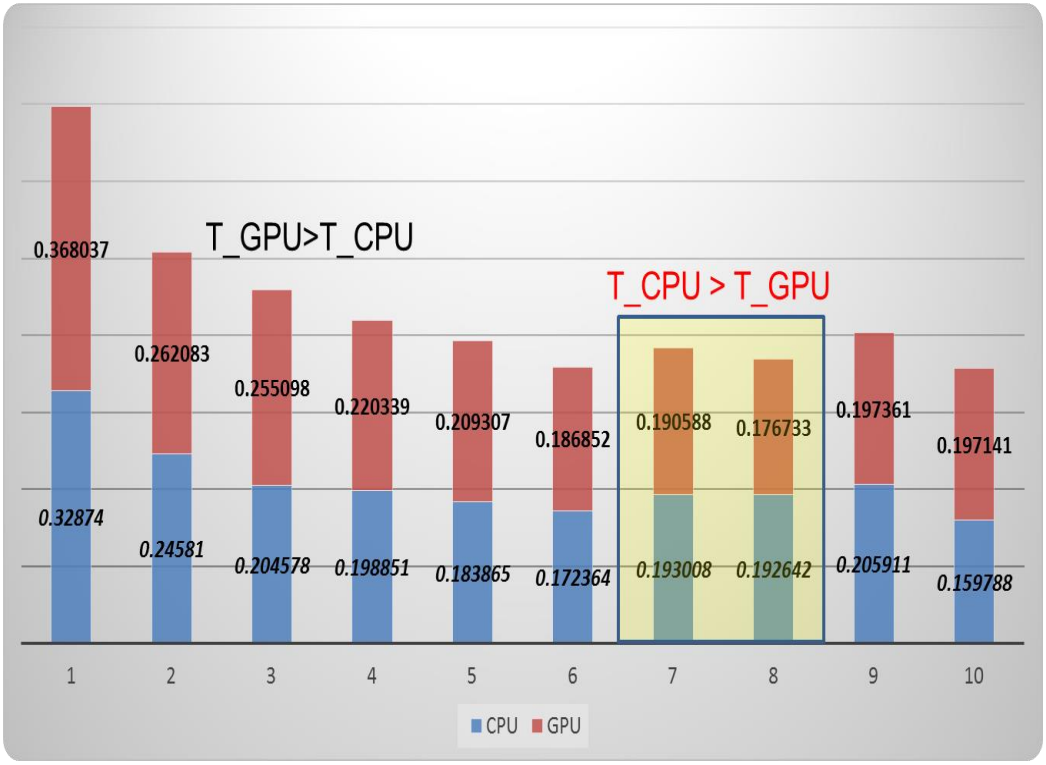

Figure 6.4 GPU and CPU Sequence Runtime Comparison

Figure 6.4 shows GPU and CPU sequence runtime comparison of path planning result from Buzz model. From the result we can see that although GPU runs large workload faster than CPU, due to communication of data sharing, small workload runtime by GPU may be larger than CPU runtime. Therefore, data sharing bottleneck is one tradeoff we need to consider while running GPU workload. Larger workload is more suitable running on GPU for faster performance.

6.3.3 Predictive Modeling for Path Sequence Control

The purpose of predictive modeling is to give hint for reference of fast performance by simulation as well as learning of user behaviour for optimization. It may

enhance parameter tuning precision of sequences for next simulation freedom trial for experimental purpose.

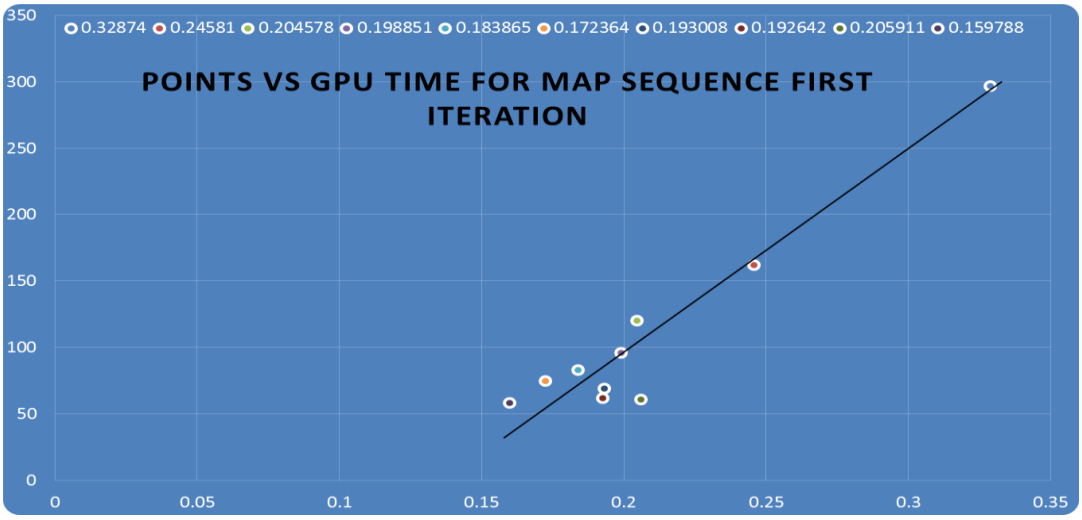

Figure 6.5 Linear Modeling of Path Sequence Points for 1st Iteration Depth for Cutting

The prediction precision of sequence is a value of how software stochastics may help analysing the linear modeling of path. The time performance generating each point is quite linear according to the mapping of linear data modeling. The linear curve intersection shows the mapping linear behaviour for a linear model. Figure 6.5 shows the process of path-point modelling for map sequence generation for the first iteration. Figure 6.6 shows the process of path-point modelling for map sequence generation for the second iteration with same cutting depth.

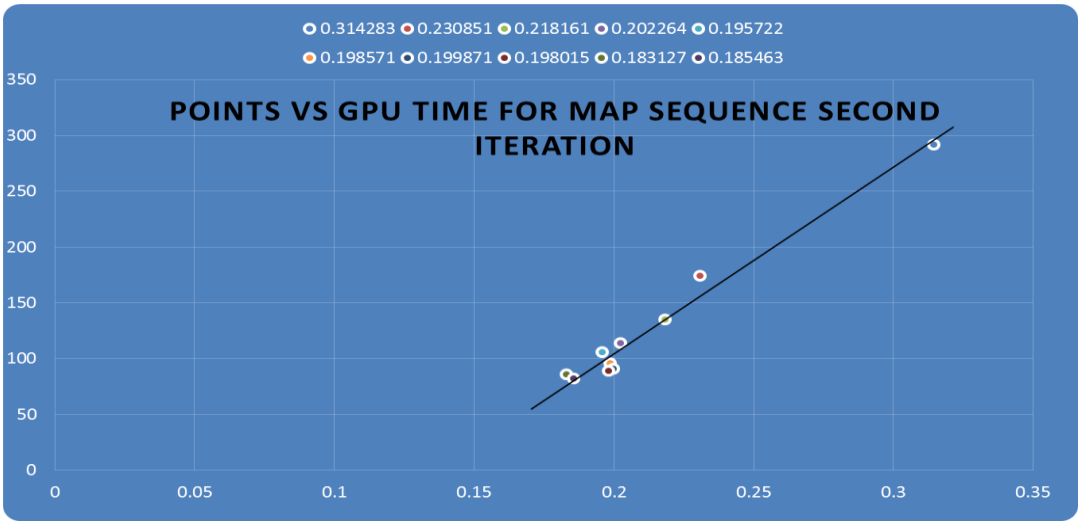

Figure 6.6 Linear Modeling of Path Sequence Points for 2nd Iteration Depth of Cutting

From the linear prediction and modeling results, we could see that

- As formulated in Equation 6.9, points of path sequence follow near linear relation for time response:

$$H_i = A_i X_r + B_i \tag{6.9}$$

- Cutting depth 3 mm for GPU simulation of Buzz follows linear behavior as the above data simulation is generated from 3mm cutting depth input of ring.

- Feedback control set the goal of error with reference for minimization within boundary so that the time response of path sequence is within the time limit.

- In addition, path planning by depth volume removal the almost follows by path iteration in linear space partition by cutting depth within 3mm; Data points deviation via time prediction is be higher for deeper depth-based path planning

6.3.4 Evaluation of Predictive Sequence Modeling Accuracy and Success Metrics

Mean square error (MSE) calculation can be used for linear modeling accuracy and measurement of linear fitting model, and also for linear prediction success measurement. Equation 6.10 shows the metric.

$$\sum_{i=1}^{n}(\widehat{T}_{\iota}\text{-}\mathrm{T}_{\mathrm{i}})^{2} \tag{6.10}$$

$\frac{1}{n}\widehat{T}\iota$ is the vector of n predictions, consideration of data attribute may also include:

- Distribution of Data
- Remote Deterministic for Variation
- Majority Counted (e.g. False positive by predictor)
- Ignore Large Variation Point as Random

6.4 Grid Modeling Application for Buzz Geometry Representation

In subtractive 3D printing, user pick model they desire to make at the given format allowed by software, and the model is then processed with path planning model in order to have ready to make G-code for production line. Grid modeling and dynamic tree form the data structure support of running workload from software perspective of workload request based on user need regarding model as input, and the grid density provides estimated approximation measurement for detailed model positioning and shape identification in computer vision perspective. The size of model can be analyzed by rough kernel size of grid density when there are intersection of model edge and grid lines.

These grid lines kind formulate the structure of model in a numerical grid lines that is more like similar form in size but in cubic shapes, then any curve line can be similarly represented as the number of grid near these edge curves around the model geometry surface. The topology of grid shape inside the model can then give an identified function of different geometry in simple kernel pattern.

In order to have an application perspective of how grid modeling by different tree depth input may affects the accuracy of modeling by numerical measurement after sampling, we pick various depth input and display the model geometry in grid kernel mapping with the image of model intersection in shape. This way, the geometry filled with grid kernel lines can be represented in numerical form if we want to do further sampling based on the required density as we want. For depth variation input based on model geometry with tree structure, we tend to have the mapping between model and the 3D structure of tree with kernel rendering to analyze the model geometry and shape quality for early phase of planning.

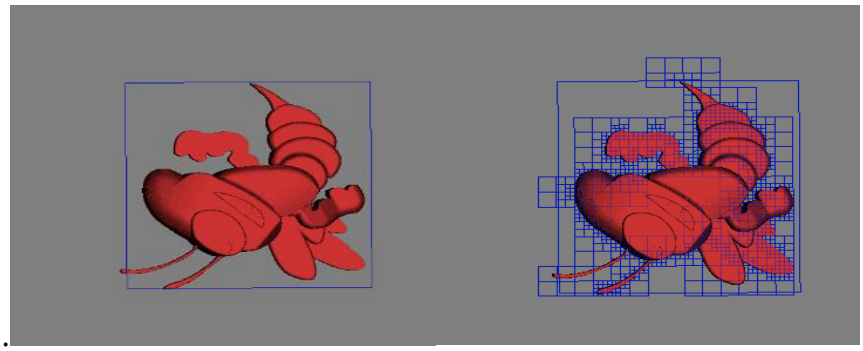

Figure 6.7 Buzz model and Tree Formulation View

As Figure 6.7 displays of the 3D visualization of original Buzz model, which runs by the HDT(hybrid dynamic tree)-based grid intersection of Buzz model geometry.

Depth based tree model not only depicts the graph geometry accuracy on a displayed grid form but also gives a rough estimate of the complexity of model geometry and sizes. Figure 6.8 and 6.9 display the tree depth input from 0, 1 and 2, 3 as depth inputs in order to have a comparison between the geometry with grid modeling measure so that the estimation of model can be relatively represented by grid kernel. We apply 3D simulation data regarding Buzz model in subtractive 3D printing for path planning using mostly point cloud of data based on STL model.

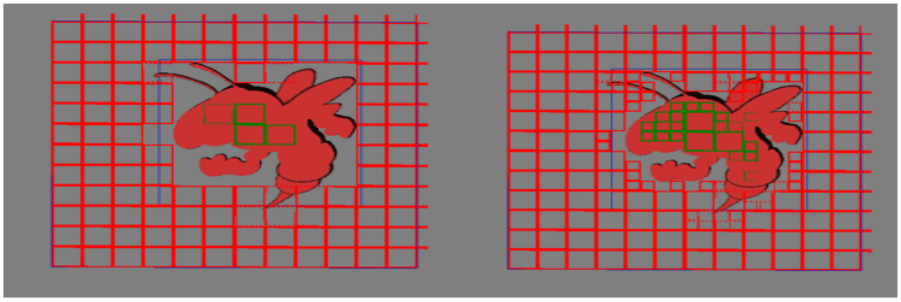

Figure 6.8 Buzz with Input Tree Depth of 0, 1

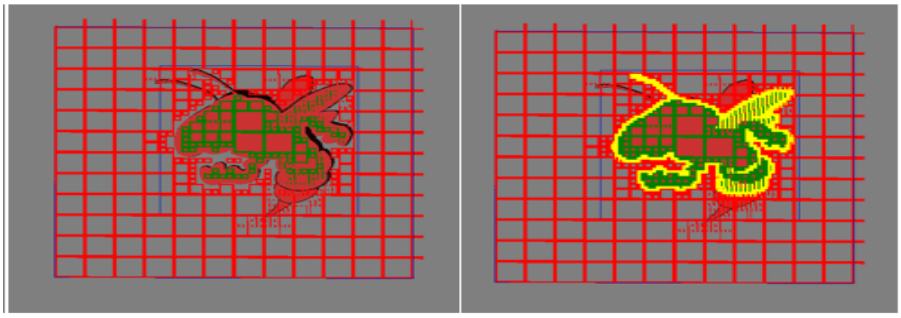

Figure 6.9 Buss with Tree Depth of 2 and 3

6.4.1 Image Processing Application for Feature Remodeling

Besides measurement of approximation accuracy in numerical form of sampling, another grid application is that we can enhance image feature or ignore inner local geometry feature for rough modeling perspective for feature enhancement or feature highlighting such as edge remodeling shown in Figure 6.11. In order to do that, we have feature lines extracted in order to have desired depth analysis. For tree depth with maximum 3 for 3D structure representation, we tend to change the min depth of tree so that we can have a comparison look. The edge curve can then be extracted and formulated as output for further 3D printing such as foot print image or highlighted view of boundary image feature in shape. Figure 6.10 depicts the above process of adaptive depth input leading to remodeling output by edge lines. Figure 6.11 is the application output of feature remodeling based on Figure 6.10 processed data, compared with the original model remodeling output for STL remodeling formulation by 3D structure image view. From the results, we can tell the inner feature of image is filtered out after grid adaptive processing of model 3D structure processing. There are also some resolution losses for feature remodeling application. Here we apply remodeling by image transformation into STL model based on 3D adaptive depth.

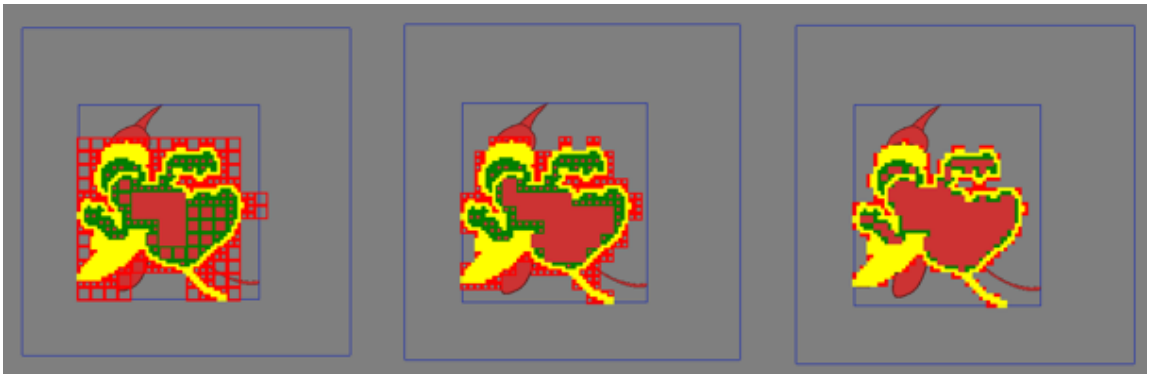

Figure 6.10 Grid Depth Variation from 0,1,2,3 for Buzz in 3D Structure View

Figure 6.11 Feature Remodeling after Grid Application

6.4.2 Color Comparison

The color difference in image grid structure reflects the 3D depth in space formulation. Figure 6.12 shows feature remodeling view of Buzz before and during remodeling with 3D grid structure. The gray image and color image of 3D grid view after processing and remodeling shows the contrast of feature highlighted in order to have local key body region classified as only one wing and one antenna are displayed on the same plane due to height plane difference in 3D space of model geometry rendering.

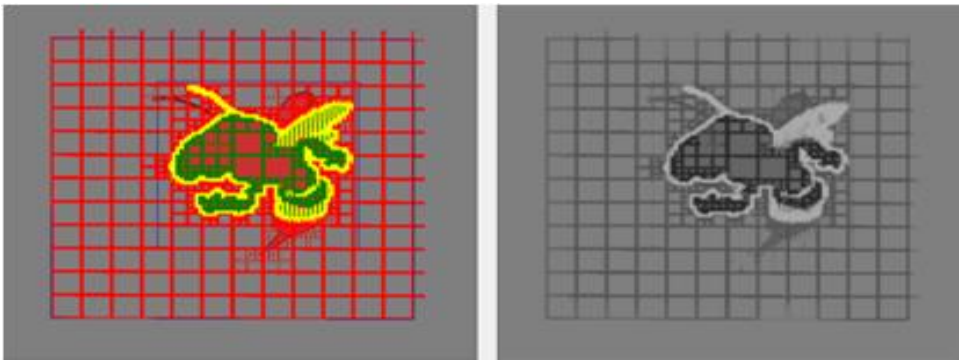

Figure 6.12 Gray and Color Comparison of 3D view

6.4.3 Modeling GPU Time and Volume Density for Load Forecast

We observe that modeling of GPU via adaptive tree depth get affected by geometry sizing and volume density. Assume the user interaction is stable for most user request in order to have subtractive 3D printing for whole system process, we ignore differences between various groups of users under standard operation and pick geometry size as the major targets of software modeling time cost target for large user volume analysis in system perspective. Now we see individual model Buzz and how the rendering time may have difference on GPU data formulation and dynamic tree support in model geometry mesh loading operation.

Figure 6.13 shows the visual software prototype of display monitoring window for various geometry models of 3D STL with performance response time and simulation thread data. The monitoring window with geometry and data in parallel provides better comparison and analysis for performance optimization purpose. Most simulation results in the thesis come by performance data monitoring while doing simulation in path planning process. The visual display also provides fast inspection of geometry shape and size for accuracy validation of path. The origin of ring path is later assigned to a certain geometry position that is mostly central of the target image. The models displayed are candle holder, head, fan and teapot from top view perspective. All models are bounded within the stock geometry size of cubic shape for subtractive path planning purpose.

The design of monitoring window will be discussed in later chapter with graphical map design and bounded data limit for condition analysis for evaluation purpose. Data

evaluation and condition analysis could be used for danger detection purpose towards efficiency in monitoring. Possible danger includes path collision and other problematic conditions that need protection procedure in an adaptive situation.

From the monitoring data, we can tell from monitoring tool that the model geometry size and complexity as well as density of HDT tree formulation all affect the GPU rendering time of a particular 3D STL model based on given data structure of hybrid dynamic tree in topology and dimension. We assume fixed dimension of tree leaf and tree root node of data structure by default definition in software prototype. Deeper depth of tree formulation tends to have longer latency time and longer data query due to model geometry structure and volume density of higher resolution.

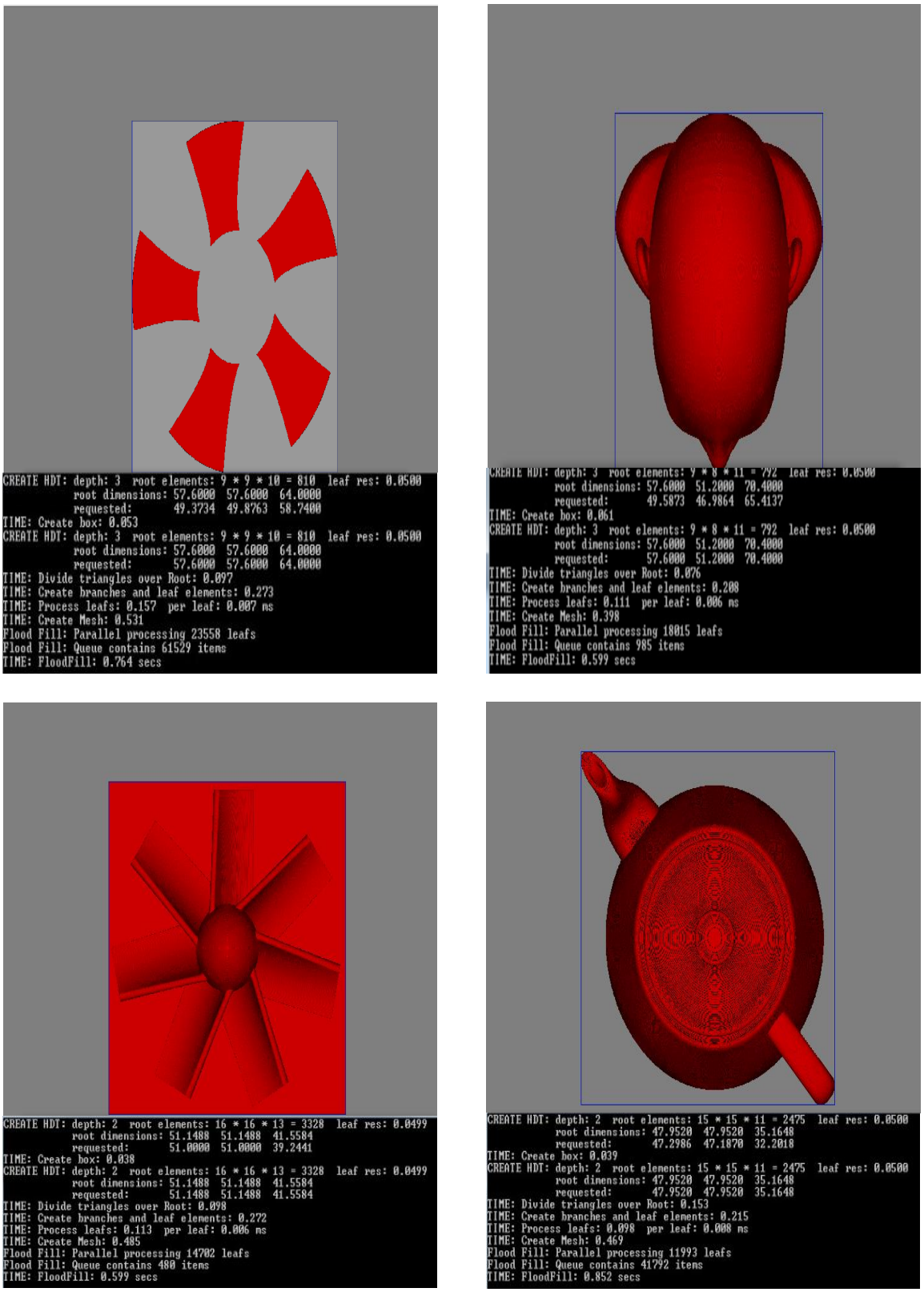

Figure 6.13 Monitoring Different 3D Geometry STL Models with Data

CHAPTER 7. DITITAL PARALLEL DATA METRICS

This chapter gives results of sampling in the path sequence generation and parallel task workload. It includes map kernel structure of parallel workload and digital metrics.

7.1 Parallelism Map Access Pattern by Data Parallelism and Task Parallelism

7.1.1 Discrete Sampling of Accessibility Map Sequence

Sequence of path generated with subdivision of linear path iteration lead to output sampling result with points and time as key parameters. We changed the code input for variable setting of accessible map resolution simulation from path planning testbed with path sequence sampling rate from 1-10.

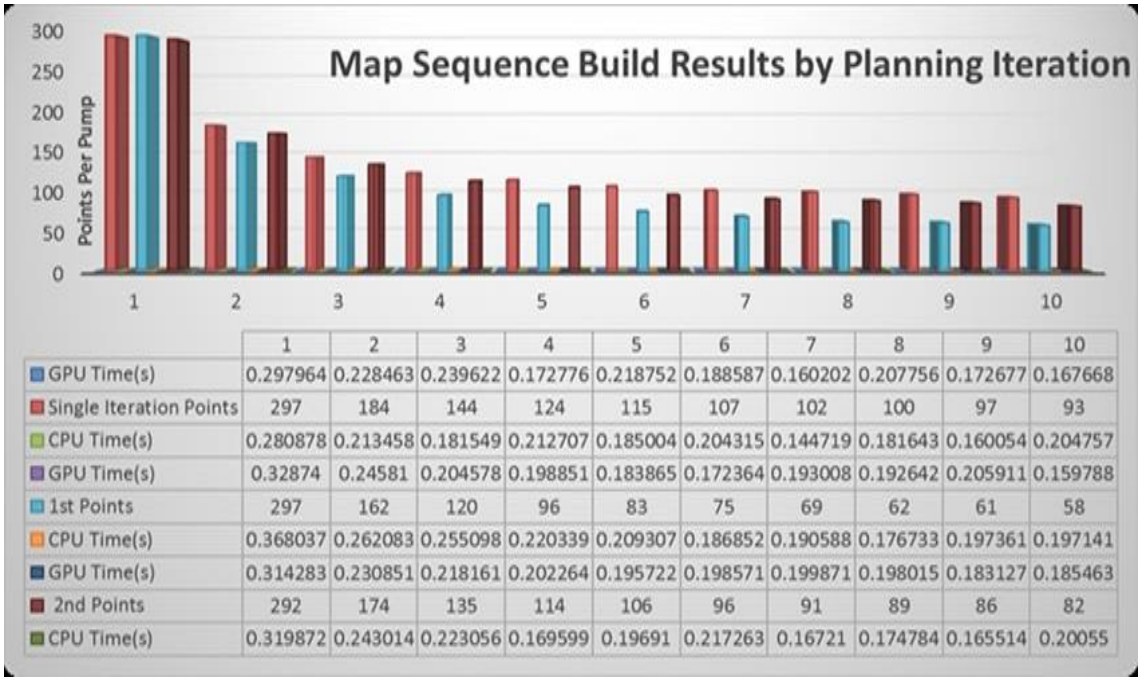

	1	2	3	4	5	6	7	8	9	10
GPU Time(s)	0.297964	0.228463	0.239622	0.172776	0.218752	0.188587	0.160202	0.207756	0.172677	0.167668
Single Iteration Points	297	184	144	124	115	107	102	100	97	93
CPU Time(s)	0.280878	0.213458	0.181549	0.212707	0.185004	0.204315	0.144719	0.181643	0.160054	0.204757
GPU Time(s)	0.32874	0.24581	0.204578	0.198851	0.183865	0.172364	0.193008	0.192642	0.205911	0.159788
1st Points	297	162	120	96	83	75	69	62	61	58
CPU Time(s)	0.368037	0.262083	0.255098	0.220339	0.209307	0.186852	0.190588	0.176733	0.197361	0.197141
GPU Time(s)	0.314283	0.230851	0.218161	0.202264	0.195722	0.198571	0.199871	0.198015	0.183127	0.185463
2nd Points	292	174	135	114	106	96	91	89	86	82
CPU Time(s)	0.319872	0.243014	0.223056	0.169599	0.19691	0.217263	0.16721	0.174784	0.165514	0.20055

Figure 7.1 Accessibility Map Resolution by Processor Time

Figure 7.1 shows point difference resolution matter mostly for first three gaps of data resolution of high frequency load samples. This is likely due to major information loss of geometry shape topology convergence after first three sampling resolutions. Larger sampling gap tend to have more information loss. GPU computation is on average faster compared to CPU running computational load regarding sequence generation of map as well as graphics and parallel simulation.

7.1.2 Parallel Map via Data Access of Accessibility Sequence

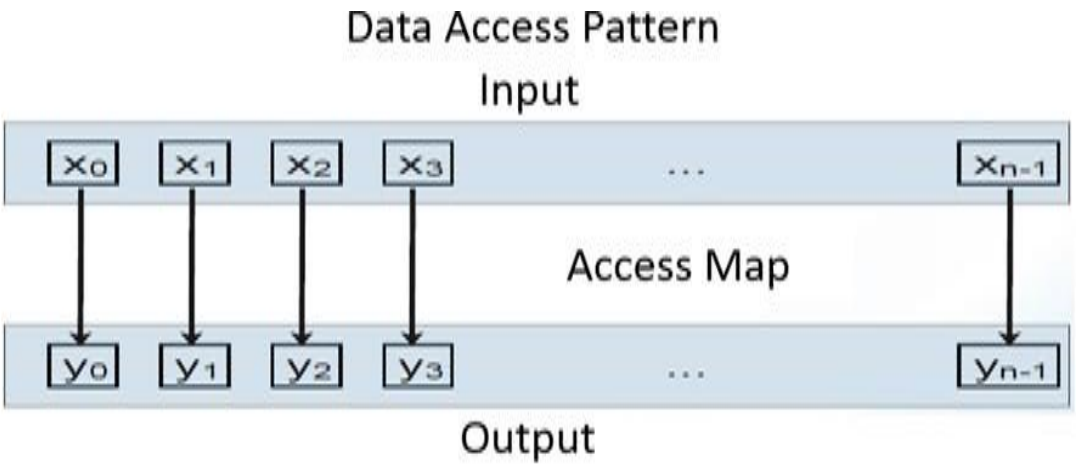

Figure 7.2 Data Access Pattern of Accessibility Map

Sequencing is important for data access especially for gene diagnosis and pattern detection. Sequence of data is generated for accessibility map computation by parallel GPU pump. Figure 7.2 is the access mapping process between data sequences and accessible region as non-zero regions.

7.1.3 Cross-Layer Parallel Computing of GPU Pump for Multi-Kernel Map

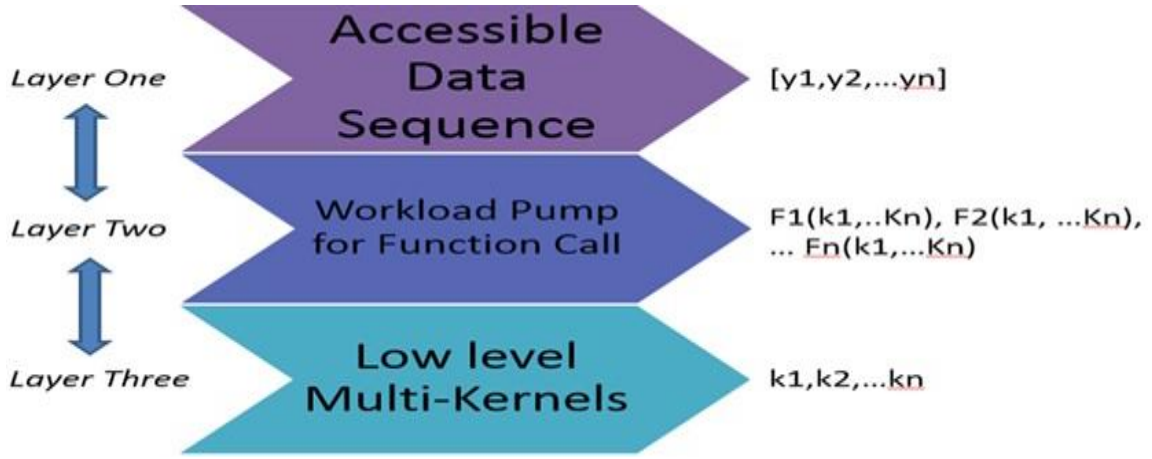

Figure 7.3 Parallel Multi-Kernel Structure of Accessibility Map

Kernel concurrency is hard due to task dependency, as multiple kernels can't be mapped to the same concurrency kernel due to their task dependency. This is why we need cross-layer structure. Multi-kernel parallel structure is shown in Figure 7.3. The first Layer takes care of sequence for data access. The second Layer takes GPU pump for each sequence for function call of the lowest kernel layer of parallel kernels.

7.2 Digital Metrics of Manufacturing Simulation Optimization in 3D Printing

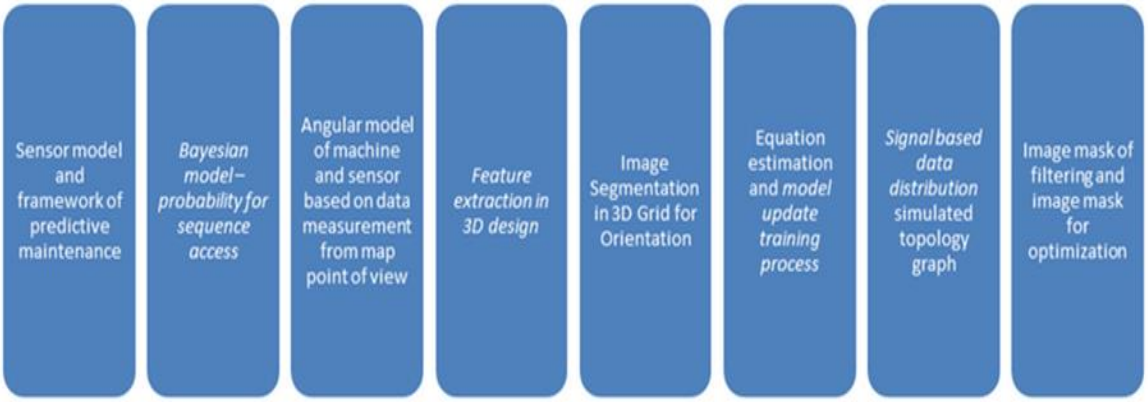

Figure 7.4 Digital Metrics of 3D Printing

The purpose why we simulate the path is to predict outcome of different path planning strategies, so that we could get optimal parameters. Figure 7.4 shows example digital metrics relevant to the 3D printing process. Digital metrics such as feature extraction or signal-based data distribution by topological graph help 3D design analysis and provide precision output for simulation optimization. Accessibility of sequence probability of certain path route based on selected digital metrics helps an effective decision making.

7.3 Scalability Study of Multi-task in Parallel Cloud/Fog Computing

Manufacturing Cloud/Manu-cloud for Simulation: The cloud provides features in manufacturing tooling like milling, turning and drilling operation to remain path generation function for manufacturer but also takes advantage of cloud computing feature to provide data synchronization. The manufacturing cloud-based data analysis provides data centered manufacturing and virtual platform for VM testing and remote experiment. To understand how each cloud feature may improve the manufacturing process in a digital way, we focus particularly how the path planning happens in software level and most of time human-centered interaction also happens a lot for decision making in 3D design.

Features of Cloud Computing Metrics In this thesis we only consider the virtual cloud for path planning in simulation as online storage of virtual machine data center and remote access platform for task assignment of online software service which is free of location. We consider features include multi-tasking, parallel processing, critical dependency, and user-oriented service and simulation as well as task distribution. By classifying groups of user simulation data and breakpoint of file reading, we may speed

up parallel tasks by scheduling group task classification by load categories in service-oriented cloud, to reduce response time or power. We will show more description in the thesis.

Cloud based Parallel Computing: The cloud platform looks like parallel computing in similar form but has its own featured design and application. It is our future research direction. It helps distribute workload and provide virtual platform simulation.

The data analysis of manufacturing cloud provides data centered manufacturing and virtual platform for VM testing and remote experiment. To understand how each cloud feature may improve the manufacturing process in a digital way, particularly as the path planning happens in software level and most of time human-centered interaction also happens a lot for decision making in 3D design.

From previous study, fog computing provides local cloud as relevant small-scale analysis while cloud computing has its featured mobile communication and robotic extension in a broad application sense. Possible ways for cloud analysis could be service-oriented cloud, map structure-based analysis, and topological graph-based analysis in a scalable way regarding accessibility and social network feature, etc. By analysis, we aim to get performance optimization tradeoff in a parallel way based on cloud platform and application extension so that software features could be further maximized for simulation benefit of path planning.

Figure 7.5 shows a service-oriented cloud structure with multiple level of layers for processing [72]. A main cloud relates to other sub-cloud through network structure.

Each cloud could become a center of task of jobs for processing data sequences and workload pump in parallel.

Since we use software path simulation for path planning optimization of 3D printing in manufacturing modeling, therefore all the simulation rest on computer is similar to cloud-oriented services running on PC machine.

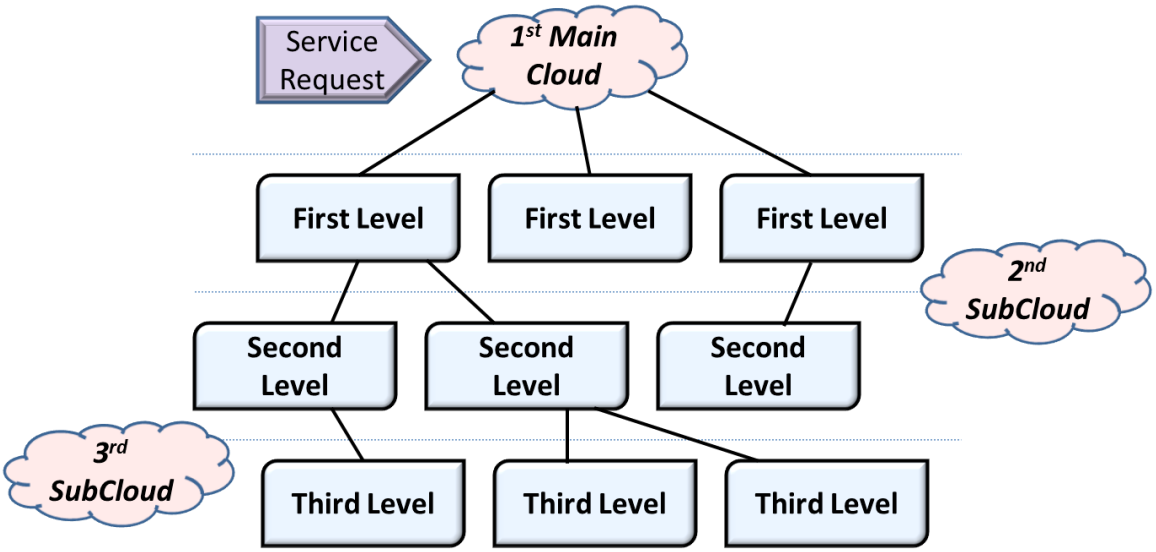

Figure 7.5 Service-Oriented Cloud [72]

7.3.1 Distribution Computing Platform

Cloud and Virtual Machine are major platforms for virtual environmental sharing of data and application in parallel. Large clusters also provide efficient tools for distribution of load across all levels given right merging schema. The key challenges involved in current information sharing system calls for better communication structure and more efficient data sharing. Enhanced system architecture could be involved to provide strong computation capability and data sharing platform for carry-on practice.

Researchers and companies select data for decision making purpose, and data should be representative of chosen service metrics with considerable care so that only key information that contribute to the performance and decision are looked at. We aim at green load decomposition of tasks that enhance service-oriented-data sharing and energy efficiency of distributed platform and data transmission with sharing platform in parallel.

7.3.2 Manufacturing System Structure

The hierarchy of systematic solution for manufacturing system usually includes: design of model, design of software and machine operation. Our work involves all three of them as follows:

- For design of model we build 3D pattern based on image feature of 3D reconstruction model and do 3D scaling for sensitivity-controlled path.
- For design of software, we put human interaction with software parameter testing and tuning, via Blackbox operation or freeform parameter selection for optimal path simulation based on geometry visualization.
- For machine operation, we consider the range of operation capability and provide collision free and multi-axis operation based on G-code path planning.

Figure 7.6 shows how path planning with current application workload processing structure and how it works in cloud service-oriented platform. The cloud provides online and remote service of software. In subtractive 3D printing, the STL model gets into mesh format and is then loaded into hybrid dynamic tree data structure to map our early input of 3D volume generation. Hybrid dynamic tree has been formulated from static structure

with enhanced dynamic structures for each of its grid division into sub-tree structures for model geometry representation. The original map can be 3D bitmap and the data are dynamically generated to fit the size and distributed location via different tree branches so that each tree element can represent analytical information of a model that gets loaded via the tree structure. Usually the model after tree representation has been divided into three HDT states: inside, boundary and outside. The part that gets outside of a tree representation structure can either be marked as empty or off-boundary. To define the surface of model and consolidation quality, the intersection of tree and model with half fulfilled state of tree leaf element is considered as boundary. The inner side of tree is usually marked as full state in its tree element representation. The hybrid dynamic tree (HDT) gets most of its operation through GPU and 3D rendering speed thus gets enhanced speed up a lot compared to CPU version as the normal tree representation over CPU incurs heavy workload even in parallel program with full workload containment for a single pc memory and load capability to sustain. The HDT data structure gets depth formulation based on model-driven workload and would have timing difference due to its topology and tree dimension set up as the data searching or rendering has to go through the tree depth level in order to reach its target. Assume the platform is fixed with given topology of data, large workload due to complex geometry shape or high computation geometry number will have longer processing time. Thus the data structure relate to the model-driven workload by platform latency and traverse time of data loading.

For analysis purpose and training data model, the information flow for data analysis that we generate order usually is:

Data → Theory→ Concept of Idea → Problem Objective Function

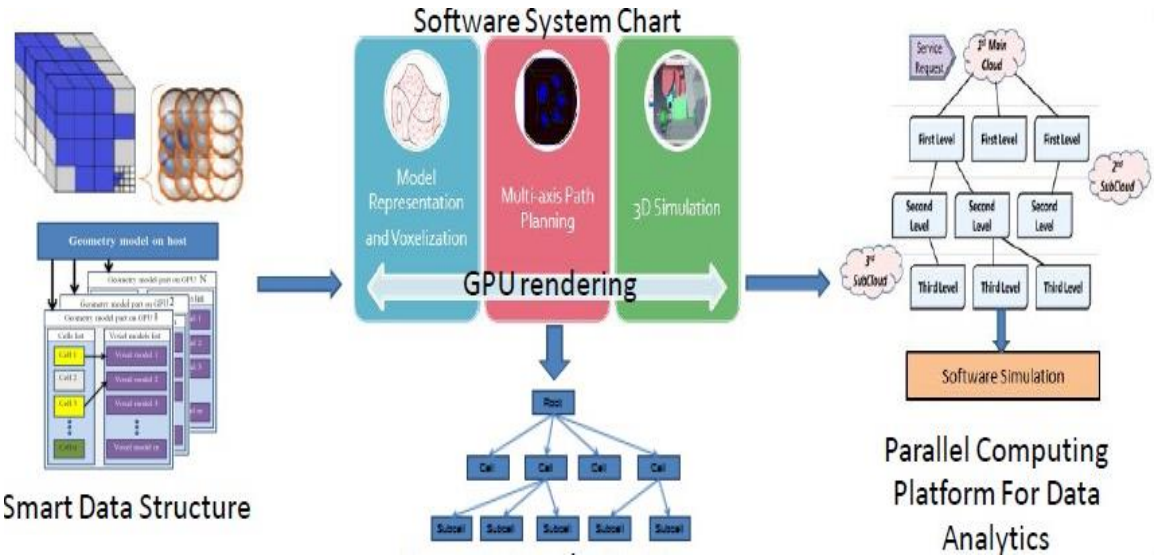

Figure 7.6 Data Integration Structure of GPU with Cloud Computing Service

7.3.3 Cloud Metrics for Data Analysis or Energy Informatics

A lot of digital metric works for data analysis purpose, we currently consider the following aspects:

- Benchmarking of simulation data
- Extending the cloud service
- Evidence theory of measurement data
- Machine learning for numerical modeling
- Focus of attention for prediction
- Network connectivity and topology
- Geographic network subsystem for distributed computing
- Failure as an option for sensing and monitoring

For cloud computing, we mostly consider data integration and the process is the same as ring path planning process shown in 3D printing. Figure 7.7 shows energy informatics and chart of cloud application orientations.

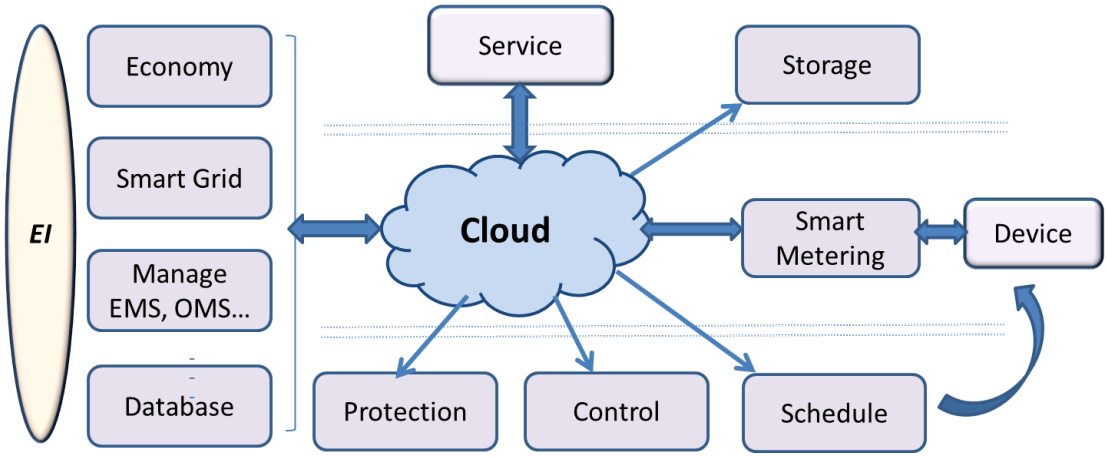

Figure 7.7 Cloud Relation to Application Areas [72]

The idea of Cloud for Energy Informatics, aiming to build the link between cloud and Energy Informatics and find out all mutual benefits between the two. Due to cloud computing's flexible computing abstraction and its functional role of linking resources. Cloud computing can work as a device control center using smart metering based on energy information or simply serves as a data hub. Additionally, for service sharing, cloud computing can have specific software developed and installed to support high performance computing in domain-specific and cross-domain applications.

7.4 Scalability of Multi-task in Cloud Computing

Cloud based Parallel Computing: The cloud platform looks like parallel computing in similar form but has its own featured design and application.

Data sharing and Distributed Computing would be potential impact based on cloud case study of path planning while data informatics for green computing may also work for computational efficiency. Data sharing is fast and convenient free of location and client machine as we could pick thin client for cloud sharing. Data synchronization is mostly applied in modern software application in mobile or PC platform. We will better understand the tradeoff of workload for each task in the 3D printing design process while we simulate the process on parallel computing platform, such as clusters or remote sharing resource online. As each computational center is connected with others by network environment, we plan to look at the optimal of connectivity regarding accessibility based on local structure of the load or task assignment for better scheduling efficiency and data communication speed if possible either through mobile application or parallel workload distribution. Possible ways we could look into the problem include discrete event simulation besides software experiment.

7.5 Speed Challenge and Service-Oriented Network Design

Cloud distribution tree is described for green computing and managing network service activity with algorithm similar to P2P logic to rank users according to their service ID and availability in a hierarchy [73]. Figure 7.8 shows its designed structure base for cloud energy management. In this paper, we keep the design of logic tree distribution for cloud and further divide service according to their priority and requirement level. The relation of service with cloud is also shown in Figure 7.8. The reason why we divide service level is because not all services are preferred by users to run in the cloud. People argue that they want the computing capability of their own personal computer.

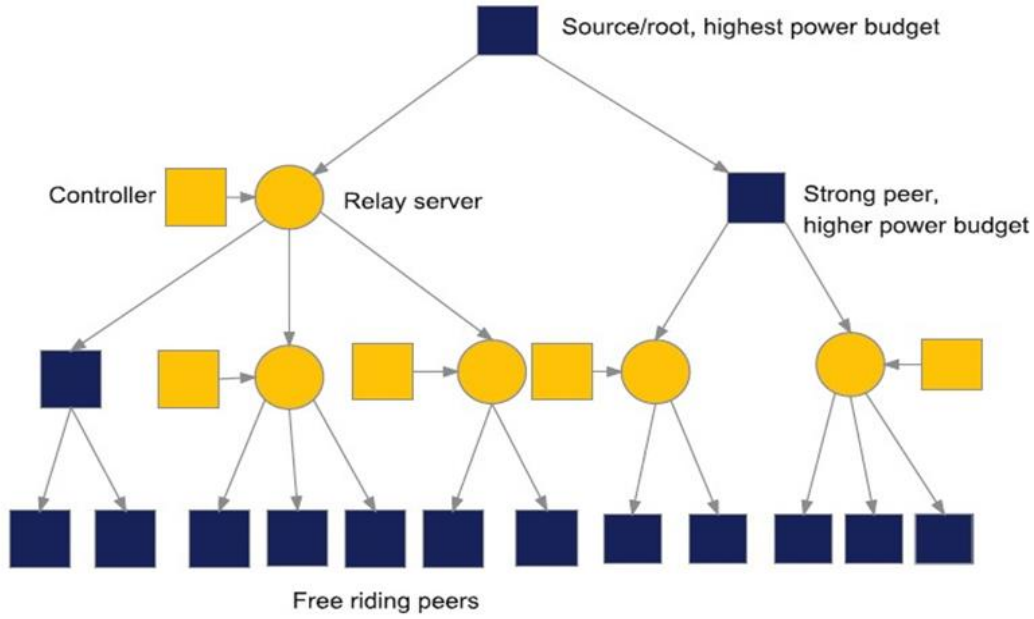

Figure 7.8 The Distribution Tree of Cloud. Rectangles are peers while circles are relay servers [73]

The P2P structure can work for query-based application and does not conflict cloud computing to provide powerful high-performance computing capability service. However, to be more efficient and give more freedom of choice regarding the services, we divide service level so that they can be handled differently in the cloud. For example, for expensive software to purchase such as Matlab and its Simulink toolbox, the cloud can provide shared service with higher level for users while for other software services of path planning users have more economic access and freedom of choice like C or Java. Therefore, it may have lower access level compared to the expensive and secured data access. Therefore, the idea of service cloud level is to classify service according to the property and requirement rank in the cloud, so that service itself has a hierarchy in the cloud tree and can be taken care by different kind of cloud center (e.g. main cloud or sub-

cloud in different level). Each cloud can have its own controller, the same as the controller shown by rectangular in Figure 7.8. On the other hand, this higher-level cloud called main cloud could then be used for sharing domain-specific solutions distributed across sub-cloud, thus enabling those sub-cloud domains to share analysis tools and programs that utilize the concepts and relationships from the main cloud.

7.5.1 Features of Cloud Computing in Manufacturing

Besides data, the features we consider include multi-tasking, parallel processing, critical dependency, and user-oriented service and simulation as well as task distribution. Multi-tasking determines whether we do multiple tasks in parallel.

- Parallel processing gives parallel solution for distributed workload or assignment that aims at the same goal for synchronization for fast speed.
- Critical dependency can be described by tree hierarchy as node is distributed over the links to higher level of node, and could be dynamically generated in simulated form to represent user interaction in the cloud.
- User-oriented service determines user input and interaction as key resource to analyze the data and input. Network simulation based on user simulation number as discrete event simulation provide ways to describe how the variation of services between users may affect the online service regarding performance.
- Task distribution is important as ways to optimize workload and reduce data to allowed level or optimal portion so that distributed manufacturing could apply distributed computing for enhanced strategies and task scheduling. Our applied

G-code partition belongs to this category solving task distribution regarding large workload.

- Rich data could include big data and compressed data with data information such as graph structure.

Software simulation for path planning operation formulates task of different sequence as user application input. Application of various domain runs on the cloud for service-oriented computation and control. The process of described cloud computing structure is shown in Figure 7.9:

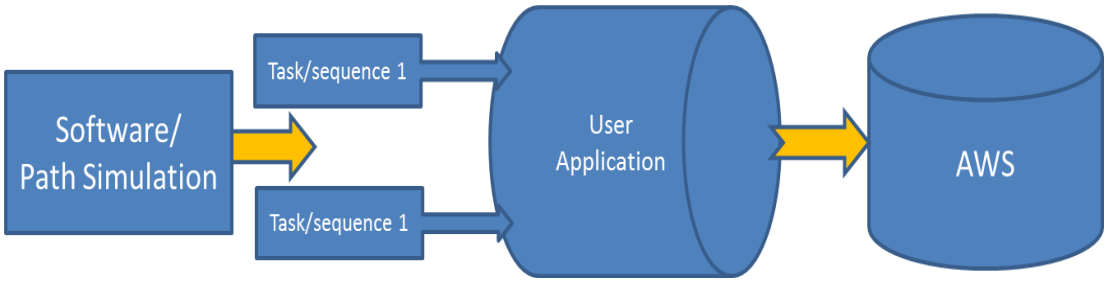

Figure 7.9 Cloud and Task Data Sequence of Path Planning Simulation

Figure 7.10 shows feature-based modeling and forecast based on data analysis system, here data include geometric feature and pattern of 3D information. The process includes six steps from Data Acquisition from Simulator to Load Forecasting with all steps formulating Data Analysis System. The major contributed steps of path planning are Data Acquisition step and Classifying/ Optimal Region step as ring path selects the optimal region with boundary. Load Modeling and Load Forecast are application steps after path planning simulation based on data selection. Data preprocessing happens before pattern recognition and feature identification. For subtractive path planning, Data

Pre−processing includes 3D reconstruction, model fitting, model scaling and reorientation. Data post-processing isn't included here as it is basically applied for G-code optimization at the last phase of subtractive path planning. The simulator generates original data that works for later analysis and pattern recognition process. Load modeling works based on these generated data and gives forecast vision for data compensation from analysis perspective for ***system automation and integration***. We could also extract feature groups of data from features of patterns based on path planning regions and classification results.

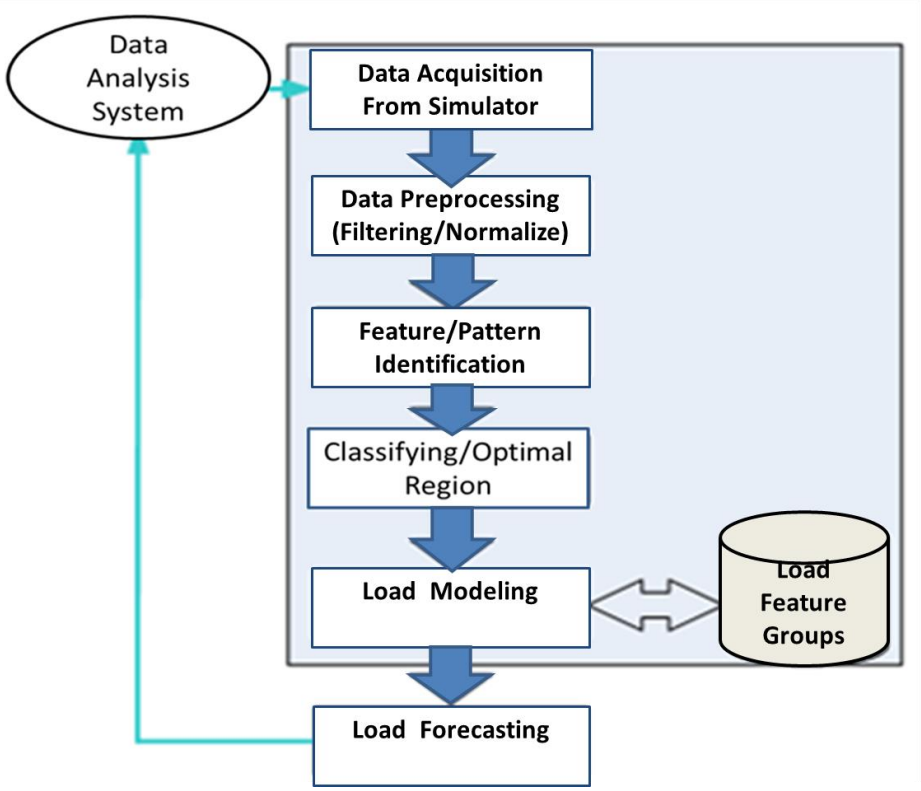

Figure 7.10 Feature-Based Modeling and Forecast of Simulation Data

7.5.2 Prediction GPU Simulation in Accessibility Map Computation for Path Planning in Subtractive 3D Printing

Algorithm 3 Extended Accessibility Map Construction Algorithm

Procedure MapAccessibility(Node A)

1 for each node B in old connected accessibility list (o-IL) of A do

2: if Node to Node accessibility (A, B) == ACCESSIBLE then

3: add B in new connected accessible list (n-IL) of A in accessible space as accessible region, label access image pixel as 1, vice versa as 0

4: add A in new connected accessible list (n-IL) of B in accessible Space as accessible region, label access image pixel as 1, vice versa as 0

5: end if

6: remove A from old accessible list (o-IL) of B

7: end for

8: for each C in children(A) do

9: MapAccessibility(C) (recursive way of functional call, assume the convergence with solution)

10: end for

Map Algorithm Structure: Given the orientation motion function of advanced CNC machine based on availability of oriented path planning in 3D space, accessibility

map is formulated by accessibility sequences from path sequences of input for angular availability computation along the geometry model in its surface area. In subtractive 3D printing, accessibility map is used in our work for 5-axis orientation calculation in path planning as the map provides reference data along the planning path that the GPU simulation curve use for planning iterations based on variable parameters such as depth of cut, step distance and margin of path planning based on 3D geometry model. **Extended Accessibility Map Construction Algorithm** with node is described as Algorithm 3. Accessibility in a broad scale can be described as the above pseudo code. The Logistics of Extended Accessibility Map define node A, which belongs to points of contact region around the surface geometry of model in 3D path planning.

Evaluation of Prediction in Accessibility Map

For evaluation purpose, we will analyze the key factors that play an important role in data simulation of path planning.

Stability: The highest time and lowest time get filtered when we want more stability time range for map generation regardless of model geometry. Then we probably take the average time as the setting bar for system points of view.

Speed: When we want the fastest map computation, we will pick the lowest sampling rate to meet minimum resolution requirement and the latency of response time threshold of map computation. The critical point is usually located where performance bottleneck is satisfied.

Sampling Rate: When we want the best path generation quality, we pick the highest time cost level regardless of where average time line as less sampling rate gives more points for high resolution data source for accessibility map computation which gets more information, although sometimes data may be redundant due to quality need.

Prediction Estimation by Refinement of Data: map generation time may be predicted when we interpolate the data by generating learning curve assume future map generation time also follows while we pick refined sampling rate in between the calculation points. The line shown in Figure 7.11 simply demonstrates the idea of average estimation following the data distribution of map sequence sample, thus the points not on the sampling rate points generated from 3D path planning simulation can also be estimated for any resolution of the map sequence based on quality requirement of the map. Thus we may do some refined tuning of parameters based on the computational geometry input.

7.5.3 Sampling Optimization

In this section we present Optimal Time Reference for Planning Budget. We can generate an average time level based on those sampling rate-based time sequence and get a bar set depending on our preference so that future reference learning curve can be made for accessibility map with default user advice coaching for model-based optimal sampling. On the other hand, we can also set the time bar based on our path generation quality requirement as ideally more resolution gets clear map information from high sampling rate. But, as the sampling rate gets higher, computation time also gets higher. Here the sampling rate is more like the gap distance between point intervals that get

extracted of model surface for accessibility map computation. The budget line works as a filter for optimal strategy generation based on software characteristics and user preference. To complement the above analysis of the sampling impact under optimization purpose, we did analysis of accessibility map sequence generation time via sampling rate on GPU so that we can see the effects of sampling on map generation based on the geometry model of Buzz we pick. Figure 7.11 shows the sampling output for accessible map sequence of Buzz path with average peak of performance for time estimation.

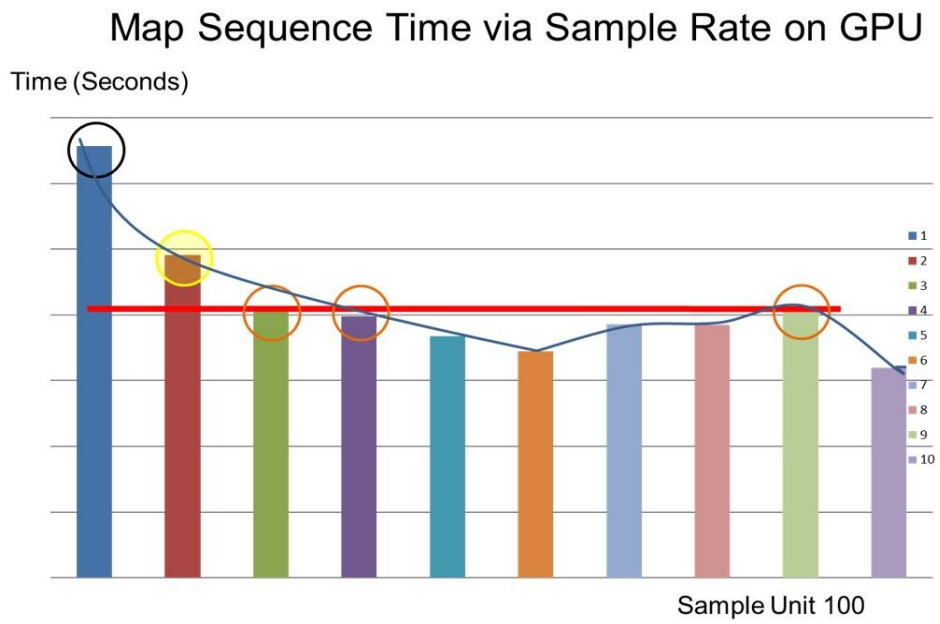

Figure 7.11 Map Sequence Time via GPU Sampling Rate of Buzz

We can vision that the actual sampling rate does affect accessibility map generation over the sampling rate from 100 to 1000 for data displayed in Figure 7.11 as GPU time cost of map sequences. The map sequences formulated in space to form accessibility space which is how the orientation get computed for path planning of 3D printing.

Optimization of data shows the time range from the lowest to highest map sequence computation given fixed model geometry and cutting depth of path planning for GPU computing. The reason we do data analysis based on sampling is because we want to see which sampling rate is best suitable for map computation while the model resolution or path resolution for planning is acceptable base on quality metrics and performance time limit.

Strategy Generation

We try to take advantage of load curve for economic analysis and demand response optimization based on the bidding strategy. Nash-equilibrium and linear programming may be useful for condition optimization and modeling with other parameters like temperature, price signal of the load models and human decision making. See if any game strategy could be used and the load profile groups or optimal cut could be achieved based on existing load forecast or error feedback. If in any case an adaptive curve fitting or forecasting algorithm could be generated, that would be useful for future fitting of load and generating load curve.

Decision Making

We need a simple simulation results for each part and a small simulation on smart meter data like load pattern or profile modeling and tie that into demand response scheduling or policy-based bidding strategy.

Scheduling decision signal is based on the optimal decision rules which can be generated by the fuzzy logic or other condition assessment based on price information.

Then we use a simple signal input as the output of the decision results and multiple that into the load data to judge whether we take any actions on the load curve by assessing whether it exceeds a certain level of power budget or cost budget of power performance boundary or platform independent quality requirement based on task execution.

7.5.4 Feature based Cloud Simulation Resource Saving Cases

As not all users are using the same service at the same time, by resource sharing using a cloud, the idle service share of a user A can be used by another user B.

a) Single Software Case

Assume there are N users at the time t, and each of them have to use a service software. Take Matlab for example, normally users have to purchase and install N times on their machine without the cloud. In comparison, by applying cloud link to provide all users the software, we can have the following situations:

When a user is using this software, the service probability of the software is 1; when not using, the service probability of using that software is 0. As users are not using Matlab all the time, so the average service probability of one user using the software is $\bar{p}_{a,b}$ at a certain time interval t_i, which belongs to a certain time period $[t_a, t_b]$ and,

$$\bar{p}_{a,b} = \sum_{i=a}^{b} p_i t_i / \sum_{i=a}^{b} t_i < 1 \qquad (7.1)$$

As formulated by Equation 7.1, p_i is the service probability of one user using a software at time period t_i. $\sum_{i=a}^{b} t_i$ represents the total time of working periods. Based on this, now we

consider N users using the cloud software. Instead of installing N pieces of the same software on each individual machine, we only need to provide a number of N_{use}

($N_{use} = p * N$) available pieces of software access for the cloud service. As the average service probability $\bar{p}<1$, which means in general the probability of individual using a software at time t is less than 1, therefore Equation 7.2 is formulated:

$$N_{use} = \bar{p} * N < N \tag{7.2}$$

Equation 7.3 calculates the portion of the software usage we can save by the cloud as

$$N_{save} = N * (1 - \bar{p}) \tag{7.3}$$

If we consider different average probabilities of N users using the same software, which is p_i, then the total available pieces of software needed are shown in Equation 7.4:

$$N_{use} = \sum_{i=1}^{N} p_i, \tag{7.4}$$

As $p_i < 1$, therefore we have Equation 7.5:

$$\sum_{i=1}^{N} P_i < N \tag{7.5}$$

Thus we still have $N_{use} < N$. In this case, the portion of the software usage we can save by the cloud is shown in Equation 7.6:

$$N_{save} = \sum_{i=1}^{N} (1 - p_i) \tag{7.6}$$

For the case of multi-threading instead of N pieces of software, we characterize energy consumption for each particular service, considering both time and power. If a service utilizes more than one thread or core, that may decrease the time to run the service, but will also increase the amount of power usage by the service.

b) Multiple Cloud-Service Software Cases that Applies for 3D printing

Considering N users using multiple software at time t, the expected usage of the total software needed at a certain time t is:

$$\mathrm{E\ (Ns)} = \sum_{j=1}^{N} \left(p_j * \mathrm{Ns_j}\right) \tag{7.7}$$

Let j represents the j[th] user, then p_j is the probability of j[th] user using cloud software at time t and, Ns_j is the number of different software needed by the j[th] user. Energy saving in the time period from time t_1 to t_2 to execute the service is:

$$E(Ns) = \sum_{j=1}^{N} \left(1 - p_j\right) * \mathrm{P} * \left(\mathrm{t_2} - \mathrm{t_1}\right) \tag{7.8}$$

In general, let $p_j = p_r$, then we have

$$\mathrm{E\ (Ns)} = \mathrm{N} * (1 - \mathrm{p_r}) * \mathrm{P} * (\mathrm{t_2} - \mathrm{t_1}) \tag{7.9}$$

Assume p_j is real time probability with variation and p_r is actual running probability with relatively stable condition. P is the general power consumption related to the cloud to run Ns software services with p_r as given average probability. Therefore, cloud can save resources by sharing its idle services to others on demand.

We extend our previous analysis of application scheduling of cloud services [72] to handle user request into application service of subtractive 3D printing in cloud for case study demonstration. We then generate simulation parameters for approximated workload for demo purpose based on model geometry type and put computer aided 3D printing in general service categories into additive 3D printing, subtractive 3D printing in 3 axis form for simple model, subtractive 3D printing in 5 axis form for complex model, and then compare the energy consumption of different techniques between models in key phase of software online data processing assuming an ordering feedback exist for recording the machine shop 3D printing services. Here we still assume total user number is 300 in the network for simplicity in a month's demand to retain our assumption in service-oriented cloud model with user web request. Next, we can then apply workload planning strategies based on system workload for behavior optimization after parallel software output and actual 3D printing operation after model processing.

We assume a cloud online ordering system is ready for handling both software input of model and machine shop product output monitoring or recording time length of each user request of particular model-based design via Computer Aided 3D Printing. In our simulation, we keep $K_{mininal}$ as the server number of cloud network in our simulation platform. We start from $K_{minimal}=1$ to $K_{minimal}=15$ and, we simulate and estimate relative

computational power in theoretical and assume ideal condition in subtractive 3D printing application without losses and no user interference or product remodeling bounce back.

Table 7-1 Cloud Application Simulation of Energy

Day	Total Users	Additive 3D Printing	Subtractive 5 axis Model	Subtractive 3 axis Model	Day	Total Users	Additive 3D Printing	Subtractive 5 axis Model	Subtractive 3 axis Model
1	294	79	61	154	16	232	70	69	93
2	171	95	49	27	17	18	10	7	1
3	92	64	26	2	18	80	38	13	29
4	73	29	38	6	19	61	58	3	0
5	287	141	6	140	20	142	7	114	21
6	51	26	12	13	21	86	67	8	11
7	159	93	44	22	22	267	122	29	116
8	277	260	1	16	23	200	100	20	80
9	108	28	39	41	24	233	193	5	35
10	71	19	20	32	25	64	13	29	22
11	138	132	4	2	26	138	80	9	49
12	226	85	117	24	27	183	96	39	48
13	237	33	28	176	28	128	106	7	15
14	25	22	2	1	29	259	4	34	221
15	164	55	26	83	30	272	202	3	67

Simulation time is the major factor that affects the energy consumption assuming average power is stable running computational workload. Here we pick numerical simulation data, and we just briefly depict that the total loaded power equals the maximum power in the cloud given the availability of user request handling and scheduling strategies that may happen in user request ordering for software feature extraction. For simulation parameters, we compare the power consumption of different techniques. As Table 7-1 reveals that for path planning in 3D printing, case study of cloud service could be extended to simulation between multi-axis paths for service-oriented cloud. For example, we could compare for two cases of service in comparison: cloud servers with 3-axis path planning model and 5-axis path planning model assuming 5-axis path takes more time for path planning simulation due to complex geometry structure. Similarly, we extend the simulation of cloud application of user event in previous work for network distribution [74] and apply here as path planning case studies.

For simplicity of the calculation, we ignore the Cooling Load Factor (CLF) and only consider Power Load Factor (PLF) [75]. We aim to show the idle switching benefits for cloud servers. According to the data efficiency concept presented in this paper, we consider useful work percentage and, we compare the outcome of different power allocation techniques using power planning and control in the cloud. This refers to power budgeting techniques in the cloud for power allocation [73].

For efficiency calculation, we assume the total power cost equals the service load power cost and set power usage efficiency to be 100% (all power spent on useful workload) for the biggest saving technique. The power costs and saving rates between

techniques are also compared, by selecting the technique with the maximum power consumption and setting its rate to be 100%.

Table 7-2 Cloud Service Simulation of Energy Efficiency by Techniques [72]

Techniques for Comparison	**Uniform Power Capping without Idle Scaling**	**Uniform Power Capping with Idle Scaling**	**Classified Power Capping with Idle Scaling**
$K_{minimal}$=1, Single Network Node Power (watts)	1450	500	500
Monthly Total Power in Unloaded Case(watts)	43500	15000	15000
Power Cost Rate	100%	34.5%	34.5%
Power Saving Rate	0%	65.5%	65.5%
Power Usage Efficiency	65.5%	100%	100%
$K_{minimal}$=15, Entire Network Power (watts)	21750	7500	7500
Monthly Total Power in Unloaded Case(watts)	652500	225000	225000
Power Cost Rate	100%	36%	36%
Power Saving Rate	0%	64%	64%
Power Usage Efficiency	64%	100%	100%
End-of-month Total Power(watts) with Load	652500	452050	394650
Power Cost Rate	100%	60 %	69%
Power Saving Rate	0%	40 %	31%
Power Usage Efficiency	60%	60/69=86%	100%
Saving Residual Efficiency	0%	31/40=77.5%	100%

The focus is to show how efficiency differs by applying different power planning and control techniques in the cloud. In addition, we compare the power usage efficiency, power cost rate and saving rate between listed techniques. The outcome of this comparison can be seen in Table 7-2. The case scenario may vary from application to application, but we focus to demonstrate the feasibility of analyzed strategy study regarding power management on the cloud service. Based on the results, we prove that Classified Power Capping outperforms the other techniques. $K_{mininal}$ is the number of server nodes in the cloud network. We still start from $K_{minimal}=1$ to $K_{minimal}=15$ which could be extended to more nodes for broad scale clusters and, we calculate related power, assuming the total loaded power consumption equals the maximum power in the cloud.

By using different planning techniques in the cloud, the actual power demand for a particular service at any given time can be allocated to match the scheduled power allocation of the underlying server hardware.

Based on the simulation and efficiency comparison, we know the total energy of a cloud is sensitive to the number of users, the virtual power consumption of a particular type of service, and the time cost of each service. On the other hand, we can see that Classified Power Capping consistently is better than the other techniques by having the minimum power cost rate, maximum power saving rate, and maximum efficiency. In fact, the idea of Classified Power Capping in the cloud belongs to smart power management techniques, including scheduling and control. The purpose is to reduce total power consumption as close as useful load demand in the cloud, so that we can maximize efficiency in the cloud. Therefore, we work on to match the total power consumption of the cloud to be close to the actual power usage on useful workloads, targeting at

maximized power savings and increased efficiencies. This gives a promising future of the "Cloud for Energy Informatics" as well as on smart manufacturing cloud.

7.5.5 Comparison to Similar Work

Compared with other methods of manufacturing design or path planning software, the key features of our path planning solution are based on parallel processing of path planning and 3D model design with ring parameter freeform testing for optimal regional strategy by human computer interaction, real-time dynamic path simulation service by high visualization resolution of geometry, feature selection by graph pattern, and scalability of the design. Our work differs by the service category of online connection, we extend the concept of data into modeling of multi-axis machining for path planning assuming 3D model costs relevant amount of time for processing path planning simulation.

7.5.6 Structure of Cloud Framework and Efficiency Metrics

A structural analysis includes but is not limited to:

- Data Structure
  - Software as a service (SaaS), Infrastructure as a service (IaaS) and Platform as a service (PaaS) as main categories of cloud computing for data structure and topology analysis (e.g. HDT branch in our case)
  - Framework of workload distribution of map kernel
  - Service-oriented cloud
  - Sub-cloud and workload classification
- Tools of Cloud Platform

  - VMs and Virtual Clusters
  - Shared cloud resources
- Data Processing and Algorithms
  - Graph partition and decomposition
  - Network topology
  - Accessibility
  - Optimization
  - Power Budgeting and informatics
- Case Study and Scalability
  - Data science and Load Distribution by Algorithm
  - Fog computing

By classifying groups of cloud data, we may speed up parallel tasks by scheduling group task classification in the service-oriented cloud [72], to reduce response time or power consumption.

7.6 Efficiency Metrics

7.6.1 Data Efficiency

The efficiency usually depicts the useful amount of power cost compared to the whole usage of power in total. According to Forrester, servers would use around 30% of their peak power consumption while sitting idle 70% of the time, although data centers are always built to suit peak load [76]. For the long term, the Green Grid [75] works on to define data center productivity (DCP) metrics, they define productivity as:

$$DatacenterProductivity = UsefulWork/TotalFacilityPower \quad (7.10)$$

According to [76], the Green Grid [75] defines two useful metrics to evaluate data center efficiency: Power Usage Effectiveness (PUE) and Data Center Infrastructure Effectiveness ($DCiE$).

$$PUE = (TotalPower)/(ITEquipmentPower) \tag{7.11}$$

$$DciE = (ITEquipmentPower)/(TotalPower) * 100 \tag{7.12}$$

Equation 7.11 measures the amount of power that goes directly to computing compared to ancillary services, Equation 7.12 calculates PUE reciprocal and indicates the percentage of actual power delivered to the servers compared to that delivered to the facility.

7.6.2 Time Efficiency

As energy is not only related to power: $Energy = Power \times Time$, therefore for a service-oriented cloud, the time spent for a particular service load is also important for the overall energy consumption and is helpful for understanding how a certain service request would cost energy in the cloud. In other words, we consider time constraints for service in our design as services tend to have the time attribute with information query involved. Therefore we apply the metrics defined in [77], and select the attribute to be time and redefine it as the flowing time efficiency metrics of cloud:

$$T_e = \sum_{i=1}^{N} p_i T_i \tag{7.13}$$

The time constraint of a particular service i and, p_i is the weight being the probability associated with each possible value T_i. Equation 7.13 gives the mean value of time

attribute associated with a weighted query of all possible time values within the selection interval [T_a, T_b].

7.6.3 Optimal Energy Saving

Optimal energy saving of service considers service task conditions: service time constraints, price range, power range and peak difference. Sometimes metrics are important for cloud measurement, such as normalized running frequency, as Equation 7.14 reveals

$$(P-Pmin)/(Pmax-Pmin) \quad (7.14)$$

Power changing rate may also be helpful to measure cloud power status. The cloud power is balanced when PD = PG − PL. Here PD is the power demand or need of cloud service load, and PG is the power generated for load. PL is the power loss of a cloud, which includes the power spent on data communication and transmission loss in network. If we can allocate the power allocation of cloud to match its power service demand, then we can have maximized power saving by classifying service cloud attributes.

7.7 Event Simulation and Task Partition towards Protection

The purpose of event simulation is to have clear understanding of task phases that contribute to the final outcome. Task partition formulates the process of path that is vital to the output of solutions. Task partition also helps parallelism as independent sub-tasks could be done in parallel. Right distribution and division of task help protect interference and independence of results. For each group, we can then relate an event with the load

data or a special feature then we can have a relative probability with each group. Here since we have PDF (probability density function), we classify the probability into decision trees so that the interrelation of different groups can be reclassified into classes in the hierarchical tree for each event, the group has a coefficient or weight for the event fuzzy logic function for decision making.

7.7.1 Graph Partition and Load Distribution

Previously for data post processing, we have talked about partition of data for G-code optimization. In order to enhance the workload partition and distribution we analyze the following aspects:

- Data load Groups (metrics for reference selection, comparison, variation)
- Event: for several load groups as its leading causes or factors of the event.

For each load group, it falls into a class in the decision tree, the tree can be seen as operation mode for each of its levels. Then we set up fuzzy logic function as (Wi*CLASSi), CLASS is the classification category of load group we used for economic decision making, and Wi is the weight metric of each class

7.7.2 Linking Data Mining to Monitoring

We address the problem of monitoring and detection systems from the data-mining and software engineering point of view. This represents a departure from traditional supervisory control and information management system approaches [78, 79]. Because data-mining encompasses solution techniques such as classification, and machine learning, we aim to divide the problem in a way that allow us to make use of

data mining methods to realize a powerful monitoring and evaluation system. On the other hand, data mining deals with identifying the relationships between behavior and data patterns. Because the decision outcomes for a given user behave as a feature pattern of space or temporal effects, if we can separate monitoring and relate its features to a single event, a clear mapping for analytics can be achieved.

To attain this objective, we use feature classification and health-analysis bars to separate individual feature monitoring based on classification. Then, we use a metric selection method to compare a single feature result against a given metric for map indication of service level. By categorizing and filtering outcomes using metric selection, the event effects and their relationship with specific features can be identified and generalized. The design of metric selection and filtering proves to be beneficial because most of the time events have only a partial effect on a set of features. The tool therefore enables separating monitoring of individual feature bar from the overall system evaluation. We assign 3 key features in our case, resulting in a classification metric selection is as follows:

- Choice1: Feature_1 classification
- Choice2: Feature_2 classification
- Choice3: Feature_3 classification
- Choice4: Composite classification_(all features)

This classification allows the system to identify the impact of a single feature under any event such as weather, mechanical failure, human action, etc.

7.7.3 Cost Optimization for Decision Making

This depends on the type of decision to be made. Regarding maintenance and service decisions, we present a classified-feature-awareness strategy. In this strategy, we assign proportional service levels to various services and application domains. We could set up cost function for optimization objective with various decision metric based on input user parameters as constraints.

7.7.4 Geographic Monitoring and Problem Detection for Protection

The system must provide geographic monitoring and detection. We apply graphical methods and symbols to display the results on a geo-referenced map and to provide data displayed in a user-friendly way. We address this by providing color classification and evaluation. We use standard meaning using green, orange, and red.

In order to implement the links that have been identified, it is necessary to overcome the barriers to the integration of software blocks. The simulation uses a weighted index, which covers the problem scope of our design regarding budget calculation and danger detection for protection. The implementation system diagram in Section 7.7.6 describes this concept.

Weighted indices link four aspects of system design: feature importance, budget allocation, danger detection, and classification. Equal weighted indices are used to represent the impact of each selected feature measure on the decision. It is beneficial to calculate the total value for danger detection and awareness evaluation, and to calculate the decision cost allocation so that optimum plans can be developed.

There are two methods to assign the weighted index. One method is by direct user input: the user can calibrate the weight as the user learns from the decisions made. Another way is to obtain automatic weighted indices from the system. This could be accomplished by machine learning algorithms that use the measured values and obtain weights that minimize the total budget allocation.

7.7.5 Protection Design using Feature Monitoring for Maintenance

Based on the conditions of the feature-classifier bar, the system detects when to send out a warning message indicating that the device is in danger. The description of the logic of how the awareness warning system works is as follows: when any key feature of a transformer test, e.g. in our simulation features 1, 2 or 3, is in a high level of awareness/maintenance, or when multiple feature analysis using weighted metrics and reference comparison is beyond a reliable threshold, the system sends a warning message. Otherwise the system is considered to be healthy.

The following metrics of comparison describe the safety condition:

(Measure_Feature1<〖Th〗_1) AND

(Measure_Feature2<〖Th〗_2) AND

(Measure_Feature3<〖Th〗_3) AND

(w_1* v_Feature1+w_2*v_Feature2+w_2*v_Feature3<Ref)

Th1, Th2, Th3 are the awareness upper thresholds of features 1, 2, 3. These represent linear constraints given the condition that any feature data should be within the

danger status upper threshold and that the overall system evaluation measure based on these feature measures is within a safe boundary.

The reference value is based on historical data and expert's setting. In the software simulation; we use normalized values of classified classes and assign each level a separate value for evaluation and budget calculation.

When the system sends out a warning signal, the map receives the data and provides a protective signal by a label with prominent color in the graphical interface.

Case1: Classified-Feature-Awareness Maintenance

Various methodologies have been developed for transformer condition assessment, including prediction and system analysis [80, 81]. None of the existing methods apply a seamless design that integrates budget saving and feature classification. In addition, analysts and decision-makers usually would like to have an easy-to-use operating tool for analytics and decision coaching. In this section we analyze optimal maintenance policy design and savings maximization based on feature-classified maintenance level. As a result of the design, we can manage key measures while considering policy making and optimal budget strategies for asset management. Asset management with budget saving and feature classification could also work for subtractive 3D path planning with data simulation feature for condition assessment and maintenance.

Case2: Generic Maintenance Strategy

The maintenance strategy may include a) routine testing and checking on a periodic basis, or b) maintenance based on failure or severe condition detection.

Rather than using different maintenance level analytics, in the generic maintenance strategy there is a default maintenance plan and the crew performs the scheduled tests regardless of service level and key feature analytics. For maintenance based on failure detection, the maintenance effort is estimated upfront. Worst-case conditions are considered so that the solution can solve all plausible conditions. We utilize generic maintenance strategies without the described methods integrated, leading to suboptimal decisions. We consider this generic strategy as the usual reference of business.

7.7.6 Classified-Feature-Awareness Protection

Based on the classification level, we apply a classified-feature-awareness maintenance for protection to extend our previous published methodology [82]. The key idea is to realize user awareness leading to a maintenance strategy proportional to the classified feature levels. Higher levels receive more concern, and are assigned higher levels of maintenance with the highest cost. Differentiating the maintenance levels tends to increase system reliability at optimal cost. The tool can help decision-makers decide on an optimal point between maximizing reliability and minimizing cost. At the same time, engineers and decision-makers can decide to alter the maintenance level and schedule based on the transformer condition and life expectancy. This procedure intends to assign the necessary precaution and safeguards according to the relevant key features before an event associated with the device occurs. The method we described could be viewed as a proportional status care for reliability and cost minimization.

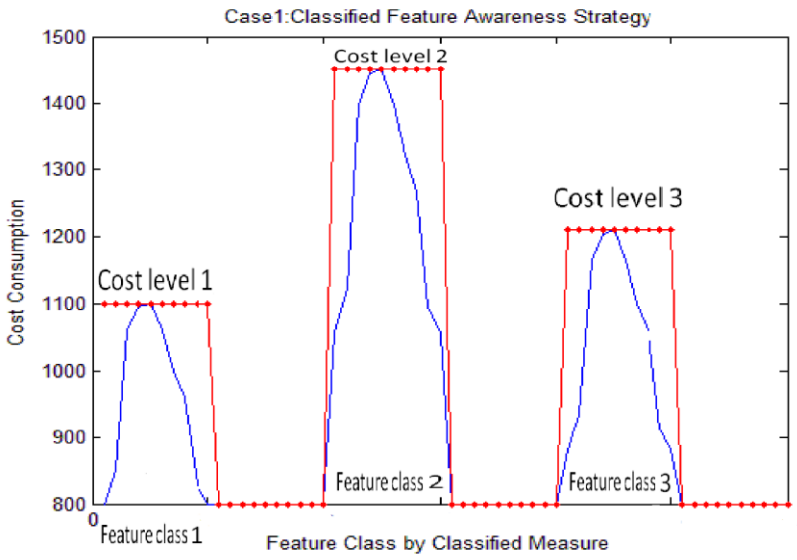

Figure 7.12 Cost Allocation Strategy of Optimization Comparison (Case1)

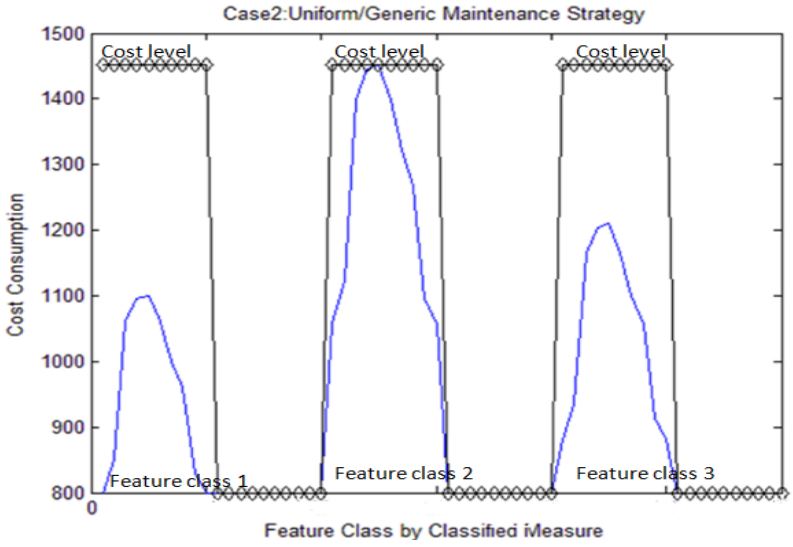

Figure 7.13 Cost Allocation Strategy of Optimization Comparison (Case2)

Most users are interested in high reliability design to avoid losses. Engineers could determine the strategy level according to their customers' reliability on satisfaction

functions. For example, they can pay more for ultra-reliable service or purchase reliability with pre-ordered design. Customer satisfaction levels could directly affect the design, such as the tool selection factors in the associated costs in our case. The classified-feature awareness tool provides advice for the service level that the utility has agreed to with the customer. Figure 7.12 and Figure 7.13 show the demonstration idea between cost allocation strategies of classified maintenance by cost compared to generic maintenance strategy. We derive the system implementation diagram in Figure 7.14. The danger condition includes path collision or other problem fault condition beyond tolerance that needs to apply protection procedure. We can see that the feature classification step is essential to linking the various blocks together. Budget calculation and danger detection are enabled based on the values determined during this step. This provides a protective logic for feature-based budget optimization with user interactive weights in map design. Note the difference of simulated monitoring map is different from accessibility map computation. The purpose of monitoring map optimization considers more user input parameter optimization in visualization interface while accessible map computation in path planning considers more searching orientations of accessible space. Accessible map computation in path planning generates map sequences for 2D sequences of data based on 3D space decomposition while map interface computation with budgets and cost allocation is designed with map visual platform for convenience of displaying data for comparison and analysis. The inner logics of computation for the two map concepts are also different in their flow diagram design, though both consider user input parameters with a specified focus.

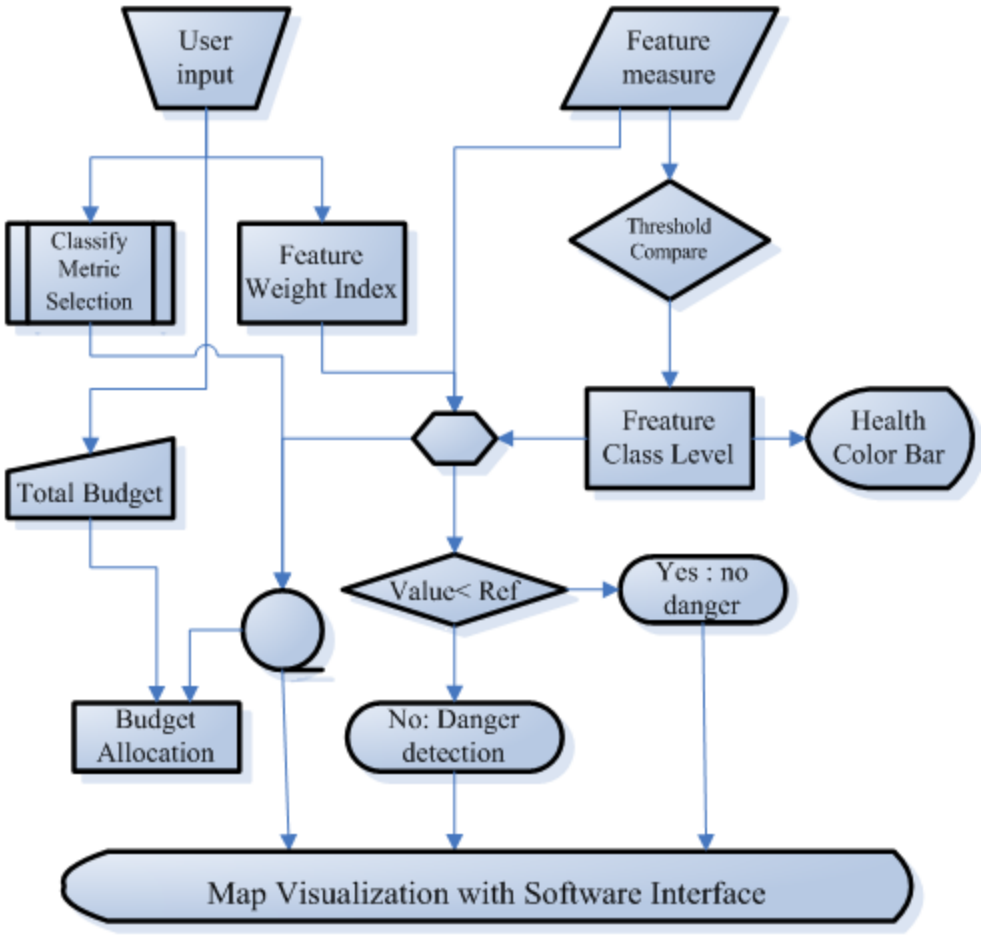

Figure 7.14 System Diagram for Classified Maintenance via Problem Detection

7.8 Evaluation of Results for Optimization with Asset Monitoring Interface

Result evaluation determines the accuracy of design and feedback of automation system, and it affects user decision in a broad range of solutions. In addition, the demo method calculates and displays the cost data using the classification metrics defined within the system. We derive visualization scorecard information based on the classification and evaluation of different feature levels and calculate budget saving for each strategy. In this way, an optimal budget assignment can be derived.

1st, the system needs to decide which type of features must be used for the simulation. The feature classification uses a generic design that can be applied to many types of feature measures and types of electric power assets. The feature classification allows better system status monitoring in terms of the key features selected for danger detection and warning. This is utilized in 3D visualization of condition assessment and feature description. The bar can be further extended to the policy setting for special cases such as collision of path or cost over-budget of service.

The warning detector is implemented by the safety conditions previously discussed. In our simulation, we apply the following *Protection Logic* to define safety condition as

$$(F\_1<0.9)\ \&\&(F\_2<0.9)\ \&\&(F\_3<0.9)$$

$$\&\&(W\_1*F\_1+W\_2*F\_2+W\_3*F\_3<0.9)$$

2nd: Metric selection panel and classification visualization with map indication.

Figure 7.15 shows the idea of feature monitoring with map interface design. Our theoretical design of the classification strategy is based on the key feature classification. Each feature is assigned with weighted evaluation function for total health estimation and measurement evaluation. Transformer is one example of asset management target. Here we want to demonstrate the idea of data simulation and classification with map interface design by transformer as case study of feature monitoring and protection regardless of the target. The asset target could also be machine design and path planning models by selection of feature monitoring purpose.

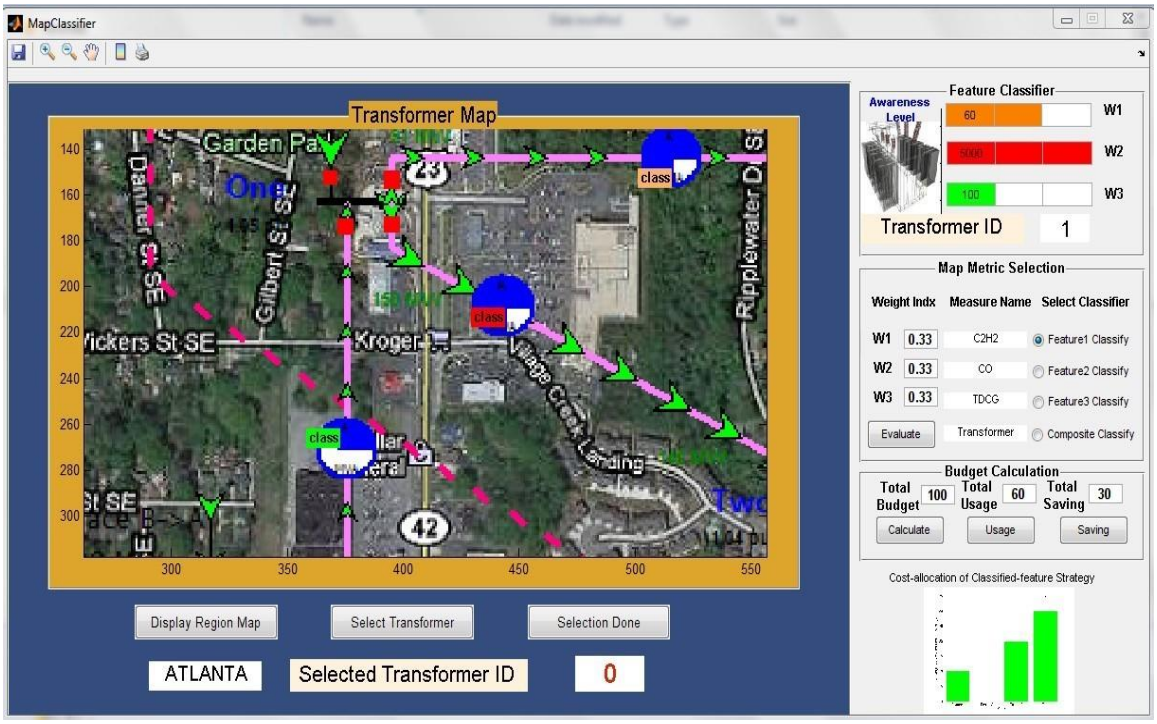

Figure 7.15 Map Interface and Panel with Feature Monitoring

In general, we like to extend the case study for importance of each selected feature to protect the overall health of feature-selection target, such as system health in case study of component condition analysis or quality of path in 3D path planning for Subtractive 3D Printing. For this purpose, we designed a weighted index for the system evaluation inputs. The feature classification by measure can be evaluated based on the role of each key feature. In our simulation, we simply initialize the weighted indices to be equal for all the key features. As mentioned, a learning loop can be done to enhance the weights using supervised learning.

3rd: User-selection of cloud server on a map.

By selecting a given cloud service such as a virtual machine on the map, users access the machine ID and open a menu where they can perform deeper path planning for

3D printing simulation and place order. The map interface design therefore could be an indication of analysis tools for cloud-based application in subtractive 3D printing.

4th: Budget allocation and cost-saving evaluation by classified strategies.

A user can input the total budget to be assigned for asset maintenance. The software will calculate the saving of maintenance cost of our classified-feature awareness strategy compared to generic maintenance. The actual usage of the budget will be displayed as well.

Benefits of Result with Design Monitoring Interface

The simulation results and software demonstration of the applied asset data monitoring system suggests the following:

- The design is able to capture key features and link multi-domain information to provide advanced analytics and decision-making.

- Monitoring and evaluation by a weighted index and budget calculation allows determining the effect of each feature to the budget allocation and cost savings.

- Warning and danger detection based on key feature-classification play a key role in prompting the decision-maker for action.

- System classification and similarity comparison regarding key feature selection enables determining which feature contributes more to the system health and cost savings.

- The classified feature-awareness strategy could be later linked to service quality and performance levels. The classification connects service levels based on feature measure. User satisfaction could be ensured based on their preference of the service quality setting.

- Maintenance strategies and decision coaching are better addressed by classification mechanisms leading to optimal cost saving, and reliability assurance. The higher level of maintenance requires more awareness on key features and user involvement.

7.8.1 Evaluation of Classified-Feature Protection Compared to Generic Strategy

During the simulation, we determine the cost associated with each strategy level based on the total budget. This includes maintenance, normal checking, and services.

The key idea of our strategy is to maximize cost savings and minimize the maintenance effort. For evaluation purposes we assign values of 0.3, 0.6, 0.9 to low, medium, and high feature levels, $F_{(i\_class),}$ respectively. The value of 0.9 is the highest awareness for dangerous conditions and maintenance care with the highest cost. We assume this is also the value for generic maintenance, in which case feature levels are all based on routine checking. The data values are set by user experience of estimated target for evaluation goal. We just list sample number here for calculation purpose.

Figure 7.16 I-IV shows the medium case considering low, medium and high attention for each feature. Compared to generic maintenance strategy, our solution saves the incremental cost of up to 30% in medium case and up to around 60% in the best case.

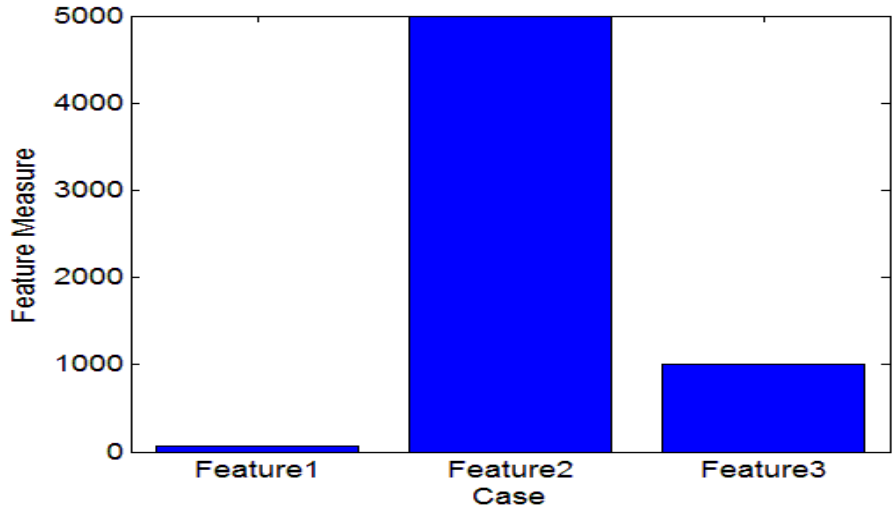

I. Input Feature Measure

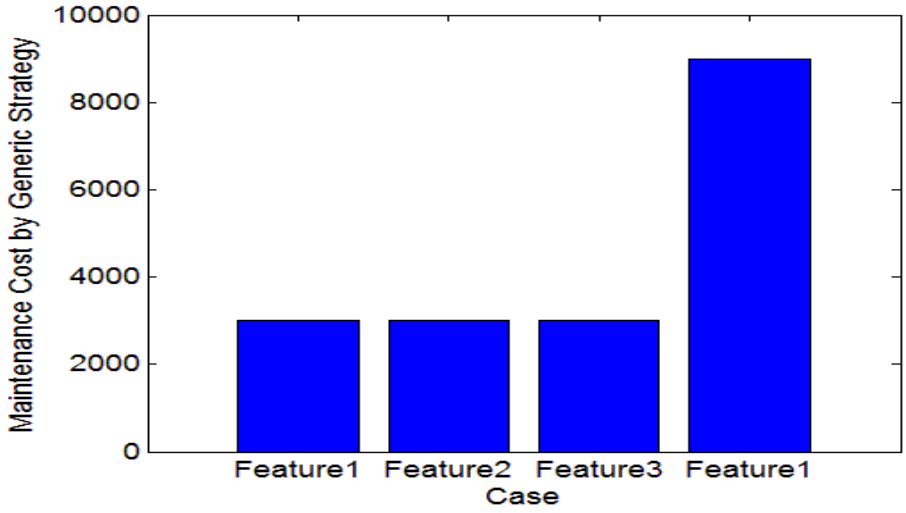

II. Generic Strategy Cost of All Features

Figure 7.16 Cost Comparison of Classified Feature-Protection with Generic Maintenance Strategy

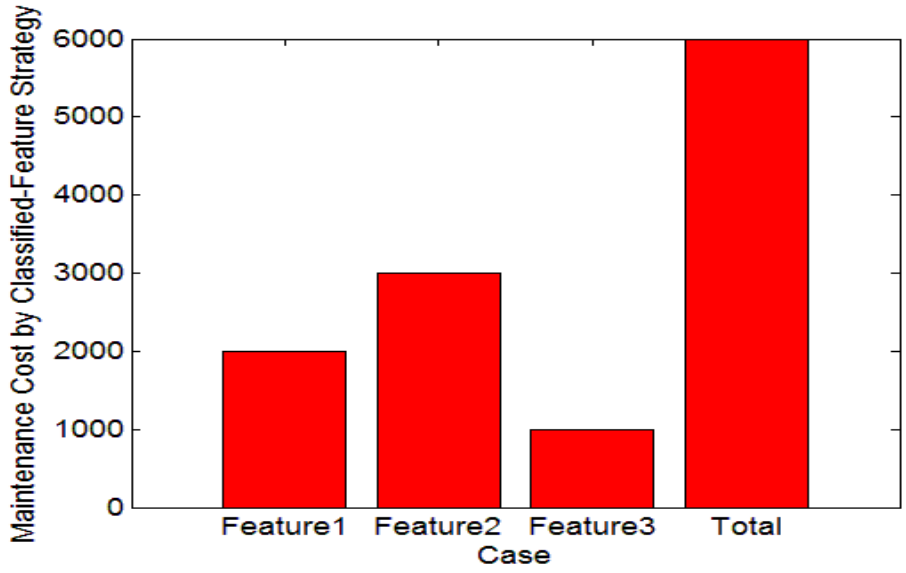

III Maintenance Cost of Classified Strategy

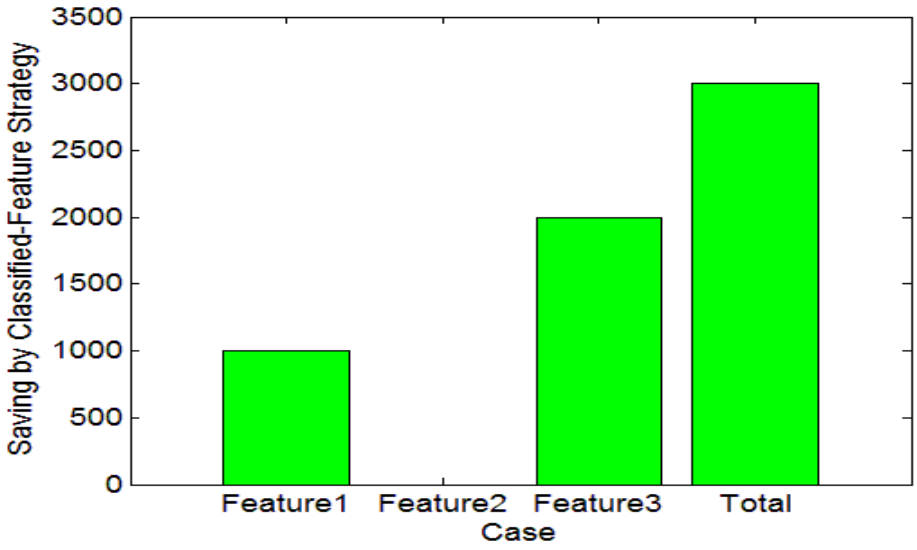

IV. Cost Saving of Classified Strategy

Figure 7.16 Continued

For general problem, we implement the following metric for evaluation:

$$Cost\_saved=total\_budget*sum\{(w_i/w)*(0.9-F_{(i\_class)})\} \;;$$

$$Cost\_usage=total\_budget*sum\{(w_i/w)*(F_{(i\_class)})\} \;;$$

$$Extra\_budget=0.1*total\_budget, \text{ for reliability concern} \;;$$

$$W=W\_1+W\_2+W\_3\ldots, i=1,2,3\ldots:$$

7.8.2 Multi-Domain Analysis

We build the system to support integrated multi-domain solutions. The system spans five areas: a) data-mining, b) condition assessment and geographic area evaluation c) decision-making, d) budget allocation, and e) detection and monitoring. To integrate these domains, we identify the links between them. The strategy does not consist in addressing deeper theoretical issues within each domain, but rather in designing a framework that integrates the five domains, with their corresponding links. Progress in each domain will hence be abstracted from the others, still providing a superior composite system capability.

The simulation results and software demonstration of the described classified service method suggests the following:

- The design is able to capture key features and link multi-domain information to provide advanced analytics and decision-making.
- Monitoring and evaluation by a weighted index and budget calculation allows determining the effect of each feature to the budget allocation and cost savings.

- Warning and danger detection based on key feature-classification play a key role in prompting the decision-maker for action.
- System classification and similarity comparison regarding key feature selection enables determining which feature contributes more to the system health and cost savings.
- The classified feature-awareness strategy could be later linked to service quality and performance levels. The classification connects service levels based on feature measure. User satisfaction could be ensured based on their preference of the service quality setting.
- Maintenance strategies and decision coaching are better addressed by classification mechanisms leading to optimal cost saving, and reliability assurance. The higher level of maintenance requires more awareness on key features and user involvement.

7.9 Domain Specific Solution for Ring Scale Optimization

7.9.1 Local Ring Optimization

Local optimal ring adapts to flexible platforms and path efficiency via domain specific solution, which defines 3D geometric pattern of linear 3-axis path region. For ring selective domain of path tolerance, Equation 7.15 shows the search of ring path solution as an optimization problem, which becomes a domain selective filtering process as well:

$$\text{Min Obj} = \sum r^2(\text{xi, Ring(S, N, d)}) \quad (7.15)$$

- Ring set the zone of tolerance as a black-box simulation function of ring parameter step-over distance and offset steps N and cutting depth d
- Each ring is an objective function r^2 in search of solution in parameter subspace
- where $x_i = \mathrm{R}(\theta, \emptyset, \varphi)[p_i + \mathrm{t}(t_x + t_y + t_z)]$ is contact points from set of selected feature as a function of $\theta, \emptyset, \varphi, t_x, t_y, t_z$ as selected with ring boundary to filter.

7.9.2 Subsurface of Ring Scale Optimization

The subsurface area may be described by Ω^m for 3D structure to be optimized, which is assigned a domain with a subset of reference domain $\boldsymbol{\Omega}$. The overall subtractive material removal and target 3D design geometry have a summation relation mapping the original stock material. We aim to optimize with minimal material to match the design:

$$\min \int_{u \in U, \varepsilon} f_\Omega \, u d\Omega + \int_{T_R} T u dS \tag{7.16}$$

$$\text{Subject to } \int_a E_{ij} K_i(x) \varepsilon_{ij}(u) \varepsilon_{ki}(v) d\Omega = \int_\Omega f v d\Omega + \int_{T_R} T v dS \tag{7.17}$$

As formulated in Equation 7.16 and Equation 7.17, T is the target shape and 3D design we aim to achieve, S is the surface of area of the target design. $\boldsymbol{\Omega}$ is the space of material we aim to remove and is selected by ring defined domain for filter. Analysis of sensitivity for linearized step is shown in the thesis Chapter 4.4.9 (page 67).

7.9.3 Domain Distribution Function for Digital Data by Sampling

To better understand controllable path and its protection function based on sampling, we try to describe the path distribution from stochastic perspective. For continuous form of data, the ring accumulated data of region is more like integration

operation within selected surface area. The root mean square (RMS) value of selected area Sq is expressed by Equation 7.18:

$$S_q = \sqrt{\frac{1}{A}\iint_A Z^2(x,y)dxdy} \tag{7.18}$$

For sampling form of data, A is the ring sampling area, Z(x, y) is a continuous function for discrete points within the region. The discrete form and stochastic perspective is shown similarly by Equation 7.19:

$$S_q = \sqrt{\frac{1}{N}\frac{1}{M}\sum_{i=1}^{N}\sum_{j=1}^{M} Z_{ij}^2} \tag{7.19}$$

S_q is chosen by general statistical parameters with N, M in x, y direction for points of path simulation. These models enable evaluation of path validation and data distribution.

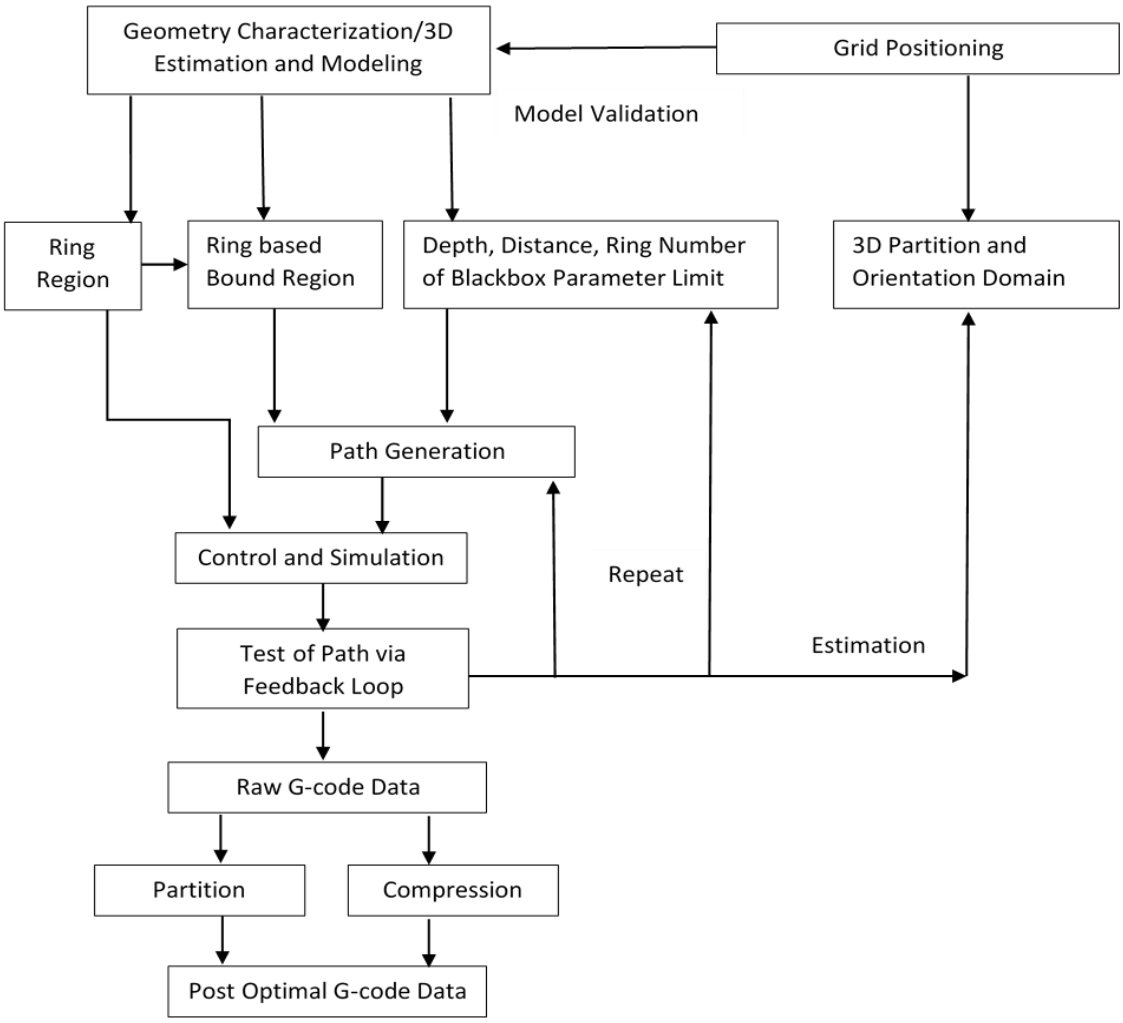

Figure 7.17 Tested Ring Step Path Planning Workflow Framework

Figure 7.17 shows the relation of ring step path planning framework after selecting the tool size. Compared with existing techniques, the key features of path planning solution based on parallel processing are 3D freeform testing for optimal strategy by human computer interaction, real-time dynamic path simulation by high visualization resolution of geometry, feature selection by graph pattern, and scalability of the design for local and global optimization. The framework helps understanding key parameters and simulation steps involved in Step Ring path planning in subtractive 3D printing.

CHAPTER 8. CONCLUSIONS AND FUTURE WORK

8.1 Conclusions

We presented and applied 3D ring step path planning for subtractive 3D printing integrating 3D modeling and CNC machine techniques for intelligent control. For software simulation, we considered system framework of software design with cost optimization interface and data integration solution with post-processing and preprocessing perspectives. Software parameter tuning is based on user interactive design with Blackbox simulation process for feature analysis and control feedback of testing from both the machine and G-code simulator. The contributions of this thesis are summarized in subsections 8.2, 8.3. Thoughts for future research directions are provided in subsection 8.4.

8.2 Contributions to Ring Step Path Planning Framework

Our contributions to ring step path planning includes accessible map filters and searching results for final region of accessible path sequence through non-zero access map data for direction decisions. Path sequence generation formulates slices of accessible route. The ring determines the distance of the k nearest neighbours around the ring start center within ring searching boundary that we estimate. The step ring path planning algorithm is based on ring predictive path planning. Bounded path solution of surface intersection with tool cutter is simulated with controllable path via volume removal visualization. The results of step ring path demonstrated successful 3D complex geometry of path planning in Subtractive 3D Printing. The local path analysis promotes scalable

design of domain specific solution and strategic path planning partition for workload distribution. We have proposed and tested a ring step path planning framework. The key features of our path planning solution are: (a) parallel processing of 3D freeform testing for optimal strategy by human computer interaction, (b) real-time dynamic path simulation by high visualization resolution of geometry, (c) feature selection by graph pattern, and (d) scalability of the design for local and global optimization.

The research has been performed by simulation and experimental testing not only theoretically but also in actual physical implementation on a CNC machine. Chapter 3 and Chapter 4 described the experimental testing based on a given platform including both software test of path planning by ring boundary prediction and mechanical test of G-code machining. The result shows a matching G-code graphic shape and mechanical product after machining compared with the original STL model. Chapter 5 provided the results i.e. the output of software function on path sequence via Buzz input, particularly the ring scale and volume rendering by domain via CPU vs. GPU.

8.3 Other Key Contributions

Other key contribution aspects include: (a) step ring based optimal region for path planning of 3D Manufacturing, (b) feature awareness protection and classification, (c) multi-domain analysis and data integration, (d) visualization and interactive map of feature classification, and (e) links between numerical modeling and path efficiency by 3D graphics. A short description of these contributions is provided next.

8.3.1 Step Ring based Optimal Region for Path Planning of 3D Manufacturing

The innovations of our scheme are a scalable path planning solution based on local ring prediction fitting tolerance geometric zone and accessibility map sequence based on optimal region. The accessible sequence modeling is based on 2D image feature Buzz reconstructed into 3D model for data fitting to pass the entire simulation process as 3D printing model into a CNC product. GPU allocation and smart data modeling is going to drive low-cost and highly-efficient-quality machining for both time-saving and event planning by classification of geometric features. High-precision 3D simulation helps parallel analysis over complex functions of machining and software simulation towards optimal solutions across flexible application platforms connecting CNC machine and even mobile application, so that distributed computing and digital manufacturing are facilitated with Computer-Aided Design (CAD).

We demonstrated that through cloud computing such as manufacturing cloud or fog computing and strategic path planning of regional ring path provide efficient morphological filtering of model decomposition for model-specific design and precision of path planning simulation. Users can design and implement pattern-oriented geometric interface combining similar techniques in 3D printing so that image features can be reconstructed into 3D modeling and CAD designs for multiaxis machining in smart manufacturing. In order to apply digital metrics and service-oriented cloud, we apply simulation and use feature classification of protection for maintenance of load monitoring and distribution.

8.3.2 Feature Awareness Protection and Classification

We have explored the potential of analytics using classification and graphical 3D modeling methods. We have simulated an evaluation and danger detection system based on the classification of key feature measures with suboptimal result. Based on this, a maintenance strategy that uses feature-classification levels is derived. A software demo is implemented for illustration by providing a weighted index as the generic link between blocks.

Simulations have demonstrated that the proposed system results in maintenance cost minimization and reliability maximization. Critical cases requiring higher awareness and attention are correctly detected. By design, the system provides the following simultaneous capabilities:

- Danger detection and feature evaluation
- A geographic map with evaluation and metric selection for monitoring.
- Budget optimization for service allocation.
- Human interface design

Reliability and cost awareness are related to feature classification for both maintenance awareness and service quality. Optimal strategy of decision-making is facilitated by comparing the weighted indices and the budget calculation.

8.3.3 Multi-Domain Analysis and Data Integration

We link the 3D path planning system components as improvement to support integrated multi-domain solutions both from data analysis and cloud computing

perspectives. 3D manufacturing via GPU path planning spans five areas: a) data-mining, b) condition assessment and geographic area evaluation c) decision-making, d) budget allocation, and e) feature detection and monitoring. To integrate these domains, we identified the links between them. The strategy does not focus in addressing deeper theoretical issues within each domain, but rather in designing a framework that integrates the five domains, with their corresponding links.

8.3.4 Visualization and Interactive Map of Feature Classification

The accessibility map is designed to work interactively with user metrics and parameters of ring path steps besides feature selection. Classification of features help diagnosis of problem and monitoring. To put data across geographic area, distributed partition of workload is necessary and thus graph partitioning for G-code optimization. Geographic information and service simulation graphs are linked with the feature classification of cost measurement, whether it be time or material. The user can choose to further investigate the information of a given service or to further perform analysis by geographical data. Metric selection is independent of the accessibility map. Extension of accessibility map in a broad scale become accessibility graph for discrete event simulation. The benefit of our design is to allow user to focus on a certain metric, e.g., an individual feature, and analyze how the status of each component is classified based on the selected metric and related to the map.

The classification feature simply receives the user defined path planning metric depending on the selected geometric choices and shows the classified weighted results.

As mentioned, the weights of each feature (w1, w2, w3 in our design) represents the importance of the individual features to the overall system health. In this manner, the weight contributes directly to the warning system design and budget allocation.

8.3.5 Links between Numerical Modeling and Path Efficiency by 3D Graphics

After we map the tasks in the cloud into local data centers, we can apply heuristic consolidation based on given Service Level Agreement (SLA) on virtual machine and resource management target in the system.

Energy is usually depicted as a given variation of data center power consumption P(t) at each time interval dt. System energy cost is recorded based on time of workload runtime with metering data from a data center platform. Energy efficiency metrics on data center [49] can then be applied based on given standard with performance standard satisfied in subtractive 3D printing.

The cloud data metric measured by cost function service application can represents the workload simulation consumed in the system given the sole mission of a particular function of path planning multi-axis model. We also researched how to apply adaptive forecast based on measurement of this simulation data so that we can correlate cloud informatics for data analysis and software integration features of 3D ring step path planning via optimal region in system analytic perspective.

8.4 Future Research Directions

The thesis already made contributions towards several aspects of the path planning problem. Additional research targets to enhance 3D step ring path planning with bounded control in subtractive 3D printing include but are not limited to:

- Classifier of advanced condition analysis by geometry feature and path filter, to extend Chapter 3.4 for path retraction and data compression in G-code optimization
- Ring stochastic variation by input geometry variables and control optimization with state estimation as path dynamics could be very complex but can advance the state of art.
- Cloud computing case studies of software service in diverse virtual machine platforms and better system integration with control as well as response times of cloud computing to support real time machining.

These tools have the potential to generate large sets of path planning data, which can be used to better train the stochastic modeling based on simulation output and use adaptive data fitting for graphical output and input to build better objective function and linear and nonlinear path model. Path protection based on these models help us understand the benefits and limitations of 3D STL model and provide estimation of path retraction condition for collision avoidance. To attain this goal, future work can be extended in several directions:

a) Machine learning applications for automatic parameter tuning regarding modeling and data compression with intelligent workload distribution, such as G-code data compression for optimization.

b) Extension to a robust coaching system that integrates automation and provides protective solution by various alternative analysis towards path optimization. Protection approach is already mentioned in system perspective for simulation data.

c) Utilization of feature-aware logic that is dependent on the user of the engineering system: maintenance technician, engineer, or financial decision maker.

d) Green computation with digital metric and optimal workload distribution.

REFERENCES

[1] D. Konobrytskyi, “Automatic CNC Toolpath Planning and Machining Simulation on Highly Parallel Computing Architectures”, Ph.D. Thesis, Clemson University, 2013.

[2] Zhang, H., Calvo-Amodio, J., and Haapala K.R., 2013. “A conceptual model for assisting sustainable manufacturing through system dynamics.” Journal of Manufacturing Systems, 32(4): pp. 543-549.

[3] Tao, F., Zhang, L., Venkatesh, V.C., Luo, Y., and Cheng, Y., 2011. “Cloud manufacturing: a computing and service-oriented manufacturing model.” Journal of Engineering Manufacture, 225(10), pp.1969-1976.

[4] Kathryn, E. S., 1983. “Formulation and Solution of Nonlinear Integer Production Planning Problems for Flexible Manufacturing Systems.” Management Science, 29(3), pp. 273-288.

[5] Torigaki, T., and Fujitani, K., 2000. "Power of a voxel approach to structural analysis and topology-shape optimization in automobile industries." Japan Journal of Industrial and Applied Mathematics, 17, pp. 129-147.

[6] Tao, F., Hu, Y. F., and Zhang, L., 2010. “Theory and practice: Optimal resource service allocation in manufacturing grid.” China Machine Press, Beijing, 1st ed. pp. 1–18.

[7] Tao, F., Zhang, L., and Nee. A. Y. C., 2011. “A review of the application of grid technology in manufacturing.” Int. J. Production Research, 49(13), pp. 4119–4155.

[8] Tao, F., Zhao, D., Hu, Y., and Zhou, Z., 2008. “Resource service composition and its optimal-selection based on particle swarm optimization in manufacturing grid system.” IEEE Transactions on Industrial Informatics, 4(4), pp. 315–327.

[9] Tao, F., Hu, Y., and Zhou, Z., 2008. "Study on manufacturing grid & its resource service optimal-selection system." The International Journal of Advanced Manufacturing Technology, 37(9), pp. 1022-1041.

[10] Tao, F., Hu, Y., and Zhou, Z., 2009. "Application and modeling of resource service trust-QoS evaluation in manufacturing grid system." International Journal of Production Research, 47(6), pp. 1521-1550.

[11] Geiss, Ryan (2007). “Generating Complex Procedural Terrains Using the GPU." GPU Gems 3, Chapter 1.

[12] Hamada, S., 2013, “Performance comparison of three types of GPU-accelerated indirect boundary element method for voxel model analysis.” Int. J. Numer. Model., 26, pp. 337–354.

[13] Crassin, C.. 2011. “GigaVoxels: A Voxel-Based Rendering Pipeline for Efficient Exploration of Large and Detailed Scenes”, Thesis, Université de Grenoble.

[14] Crassin, C., Neyret, F., Lefebvre, S., and Isemann, E., 2009. “GigaVoxels: Ray-Guided Streaming for Efficient and Detailed Voxel Rendering.” ACM SIGGRAPH Symposium on Interactive 3D Graphics and Games (I3D), Proceedings of the 2009 symposium on Interactive 3D graphics and games, ACM Press, Feb, Boston, United States., pp.15-22.

[15] Rees, E., and McColgan, P., 2013. “Voxel Based Morphometry.” Methods for Dummies 2013, (ppt slides)

[16] Sugiyama, K., Ii, S., Takeuchi, S., Takagi, S., Matsumoto Y., 2011. "A full Eulerian finite difference approach for solving fluid–structure coupling problems." Journal of Computational Physics, 230(3), pp. 596-627.

[17] Scahill, R. I., Schott, J. M., Stevens, J. M., Rossor, M. N., and Fox, N. C., 2002. "Mapping the evolution of regional atrophy in Alzheimer's disease: Unbiased analysis of fluid-registered serial MRI." Proc Natl Acad Sci USA 2002, 99(7), pp. 4703–4707.

[18] "Thermoregulation Mode", Innovative New Software: 3-D Voxel-Based Bio-Heat Transfer Code, available at (downloaded on Mar 28, 2016) http://www.thermoanalytics.com/products/humanthermal/thermoregulation.

[19] Sugiyama, K., Takeuchi, S., Ii, S., Takagi, S., and Matsumoto, Y., 2010. "An Eulerian Approach to Fluid-Structure Coupling Problems Suitable for Voxel-Based Geometry." The 6th international Symposium on Multiphase Flow, Heat Mass Transfer and Energy Conversion, Xi'an (China), AIP Conf. Proc. 1207, 324.

[20] University of Hull, School of Medical & Biological Engineering, 2013. "Voxel based finite element analysis." http://www2.hull.ac.uk/science/mbe.aspx.

[21] Banglawala, N., Bethunel, I., Fagan, M., and Holbrey, R., 2015. "Voxel-based finite element modelling with VOX-FE2." White paper funded under the embedded CSE programme of the ARCHER UK National Supercomputing Service, Ver. 1.0 (May 20, 2015).

[22] Shokrollahi, N., and Shojaei, E., 2014. "Experimental comparison of iso-scallop, iso-planar and iso-parametric algorithms in machining sculptured surfaces." Indian J. Sci. Res. 1(2), pp.475-481.

[23] Mohammad M. Hossain, Chandra Nath, Thomas M. Tucker, Rich Vuduc, Thomas Kurfess, A graphical approach for freeform surface offsetting with GPGPU acceleration for subtractive 3D printing, The 11th ASME International Manufacturing Science and Engineering Conference (MSEC), Virginia Tech, Blacksburg, VA, USA, 27 Jun–01 Jul, 2016.

[24] Łukasz CZERECH (2013). “Selection of Optimal Machining Strategy in the Manufacturing of Elements bounded by Curvilinear Surfaces.” Acta Mechanica et Automatica, 7(1), pp. 5–10, ISSN (Online) 2300-5319, January 2014.

[25] U. Firat, S. N. Engin, M. Saraclar, and A. B. Ertuzun, "Wind Speed Forecasting Based on Second Order Blind Identification and Autoregressive Model," in Machine Learning and Applications (ICMLA), 2010 Ninth International Conference on, pp. 686-691.

[26] N. Abdel-Karim, M. Small, and M. Ilic, "Short term wind speed prediction by finite and infinite impulse response filters: A state space model representation using discrete markov process," in PowerTech, 2009 IEEE Bucharest, 2009, pp. 1-8.

[27] J. Xin, D. Yao, W. Jie, and W. Jujie, "An Improved Combined Forecasting Method for Electric Power Load Based on Autoregressive Integrated Moving Average Model," in Information Science and Management Engineering (ISME), 2010 International Conference of, pp. 476-480.

[28] C. Hao, L. Fangxing, W. Qiulan, and W. Yurong, "Short term load forecasting using regime-switching GARCH models," in Power and Energy Society General Meeting, 2011 IEEE, 2011, pp. 1-6.

[29] C. Hao, W. Jie, and G. Shan, "A Study of Autoregressive Conditional Heteroscedasticity Model in Load Forecasting," in Power System Technology, 2006. PowerCon 2006. International Conference on, 2006, pp. 1-8.

[30] M. Hassanzadeh and C. Y. Evrenosoglu, "Power system state forecasting using regression analysis," in Power and Energy Society General Meeting, 2012 IEEE, pp. 1-6.

[31] E. Mangalova and E. Agafonov, "Time series forecasting using ensemble of AR models with time-varying structure," in Evolving and Adaptive Intelligent Systems (EAIS), 2012 IEEE Conference on, 2012, pp. 198-203.

[32] D. Ni, Y. Besanger, F. Wurtz, G. Antoine, and P. Deschamps, "Time series method for short-term load forecasting using smart metering in distribution systems," in PowerTech, 2011 IEEE Trondheim, pp. 1-6.

[33] L. Shu-liang, H. Zhi-qiang, and C. Xiu-kai, "Power Load Forecasting Based on Neural Network and Time Series," in Wireless Communications, Networking and Mobile Computing, 2009. WiCom '09. 5th International Conference on, 2009, pp. 1-5.

[34] K. Feng and W. Xiaojuan, "Time Series Forecasting Model with Error Correction by Structure Adaptive Support Vector Machine," in Computer Science and Software Engineering, 2008 International Conference on, 2008, pp. 1067-1070.

[35] W. Yi and Y. Songqing, "Annual electricity consumption forecasting with least squares support vector machines," in Electric Utility Deregulation and Restructuring and Power Technologies, 2008. DRPT 2008. Third International Conference on, 2008, pp. 714-719.

[36] M. Ghofrani, M. Hassanzadeh, M. Etezadi-Amoli, and M. S. Fadali, "Smart meter based short-term load forecasting for residential customers," in North American Power Symposium (NAPS), 2011, pp. 1-5.

[37] K. S. K. Weranga, D. P. Chandima, S. R. Munasinghe, S. P. Kumarawadu, and A. M. Harsha S, "Short-term electricity demand forecasting method for smart meters," in Information and Automation for Sustainability (ICIAfS), 2012 IEEE 6th International Conference on, pp. 266-272.

[38] I. Fernandez, C. E. Borges, and Y. K. Penya, "Efficient building load forecasting," in Emerging Technologies & Factory Automation (ETFA), 2011 IEEE 16th Conference on, pp. 1-8.

[39] C. Hao, W. Qiulan, Z. Bing, L. Fangxing, and W. Yurong, "Short-term load forecasting based on asymmetric ARCH models," in Power and Energy Society General Meeting, 2010 IEEE, pp. 1-6.

[40] Y. K. Penya, C. E. Borges, and I. Fernandez, "Short-term load forecasting in non-residential Buildings," in AFRICON, 2011, 2011, pp. 1-6.

[41] D. De Silva, X. Yu, D. Alahakoon, and G. Holmes, "Incremental pattern characterization learning and forecasting for electricity consumption using smart meters," in Industrial Electronics (ISIE), 2011 IEEE International Symposium on, pp. 807-812.

[42] C. Guowei, D. Yang, J. Ying, and P. Chao, "The characteristic analysis and forecasting of mid-long-term load based on spatial autoregressive model," in Sustainable Power Generation and Supply, 2009. SUPERGEN '09. International Conference on, 2009, pp. 1-5.

[43] J. Z. Kolter, and Joseph Ferreira, "A Large-Scale Study on Predicting and Contextualizing Building Energy Usage," AAAI, 2011.

[44] M. Torabi and S. Hashemi, "A data mining paradigm to forecast weather sensitive short-term energy consumption," in Artificial Intelligence and Signal Processing (AISP), 2012 16th CSI International Symposium on, pp. 579-584.

[45] AbdelSalam, H., Maly, K., Mukkamala, R., Zubair, M., Kaminsky,D.: Towards energy efficient change management in a cloud computing environment. In: Scalability of Networks and Services. Lecture Notes in Computer Science, vol. 5637. Springer, Berlin (2009)

[46] Amazon Elastic Compute Cloud: http://aws.amazon.com/ec2

[47] Chandra, A., Gong, W., Shenoy, P.: Dynamic resource allocation for shared data centers using online measurements. In: SIGMETRICS'03, San Diego, California, USA, June 10–14, 2003. ACM, New York (2003). 1-58113-664-1/03/0006

[48] Chase, J., Anderson, D., Thakar, P., Vahdat, A., Doyle, R.: Managing energy and server resources in hosting centers. In: Proceedings of the 18th Symposium on Operating Systems Principles (SOSP)(2001)

[49] Chen, Y., Das, A., Qin,W., Sivasubramaniam, A.,Wang, Q., Gautam, N.: Managing server energy and operational costs in hosting centers. In: ACM SIGMETRICS Performance Evaluation Review (2005)

[50] Data Center Energy Efficiency with Intel Power Management Technologies, Intel Information Technology, Data Centers, February 2010

[51] Femal, M., Freeh, V.: Boosting data center performance through non-uniform power allocation. In: Proceedings of the IEEE International Conference on Autonomic Computing (ICIA) (2005)

[52] Fouquet, M.: Position Paper. Technische Universität. Cloud Computing for the Masses, U-NET'09, December 12009. Rome, Italy, ACM (2009)

[53] Ge, R., Feng, X., Feng, W., Cameron, K.: CPU miser: a performance-directed, run-time system for power-aware clusters. In: Proceedings of the International Conference on Parallel Processing (ICPP) (2007)

[54] Heller, B., Seetharaman, S., Mahadevan, P., Yiakoumis, Y.,Sharma, P., Banerjee, S., McKeown, N.: ElasticTree: saving energy in data center networks. Usenix (2010)

[55] Khalid, F.: Cloud computing: local user expectations. In: Open Cirrus Summit, 28–29 January 2010

[56] Kishimoto, Z.: Can cloud computing be energy efficient? http://tek-tips.nethawk.net/blog/can-cloud-computing-be-energy-efficient

[57] Lefurgy, C., Wang, X., Ware, M.: Server-level power control. In Proceedings of the IEEE International Conference on Autonomic Computing (ICAC), June 2007

[58] Nathuji, R., Schwan, K., Somani, A., Joshi, Y.: VPM tokens: virtual machine-aware power budgeting in datacenters. Cluster Comput. 12(2), 189–203 (2009). doi:10.1007/s10586-009-0077-z

[59] Pakbaznia, E., Pedram, M.: Minimizing data center cooling and server power costs. In: Proceedings of the 14th ACM/IEEE International Symposium on Low Power Electronics and Design (2009)

[60] Pfleeger, S.L., Atlee, J.M.: Testing the programs, 4th edn. In: Software Engineering: Theory and Practice

[61] Raghavendra, R., Ranganathan, P., Talwar, V., Wang, Z., Zhu, X.:No “power” struggles: coordinatedmulti-level powermanagement for the data center. doi:10.1145/1346281.1346289

[62] Rajamani, K., Lefurgy, C.: On evaluating request-distribution schemes for saving energy in server clusters. In: Proceedings of the IEEE International Symposium on Performance Analysis of Systems and Software (ISPASS), March 2003

[63] Ranganathan, P., Leech, P., Irwin, D., Chase, J.: Ensemble-level power management for dense blade servers. In: Proceedings of the International Symposium on Computer Architecture (ISCA) (2006)

[64] Srikantaiah, S., Kansal, A., Zhao, F.: Energy aware consolidation for cloud computing. In: USENIX Workshop on Power Aware Computing and Systems in Conjunction with OSDI, San Diego, December 2008

[65] Wang, L., von Laszewski, G., Kunze, M., Tao, J.: Cloud computing: a perspective study. New Gener. Comput. 28(2), 137–146 (2010). doi:10.1007/s00354-008-0081-5

[66] Wang, L., Khan, S.U., Dayal, J.: Thermal aware workload placement with task-temperature profiles in a data center. J. Supercomput.1–24 (2011). doi:10.1007/s11227-011-0635-zAa

[67] Wang, L., von Laszewski, G., Huang, F., Dayal, J.: Task scheduling with ANN based temperature prediction in a data center: a simulation based study. Eng. Comput. Int. J. Simul.-Based Eng. doi:10.1007/s00366-011-0211-4

[68] Wang, X., Chen, M., Lefurgy, C., Keller, T.W.: SHIP: scalable hierarchical power control for large-scale data centers. In: PACT (2009)

[69] Wu, et al., “Step Ring Based 3D Path Planning via GPU Simulation for Subtractive 3D Printing,” Paper No. MSEC2016-8751, pp. V002T04A006; 11 pages, doi:10.1115/MSEC2016-8751 in Proceedings of the 11th ASME Manufacturing Science and Engineering Conference (MSEC), June 27-July 1, 2016, Blacksburg, VA, USA

[70] Wu, et al., “Step Ring-Based Three-Dimensional Path Planning Via Graphics Processing Unit Simulation for Subtractive Three-Dimensional Printing”, J. Manuf. Sci. Eng 139(3), 031010 (Oct 06, 2016) (10 pages) Paper No: MANU-16-1415; doi: 10.1115/1.4034662

[71] Choi, W. and T. R. Kurfess (1999). "Dimensional Measurement Data Analysis, Part 1: A Zone Fitting Algorithm." Journal of Manufacturing Science and Engineering 121(2): 238-245.

[72] Wu, et al., “Towards a Cloud Infrastructure for Energy Informatics”, Conference: Proceedings of the 2012 Energy Informatics Conference (EI'12), October 2012

[73] Wu, et al., “Power Control by Distribution Tree with Classified Power Capping in Cloud Computing”, 2010 IEEE/ACM International Conference on Green Computing and Communications & 2010 IEEE/ACM International Conference on Cyber, Physical and Social Computing

[74] Wu, et al., “Classified Power Capping on Network Distribution Trees for Green Computing”, Journals of Cluster Computing, 2011, DOI:10.1007/s10586-011-0173-8

[75] Christian Belady, A. R., Pfleuger, J., and Cader, T. (2007). The green grid data center power efficiency metrics: Pue and dcie. The Green Grid. Whitepaper.[online].

[76] Singh, T. and Vara, P. (2009). Smart metering the clouds. In Enabling Technologies: Infrastructures for Collaborative Enterprises, 2009. WETICE '09. 18th IEEE International Workshops on, pages 66 –71.

[77] Jiang, Z. (2012). A decision-theoretic framework for numerical attribute value reconciliation. Knowledge and Data Engineering, IEEE Transactions on, 24(7):1153–1169.

[78] "IEEE Recommended Practice for Monitoring Electric Power Quality," in IEEE Std 1159-2009 (Revision of IEEE Std 1159-1995) , vol., no., pp.c1-81, 26 June 2009, doi: 10.1109/IEEESTD.2009.5154067

[79] G. L. Martin, "The Hydran@ -a system for the detection and monitoring of failure conditions in power transformers," IEE Colloquium on Monitors and Condition Assessment Equipment (Digest No. 1996/186), Leatherhead, UK, 1996, pp. 3/1-3/5. doi: 10.1049/ic:19961066

[80] A. E. B. Abu-Elanien, M. M. A. Salama and R. Bartnikas, "A Techno-Economic Method for Replacing Transformers," in *IEEE Transactions on Power Delivery*, vol. 26, no. 2, pp. 817-829, April 2011. doi: 10.1109/TPWRD.2010.2091289

[81] E. Duarte et al., "Prioritizing transformers for condition-based asset replacement," IEEE PES General Meeting, Providence, RI, 2010, pp. 1-7. doi: 10.1109/PES.2010.5590002

[82] Wu, et al., “Electric Power Asset Monitoring and Danger Detection using Classified-Feature Awareness”, Journal of Pervasive Technology, Journal of Pervasive Technology, Vol. 1., No. 1, 2012.

[83] A focus on visualizations: Spider charts, published on 6 August, 2014, https://www.sweetspot.com/en/2014/08/06/focus-visualizations-spider-chart/

VITA

Ms. Zhengkai Wu was born in Xi'an, and grow up in Northwestern Polytechnical University in China. Her grandfather previously served as the vice president of Northwestern Polytechnical University and earned his Ph.D degree in Imperial College London with Gengzi Scholarship between British and Chinese government. All her family was teaching on campus, that highly inspires her to pursue the Ph.D study abroad. Since 2011, Dr. Wu has joined as a research assistant in Electrical and Computer Engineering department at the Georgia Institute of Technology, while pursuing a Doctor of Philosophy. During 2012 Summer, she served as a researcher in an internship co-op with the National Renewable Energy Laboratory in Denver, Colorado and won an idea prize from director of Energy System Integration lab. Prior, she was awarded with the provost fellowship and served as both a teaching and a research assistant for the University of Central Florida, and later graduated with a Master of Science degree in Computer Science in 2010 Fall.

In 2016, Ms. Wu was awarded with 70th Who's who in America for contributing articles and scientific papers to professional journals in her field. Her doctoral research focused on subtractive 3D printing and CAD Buzz modeling design and path planning optimization as well as system integration. Her work was published to MSEC, JMSE and several poster workshops including NSF-CPS (Cyber Physical System), GSSC (Georgia Scientific Computing Symposium), AeroDef (2017) and SC(HWPC 2016). She joined various memberships, such as e.g. IEEE Smart Grid, IEEE Communications Society, IEEE Power and Energy Society, IEEE Computer Society, SIAM, etc.